BRAIN COMMUNICATIONS

Passive immunotherapy for N-truncated tau ameliorates the cognitive deficits in two mouse Alzheimer's disease models

Veronica Corsetti,[1]* Antonella Borreca,[2,3]* Valentina Latina,[1]* Giacomo Giacovazzo,[4]
Annabella Pignataro,[4] Paraskevi Krashia,[4,5,6] Francesca Natale,[7] Sara Cocco,[7]
Marco Rinaudo,[7] Francesca Malerba,[1] Rita Florio,[1] Roberta Ciarapica,[1]
Roberto Coccurello,[4,8] Marcello D'Amelio,[4,5,6] Martine Ammassari-Teule,[4]
Claudio Grassi,[7,9] Pietro Calissano[1,†] and Giuseppina Amadoro[1,10,†]

*These authors equally contributed to this work.

†These authors equally shared the seniorship of the work.

Clinical and neuropathological studies have shown that tau pathology better correlates with the severity of dementia than amyloid plaque burden, making tau an attractive target for the cure of Alzheimer's disease. We have explored whether passive immunization with the 12A12 monoclonal antibody (26–36aa of tau protein) could improve the Alzheimer's disease phenotype of two well-established mouse models, Tg2576 and 3xTg mice. 12A12 is a cleavage-specific monoclonal antibody which selectively binds the pathologically relevant neurotoxic $NH_2$26-230 fragment (i.e. NH_2htau) of tau protein without cross-reacting with its full-length physiological form(s). We found out that intravenous administration of 12A12 monoclonal antibody into symptomatic (6 months old) animals: (i) reaches the hippocampus in its biologically active (antigen-binding competent) form and successfully neutralizes its target; (ii) reduces both pathological tau and amyloid precursor protein/amyloidβ metabolisms involved in early disease-associated synaptic deterioration; (iii) improves episodic-like type of learning/memory skills in hippocampal-based novel object recognition and object place recognition behavioural tasks; (iv) restores the specific up-regulation of the activity-regulated cytoskeleton-associated protein involved in consolidation of experience-dependent synaptic plasticity; (v) relieves the loss of dendritic spine connectivity in pyramidal hippocampal CA1 neurons; (vi) rescues the Alzheimer's disease-related electrophysiological deficits in hippocampal long-term potentiation at the CA3-CA1 synapses; and (vii) mitigates the neuroinflammatory response (reactive gliosis). These findings indicate that the 20–22 kDa NH_2-terminal tau fragment is crucial target for Alzheimer's disease therapy and prospect immunotherapy with 12A12 monoclonal antibody as safe (normal tau-preserving), beneficial approach in contrasting the early Amyloidβ-dependent and independent neuropathological and cognitive alterations in affected subjects.

1 European Brain Research Institute (EBRI), 00161 Rome, Italy
2 Humanitas University Laboratory of Pharmacology and Brain Pathology, Neuro Center, 20089 Milan, Italy
3 Institute of Neuroscience, 20129 Milan, Italy
4 IRCSS Santa Lucia Foundation, 00143 Rome, Italy
5 Department of Medicine, University Campus Bio-Medico, 00128 Rome, Italy
6 Department of Science and Technology for Humans and Environment, University Campus Bio-medico, 00128 Rome, Italy
7 Fondazione Policlinico Universitario A. Gemelli IRCCS, 00168 Rome, Italy
8 Institute for Complex Systems (ISC), CNR, 00185 Rome, Italy
9 Institute of Human Physiology, Università Cattolica del Sacro Cuore, 00168 Rome, Italy
10 Institute of Translational Pharmacology (IFT)–National Research Council (CNR), 00133 Rome, Italy

Correspondence to: Giuseppina Amadoro, PhD Institute of Translational Pharmacology (IFT)–National
Research Council (CNR), Via Fosso del Cavaliere 100, 00133 Rome, Italy
E-mail: g.amadoro@inmm.cnr.it

Graphical Abstract

12A12mAb | N-truncated tau fragment(s)
Glutamate Receptors | Synaptic vesicles | Neurotransmitter
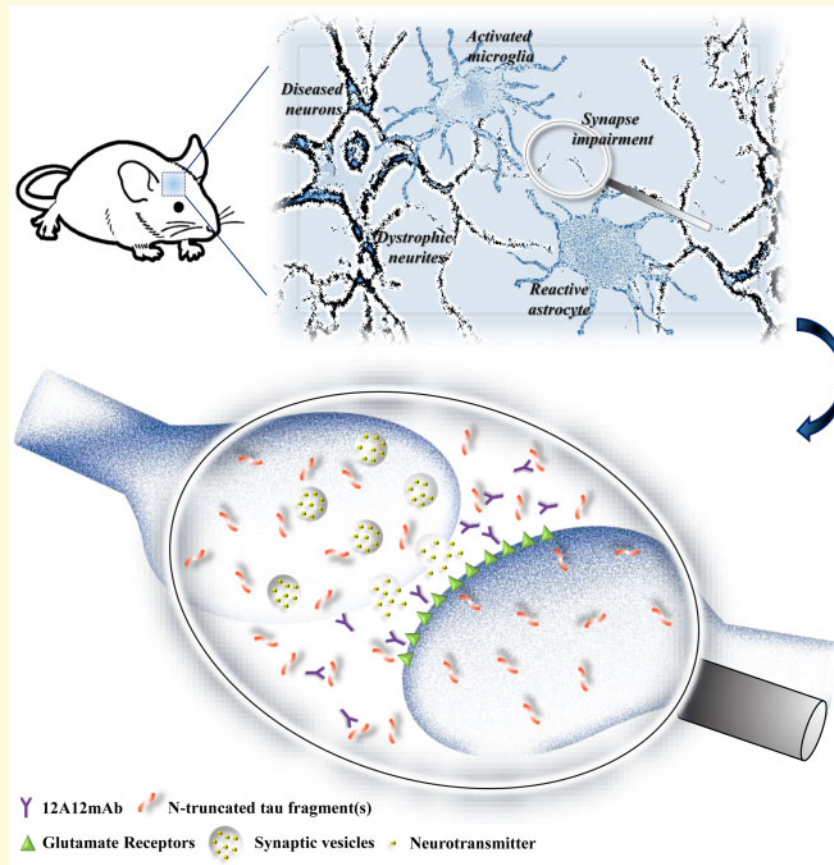
Introduction

Recent *in vitro* and *in vivo* data have highlighted a crucial role of proteolytic fragments of tau protein, in particular those derived from truncation at its N-terminal domain, in the initiation/progression of Alzheimer's disease and other related tauopathies, thus paving the way for their potential use as therapeutic targets or as biomarkers for diagnosing dementia and/or monitoring disease progression (Avila *et al.*, 2016a; Quinn *et al.*, 2018; Sebastián-Serrano *et al.*, 2018). On the one hand, tau cleavage may generate amyloidogenic fragments that initiate its aggregation which, in turn, can cause toxicity (Wang *et al.*, 2010). On the other hand, tau proteolysis

may result in production of noxious, both intracellular and extracellular, truncated species which drive neurodegeneration independently of aggregative pathway(s) and in a fragment-dependent manner as a result of their deleterious action on pre- and/or post-synaptic functions and/or their secretion and transcellular propagation (Quinn *et al.*, 2018).

Extracellular cleaved tau is toxic to neurons by increasing the $A\beta$ production (Bright *et al.*, 2015) and/or by impairing synaptic plasticity (Fà *et al.*, 2016; Florenzano *et al.*, 2017; Borreca *et al.*, 2018; Hu *et al.*, 2018). Hyperphosphorylation and caspase-3 cleavage of tau (Asp421), which promote aggregation, also favour the protein secretion *in vitro* (Plouffe *et al.*, 2012). The

amino-terminal projection domain of human tau—which interacts with the plasma membrane (Brandt *et al.*, 1995) and undergoes early conformational changes in human tauopathies including Alzheimer's disease (Combs *et al.*, 2016, 2017)—is endowed with deleterious action(s), mainly at nerve endings (King *et al.*, 2006; Ittner *et al.*, 2010; Amadoro *et al.*, 2012; Zhou *et al.*, 2017). The N-terminus extremity of tau, despite the lack of the microtubule binding domains which abnormally aggregate to form paired helical filaments, is prone to come into higher order of oligomerization (Feinstein *et al.*, 2016) and is specifically released into the extracellular space in an *in situ* tauopathy model (Kim *et al.*, 2010), suggesting a potential role for molecular 'templating' in the propagation of neurofibrillary lesions. Soluble C-terminally truncated tau species are also preferentially secreted from synaptosomes of Alzheimer's disease brains (Sokolow *et al.*, 2015) and in conditioned media from patient-derived induced pluripotent stem cell cortical neurons (Bright *et al.*, 2015; Kanmert *et al.*, 2015; Sato *et al.*, 2018). Interestingly, although full-length tau is found in CSF from healthy humans, a heterogeneous population of fragments—including the NH_2-terminal and/or prolin-rich domain—is mainly discernible in Alzheimer's disease patients (Johnson *et al.*, 1997; Portelius *et al.*, 2008; Meredith *et al.*, 2013; Amadoro *et al.*, 2014; Chen *et al.*, 2019; Cicognola *et al.*, 2019). Exosomes-associated NH_2-derived tau fragments are also detected in CSF from Alzheimer's disease patients (Saman *et al.*, 2012) and a different CSF pattern of NH_2-derived tau fragments may reflect disease-specific neurodegenerative processes (Borroni *et al.*, 2009). Consistently, passive immunotherapy with antibody targeting the N-terminal projection domain of full-length human tau has shown to be beneficial in Alzheimer's disease transgenic (Tg) mice by improving the cognitive deficits (Yanamandra *et al.*, 2013; Dai *et al.*, 2015; Subramanian *et al.*, 2017) and blocking the seeding/spreading of tau pathology (Dai *et al.*, 2018). Both intracerebroventricular infusion and peripheral administration of anti-tau antibodies specific for N-terminal 25–30 epitopes are curative in P301S mice model of tauopathy, by preventing the brain atrophy and ameliorating the motor/sensorimotor functions (Yanamandra *et al.*, 2013, 2015). Immunization with antibody directed against the N-terminal end of full-length tau protein (Dai *et al.*, 2017) significantly reduced the level of amyloid precursor protein (APP), amyloid-β peptides (Aβ40) and Aβ42 in CA1 region of Alzheimer's disease animal models, indicating that tau-based immunotherapy is actually able to restore the Aβ-dependent and/or independent synaptic dysfunction(s) which occur at early stages in Alzheimer's disease and other related dementias (Pedersen and Sigurdsson, 2015; Panza *et al.*, 2016). However, albeit tau appears to be the main factor underlying the development and progression of Alzheimer's disease (Kametani and Hasegawa *et al.*, 2018; Castellani and Perry, 2019), its expression at physiological level is required for neuronal functions underlying learning and memory (Pooler *et al.*, 2014; Regan *et al.*, 2017) and its down-regulation, even if moderate, has been proved to have deleterious effects, both *in vitro* and *in vivo* (Biundo *et al.*, 2018; Velazquez *et al.*, 2018). As a consequence, the development of selectively targeting antibodies against pathogenic tau may have a unique therapeutic advantage by leading to valuable, beneficial effects—in the absence of unwanted consequences due to the 'loss of function' of normal protein—in the cure of human, chronic neurodegenerative tauopathies which are sometimes expected to require long-term treatments with multiple and high-dose administrations of drugs (Kontsekova *et al.*, 2014; Elmaleh *et al.*, 2019).

In this framework, we developed a neo-epitope antibody directed against the N-terminal sequence of human tau protein DRKD($_{25}$)-QGGYTMHQDQE (Amadoro *et al.*, 2012) which encompasses a conserved cleavage-site sequence previously identified in cellular and animal Alzheimer's disease models (Corsetti *et al.*, 2008) and in human Alzheimer's disease brains (Rohn *et al.*, 2002). 12A12 (formerly Caspase-Cleaved protein-$NH_2$4268 tau antiserum, Amadoro *et al.*, 2012) is a monoclonal antibody (mAb) which recognizes the newly created Δ-$_{25}NH_2$tau(Q26–36aa)-terminus of degradation product(s) of tau without cross-reacting with the same amino acidic stretch from full-length isoforms of intact, normal protein (Amadoro *et al.*, 2019; Supplementary Fig. 1). The pathologically relevant NH_2tau 26–44aa stretch, which is the minimal active moiety of a neurotoxic 20–22 kDa NH_2-derived tau peptide (aka NH_2htau), accumulates at Alzheimer's disease pre-synaptic terminals (Amadoro *et al.*, 2006, 2010, 2012; Corsetti *et al.*, 2015) and is present in CSFs from living patients suffering from Alzheimer's disease and other non-Alzheimer's disease neurodegenerative diseases (Amadoro *et al.*, 2014). Interestingly, this peptide is able to negatively impact on normal synaptic function(s) *in vitro* (Florenzano *et al.*, 2017) and *in vivo* (Borreca *et al.*, 2018), suggesting that its antibody-mediated selective clearance can have important clinical and translational implications in contrasting the earliest neuropathological and cognitive alterations associated with human tauopathies, including Alzheimer's disease (Bright *et al.*, 2015; Sokolow *et al.*, 2015; Barthélemy *et al.*, 2016a, b; Sato *et al.*, 2018; Cicognola *et al.*, 2019).

In this study, we explored the potentially beneficial immunotherapeutic power of the 12A12mAb by means of its intravenous (i.v.) administration in two lines of Alzheimer's disease Tg animals with different genetic backgrounds, such as Tg2576 carrying the APP KM670/671NL Swedish mutation and 3xTg mice expressing the amyloid precursor protein KM670/671NL Swedish mutation, tauP301L, PS1M146V human transgenes. Relevantly, unlike other murine or humanized NH_2tau-directed immunotherapeutic antibodies (Yanamandra *et al.*, 2013, 2015; Dai *et al.*, 2015, 2017, 2018;

Subramanian *et al.*, 2017; Qureshi *et al.*, 2018), 12A12mAb reacts with the 20–22 kDa neurotoxic NH$_2$-truncated tau but not with the physiological full-length form of protein (Corsetti *et al.*, 2008; Amadoro *et al.*, 2012) advocating its *in vivo* use as safe, more harmless and personalized medicine treatment to slow progressing human tauopathies.

Materials and methods

Animals

All experiments involving animals were performed in accordance with the ARRIVE guidelines and were carried out in accordance with the ethical guidelines of the European Council Directive (2010/63/EU); experimental approval was obtained from the Italian Ministry of Health (protocol # 524/2017 PR; 554/2016-PR). Only male subjects were used to avoid changes in female hormone state that can affect cognitive data. All efforts were made to minimize the number of animals used and suffering.

One, 3- and 6-month-old Tg2576 and 3xTg mice (Tg-Alzheimer's disease) ($n = 8$–10 per group/treatment) and age-matched wild-type (WT) controls ($n = 8$–10 per group/treatment) were used in this study.

Heterozygous Tg2576 mice overexpressing the APP695 with the Swedish mutation (APP KM670/671NL, TgHuAPP695swe: Tg2576) in a hybrid genetic background (87% C57BL/6 × 12.5% SJL) (Hsiao *et al.*, 1996) were subsequently backcrossed to C57BL/6xSJL F1 females and the offspring were genotyped to confirm the presence of human mutant APP DNA sequence by PCR. WT littermates were used as controls.

The homozygous 3xTg mice harbouring human amyloid precursor protein KM670/671NL Swedish mutation and tauP301L transgenes with knock-in PS1M146V under the control of the mouse Thy1.2 promoter were obtained from The Jackson Laboratory (https://www.jax.org/strain/004807). Mice were bred on the mixed C7BL/6; 129X1/SvJ; 129S1/Sv genetic background and genotypes were confirmed by PCR on tail biopsies (Oddo *et al.*, 2003). B6129SF2/J strain mice, used as WT controls in the present study, were the offspring of a cross between C57BL/6J females (B6) and 129S1/SvImJ males (129S); they are commonly used as controls for genetically engineered strains generated with 129-derived embryonic stem cells and maintained on a mixed B6; 129 background (https://www.jax.org/strain/101045). The housing conditions (four or five animals per cage) in pathogen-free facilities were controlled (temperature 22°C, 12 h light/12 h dark cycles, humidity 50–60%) with *ad libitum* access to chow and water.

Immunization scheme

The N-terminal tau 12A12 antibody (26–36aa) was produced and characterized by monoclonal antibodies core

facility at EMBL—Monterotondo, Rome, Italy (Dott. Alan Sawyer), as previously described in Florenzano *et al.* (2017). 12A12mAb was purified from hybridoma supernatants according to standard procedures and its purity was determined using sodium dodecyl sulphate-polyacrylamide gel electrophoresis and Coomassie staining. In detail, the hybridoma supernatant was precipitated by ammonium sulphate (336 g/l). After precipitation, the solution was centrifuged at 10 000 g for 1 h and the pellet was dissolved in phosphate-buffered-saline (PBS) and dialyzed against the same buffer. The solution was centrifuged at 10 000 g for 30 min and loaded on a HiTrap Protein G HP (GE Healthcare) equilibrated with PBS. The column was washed with PBS (5 column volumes). 121A12mAb was eluted with 0.1 M Glycine-HCl, pH 2.7. The fractions containing the antibody were neutralized by 1 M Tris-HCl, pH 9.0, collected and immediately dialyzed against PBS. 121A12mAb concentration was determined by measuring the absorbance at 280 nm. The average yield was 8 mg/l of cell supernatant. 12A12mAb was ≥95% pure and contained ≤1 U/mg of endotoxin (LAL Chromogenic Endotoxin quantitation kit; Thermo Scientific).

To minimize experimental variability, all mice were initially grouped according to their body weight and age and mice from the same litter were finally assigned to different groups. For each animal strain (Tg2576, 3xTg), the grouped mice were randomized into: (i) WT mice treated with saline vehicle; (ii) WT mice treated with 12A12mAb (30 μg/dose); (iii) age-matched Tg-Alzheimer's disease mice treated with saline or non-specific mouse Immunoglobulin (IgG) (normal mouse IgG, Santa Cruz sc-2025, 30 μg/dose); and (iv) age-matched Tg-Alzheimer's disease mice treated with 12A12mAb (30 μg/dose) or non-specific mouse IgG (normal mouse IgG, Santa Cruz sc-2025, 30 μg/dose). Animals were infused over 14 days with two weekly injections administered on two alternate days to the lateral vein of the tail. The dose and route of immunization were based on prior studies using Alzheimer's disease Tg mice (Castillo-Carranza *et al.*, 2015). In details, mice were placed in a restrainer (Braintree Scientific), and an inch of the tail was shaved and placed in warm water to dilate veins. After injection via the lateral tail vein, mice were returned to home cages and kept under general observation. Abnormalities in overall health, home-cage nesting, sleeping, feeding, grooming, body weight and condition of the fur of animals were noted.

Tissue collection, harvesting and preparation

For biochemical analysis, tissue sampling was carried out according to Mably *et al.* (2015) with some modifications. Briefly, 2 days following the last injection, animals were sacrificed by cervical dislocation to avoid anaesthesia-mediated tau phosphorylation (Planel *et al.*, 2007)

and intra-cardially perfused with ice-cold PBS using a 30-ml syringe to remove blood contamination. Brains were collected, the meninges were carefully removed and dissected hippocampi were immediately frozen on dry-ice and, then, stored at $-80°C$ until use.

Hippocampal total protein lysates were carried out according to Castillo-Carranza *et al.* (2015) with some modifications. In details, frozen mice hippocampi were diced and homogenized in PBS with a protease inhibitor mixture (Roche) and 0.02% NaN_3 using a 1:3 (w/v) dilution. Samples were then centrifuged at 10 000 rpm for 10 min at $4°C$ and the supernatants were collected.

Tris-buffered saline (TBS) extracts were carried out according to Mably *et al.* (2015) with some modifications. Frozen mice hippocampi were homogenized in five volumes (wt/vol) TBS, pH 7.4, plus proteases inhibitor cocktail (Sigma-Aldrich P8340) and phosphatase inhibitor cocktail (Sigma-Aldrich, Oakville, Ontario, Canada P5726/P2850) with 30 strokes of a glass Dounce tissue. The homogenate was centrifuged at 90 000 g at $4°C$ for 1 h. The supernatant (TBS extract) was removed and stored at $-20°C$.

Synaptosomes preparations were carried out as previously reported (Corsetti *et al.*, 2015; Florenzano *et al.*, 2017).

Cloning, bacterial expression and purification of the 20–22 kDa $NH_2$26-230 tau fragment (aka NH_2htau)

cDNA fragment coding for the amino acids 26–230 of the isoform 4 of human tau protein (htau40) was cloned into the vector pET-11a (Novagen) suitable for the expression of recombinant proteins in BL21DE3 Gold *Escherichia coli* cells. After induction with IPTG, recombinant protein in lysates from bacterial pellet was purified to homogeneity by a two-step procedure: step 1 was a HiCood Q Sepharose 16/10; step 2 was Hitrap Phenyl 5 ml. Degree of protein purification was evaluated by Coomassie Brilliant Blue G-250 and checked by sodium dodecyl sulfate-polyacrylamide gel electrophoresis under reducing conditions by western blotting with commercial human-specific NH_2-tau antibody (DC39N1 45–73aa) and with 12A12mAb (26–36aa). The molecular identity of purified peptide fraction was finally checked by electrospray ionization mass spectrometry.

Detection of the NH_2htau fragment by 12A12mAb-based enzyme-linked immunosorbent assay

High-binding black 96 well plates (Costar 3925, Corning, NY) were coated overnight at $4°C$ following the addition of 5 µg/ml 12A12mAb capture antibody diluted in coating buffer (50 mM $NaHCO_3$, pH9.6). Plates were washed with PBST (PBS containing 0.05% Tween-20) and incubated with 5% non-fat dry milk (w/v) in PBST at room temperature (RT) for 2–4 h while shaking to block non-specific binding sites. Plates were washed with PBST and incubated (50 µl/well) overnight at $4°C$ while shaking with recombinant $NH_2$26-230 tau fragment standard curves prepared in assay buffer concentration of 5% milk (w/v) and 0.05% Tween-20 (v/v) in PBS, pH 8. Plates were washed with PBST and incubated (50 µl/well) overnight at $4°C$ with rabbit H150 antibody (1–150aa; Santa-Cruz sc-5587) diluted to the final concentration of 2.5 µg/ml in assay buffer concentration of 5% milk and 0.05% Tween-20 (v/v) in PBS. Plates were then washed with PBST and added with 50 µl/well of rabbit horseradish peroxidase-conjugated secondary antibody for 1 h at RT. Plates were washed with PBST and developed at RT using TMB substrate (T0440; Sigma-Aldrich, Oakville, Ontario, Canada). Luminescence counts were measured using Packard TopCount (PerkinElmer, MA). Log-transformed luminescence counts from individual samples were interpolated to concentration using a second-order polynomial fit to the respective standards (GraphPad Prism 5.00, GraphPad Software, San Diego).

Detection of i.v.-delivered 12A12mAb in TBS brain extracts

The concentration of i.v. delivered anti-tau 12A12mAb was measured in TBS brain extracts according to Mably *et al.* (2015) with some modifications. A solid-phase enzyme-linked immunosorbent assay (ELISA) was performed on the plate-immobilized synthetic $NH_2$26-44aa which was used as catching antigenic peptide, being the minimal Alzheimer's disease-relevant (Borreca *et al.*, 2018), active moiety of the parental longer $NH_2$26-230 (Amadoro *et al.*, 2004, 2006). Clear 96 well high-binding plates (Costar 3925, Corning, NY) were coated (50 µl/well) of 5 µg/ml synthetic $NH_2$26-44aa in coating buffer (0.05 M Carbonate-Bicarbonate, pH9.6) overnight at $4°C$. Wells were washed twice with PBST and loaded (50 µl/well) with (i) the standard curve prepared by making serial dilutions of 12A12mAb (250–0.12 ng/ml), (ii) the TBS extracts diluted 1/50, 1/10, 1/2, 1/1.3 or (iii) blanks diluted in assay buffer concentration of 5% milk and 0.05% Tween-20 (v/v) in PBS overnight at $4°C$. Plates were then washed with PBST and added with 50 µl/well of rabbit horseradish peroxidase-conjugated secondary antibody for 1 h at RT. Plates were washed with PBST and developed at RT using TMB substrate (T0440; Sigma-Aldrich, Oakville, Ontario, Canada). Luminescence counts were measured using Packard TopCount (PerkinElmer, MA). Log-transformed luminescence counts from individual samples were interpolated to concentration using a second-order polynomial fit to the respective standards (GraphPad Prism 7.00, GraphPad Software, San Diego).

Cell culture, treatment and protein lysates preparation

SH-SY5Y human neuroblastoma cells were cultured and terminally differentiated into post-mitotic neurons according to Corsetti *et al.* (2008). Culture treatment and protein lysates preparation were carried out by using standard procedures, according to Borreca *et al.* (2018).

Western blot analysis and densitometry

Western blot analysis and densitometry were carried out by using standard procedures, according to Borreca *et al.* (2018).

The following antibodies were used: anti-Aβ/APP 6E10 (4–9aa) mouse MAB1560 Chemicon; anti-Alzheimer precursor protein 22C11 (66–81aa of N-terminus) mouse APP-MAB348 Chemicon Temecula-CA; anti-pan tau protein H150 (1–150aa of N-terminus) rabbit sc-5587 Santa Cruz Biotechnology; anti-pan tau protein DC25(microtubule binding repeat) mouse T8201 Sigma-Aldrich; tau 21 (21–36aa of N-terminus) rabbit AHB0371 Biosource International (USA); anti-N-tau (45–73aa) DC39N1 mouse T8451 Sigma-Aldrich; neuronal marker β III tubulin antibody mouse ab78078 (clone 2G10) Abcam; GAPDH antibody (6C5) mouse sc-32233 Santa Cruz Biotechnology; activity-regulated cytoskeleton-associated protein (C-7) mouse sc-17839 Santa Cruz Biotechnology; glial fibrillary acidic protein antibody rabbit Z0334 Dako; Iba1 antibody rabbit Wako 016-20001 (for WB).

Novel object recognition test

Two days after the last i.v. injection, mice run the novel object recognition (NOR) task (Antunes and Biala, 2012) to check the hippocampal-dependent episodic memory (Bevins and Besheer, 2006; Akkerman *et al.*, 2012a, b). The entire task was performed in three consecutive sessions during the same day (1-day version), according to previously published protocol (Borreca *et al.*, 2018).

Object place recognition test

The object place recognition paradigm involves the activity of the hippocampus and is used to test the short-term memory (Vogel-Ciernia and Wood, 2014). The animals, which underwent the NOR paradigm with a training and test session, were tested in the object place recognition paradigm 24 h later, with a separated training and test session. The objects used for the object place recognition were different from those used previously for the NOR test in order to avoid possible confounding effects. The entire behavioural task including three phases (a common habituation phase, a training phase and a test phase) was performed by using standard protocol (Lesburguères *et al.*, 2017).

Spontaneous alternation (Y-maze) test

Evaluation of short-term working memory was carried out by using the spontaneous alternation version of the Y-maze, which involves different brain structures ranging from the hippocampus to the prefrontal cortex. Y-maze testing also indicates overall activity, or hyperactivity, based on the number of arm entries Spontaneous alternation, expressed as a percentage, was calculated by dividing the number of entries into all three arms on consecutive choices (correct choices) by number of arm entries subtracted by two, then multiplying the quotient by 100 (Hiramatsu *et al.*, 1997; Wall and Messier, 2002). A high spontaneous alternation rate is indicative of sustained working memory because the animals must remember which arm was entered last to know not to re-enter it.

Energy metabolism

Energy expenditure (EE) and oxygen consumption (VO_2) were measured by an indirect calorimeter system (TSE PhenoMaster/LabMaster System®) in vehicle- or 12A12mAb-treated mice by a constant air flow of 0.35 l/min. Mice were adapted for 6 h to the metabolic chamber before the start of recording, and VO_2 was measured every 30 min in each mouse, starting at 7:00 PM and ending automatically after 4 days (96 h later). RT was kept constant (22 ± 1°C). The EE for each sample point was evaluated across the 48 h of total recording. Locomotor activity was assessed during the indirect calorimetric assay by the number of infra-red beams broken. Each cage of the calorimeter system is equipped with the InfraMot® device that uses 'passive infrared sensors' to detect and record the motor activity of the mouse by the body-heat image and its spatial displacement across time. Any type of body movement was detected and recorded as activity counts. EE was also analysed by considering animals' steady conditions or lack of motor activity (resting EE, REE; only values between 0 and 2 activity counts were included).

Golgi-Cox staining and dendritic spine analysis

Two days after the last i.v. injection, mice were sacrificed with a lethal dose of anaesthetic (Zoletil/Rompun 800 and 100 mg/kg, respectively) and perfused transcardially with 0.9% saline solution. Brains were dissected and immediately immersed in a Golgi-Cox solution (1% $K_2Cr_2O_7$, 1% $HgCl_2$ and 0.8% K_2CrO_4) at RT for 6 days, according to a previously described protocol (Gibb and Kolb, 1998; Rosoklija *et al.*, 2014). On the

seventh day, brains were transferred in a 30% sucrose solution for cryoprotection and then sectioned with a vibratome. Staining and dendritic spine analysis was carried out according to standard criteria (Horner and Arbuthnott, 1991; Leuner et al., 2003) and by using previously published method (Borreca et al., 2018). Statistical comparisons were made on single mouse values obtained by averaging the number of spines counted on neurons of the same mouse.

Electrophysiological recordings

Two days after the last i.v. injection of 12A12mAb, mice were anaesthetized by halothane or isofluorane inhalation and decapitated. The brain was rapidly removed and put in ice-cold cutting solution (in mM: 124 NaCl, 3.2 KCl, 1 NaH_2PO_4, 26 $NaHCO_3$, 2 $MgCl_2$, 1 $CaCl_2$, 10 glucose, 2 sodium pyruvate and 0.6 ascorbic acid, bubbled with 95% O_2–5% CO_2, pH 7.4). Electrophysiological recordings were performed on hippocampal coronal slices (400 μm thick) by using standard procedures (Podda et al., 2016; Nobili et al., 2017).

Statistical analysis

In box-and-whisker plots, the centre lines denoted median values, edges were upper and lower quartiles, whiskers showed minimum and maximum values and points were individual experiments. Other data were expressed as mean ± SEM. All data were representative of at least three separate experiments (n = independent experiments). Statistically significant differences were calculated by one-way or two-way analysis of variance (ANOVA) followed by Bonferroni's, Fisher's and Dunnett's post hoc tests for multiple comparisons among more than two groups. $P < 0.05$ was accepted as statistically significant ($*P < 0.05$; $**P < 0.01$; $***P < 0.0005$; $****P < 0.0001$). All statistical analyses were performed using GraphPad Prism 7 software.

Data availability

The datasets used and/or analysed during the current study and detailed protocols/experimental procedures are available from the corresponding author on reasonable request. Western blotting fill-size images can be found in Supplementary Materials.

Results

Intravenously injected anti-NH$_2$htau 12A12mAb is biologically active in the animals' hippocampus

Tg2576 and 3xTg mice—two well-established animal Alzheimer's disease models (Hsiao et al., 1996;

Oddo et al., 2003) which express the human APP695 with Swedish mutations (K670N-M671L), alone or in combination with MAPT P301L and PSEN1 M146V, respectively—were analysed because these Tg animals are recognized to display progressive tau-dependent, hippocampus-based synaptic and cognitive impairments (Oddo et al., 2006; Castillo-Carranza et al., 2015; Amar et al., 2017). The hippocampal parenchyma was examined in the present study, since this vulnerable cerebral area: (i) selectively and disproportionally degenerates at early stages of mild cognitive impairment prior to the clinical diagnosis of full-blown dementia (Honer et al., 1992; West et al., 1994; Gomez-Isla et al., 1996; Kordower et al., 2001; Scheff et al., 2006a, b); (ii) preferentially develops tau neuropathology into synaptic compartments, whose initial deterioration is considered the best correlate of cognitive decline in Alzheimer's disease symptomatology by critically subserving the transition from normal aging to mild cognitive impairment (Braak and Braak, 1991, Arriagada et al., 1992; Guillozet et al., 2003; Markesbery et al., 2006, 2010; Pooler et al., 2014; Spires-Jones and Hyman, 2014).

Before addressing the possible benefits offered by systemic delivery of the cleavage-specific 12A12mAb (Δ-$_{25}$NH$_2$tau(Q26–36aa)-terminus), we determined an appropriate lifetime at which Tg-Alzheimer's disease mice could be employed for antibody immunization experiments. In light of these considerations, the in vivo level of the pathogenic 20–22 kDa NH$_2$htau was measured by western blotting sodium dodecyl sulphate-polyacrylamide gel electrophoresis analyses carried out on synaptosomal preparations from hippocampi of WT and Alzheimer's disease Tg animals of both genetic backgrounds at three ages (1, 3, 6-month-old Tg2576 and 3xTg). As shown in Fig. 1A and B, the signal intensity of 12A12mAb-positive NH$_2$htau immunoreactivity band was virtually undetectable in 6-month-old cognitively intact controls but appeared to be up-regulated in diseased animals (one-way ANOVA followed by Dunnett's post hoc test for multiple comparisons Tg2576 $F(3,12) = 13.34$, $P = 0.0004$; 3-month-old Tg2576 versus 6-month-old WT, $***P < 0.0005$; 6-month-old Tg2576 versus 6-month-old WT, $**P < 0.01$; 3xTg $F(3,12) = 76.79$, $P < 0.0001$; 1-month-old 3xTg versus 6-month-old WT, $*P < 0.05$; 3-month-old 3xTg versus 6-month-old WT, $****P < 0.0001$; 6-month-old 3xTg versus 6-month-old WT, $****P < 0.0001$). Consistent with previous investigations from rodent preparations (Rohn et al., 2002; Corsetti et al., 2008) and human nerve terminals specimens (Amadoro et al., 2010, 2012; Corsetti et al., 2015; Sokolow et al., 2015), the steady-state expression level of the neurotoxic 20–22 kDa NH$_2$htau truncated fragment significantly increased and time-dependently accumulated starting from 1 month of age into synaptic-enriched fractions of cognitively impaired older animals from both Alzheimer's disease Tg mouse models. The specific ability of 12A12mAb in binding the 20–22 kDa NH$_2$htau fragment in vitro, both in recombinant and native forms, was
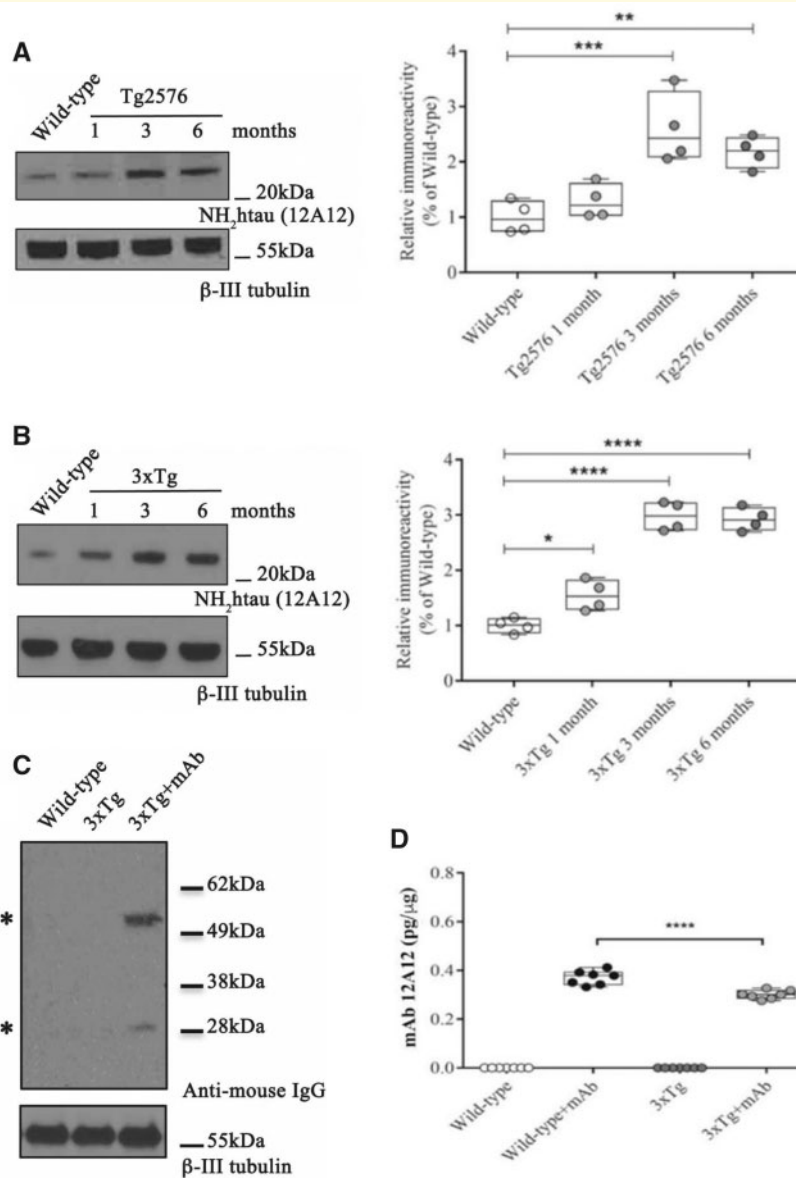
Figure 1 The i.v.-injected 12A12mAb anti-tau antibody is biologically active into the animals' hippocampus. (**A**, **B**) Western blot analysis carried out on hippocampi from Tg2576 and 3xTg Alzheimer's disease mice at different ages (1, 3 and 6 months old) and from 6-month-old WT by probing with 12A12mAb (left). β-III tubulin was used as loading control. Arrows on the right side indicate the molecular weight (kDa) of bands calculated from migration of standard proteins. Full uncropped blots are available in Supplementary Fig. 5. Pooled data and relative densitometric quantifications are reported on the right. In this and all other figures, in box-and-whisker plots the centre lines denote median values, edges are upper and lower quartiles, whiskers show minimum and maximum values and points are individual experiments. Statistically significant differences (see details in the main text) were calculated by ANOVA followed by *post hoc* test for multiple comparisons among more than two groups. $P < 0.05$ was accepted as statistically significant (*$P < 0.05$; **$P < 0.01$; ***$P < 0.0005$; ****$P < 0.0001$). (**C**) Western blotting analysis was carried out by probing with anti-mouse IgG as primary antibody (Thermo-Fisher 10400C) on hippocampal protein extracts (40μg) from animals of the three experimental groups (WT, 'naïve' 3xTg, 3xTg + mAb) which underwent i.v. injection with saline or 12A12mAb (see details in Materials and methods section). β-III tubulin was used as loading control. Arrows on the right side indicate the molecular weight (kDa) of bands calculated from migration of standard proteins. Full uncropped blots are available in Supplementary Fig. 5. Notice that 3xTg animals, which are systemically i.v. injected for 14 days with 12A12mAb (see details in Materials and methods section), exhibit high levels of cerebral mouse IgG when compared to not-vaccinated controls confirming that a fraction of mAb injected into the tail vein is present in the hippocampal parenchyma. Asterisks point to the light and heavy antibody chains (25 and 50 kDa, respectively). (**D**) Brain levels of anti-tau antibody 12A12mAb were evaluated by ELISA in the TBS-soluble fraction of hippocampal homogenates from WT and 3xTg mice that i.v. received saline or 12A12mAb for 14 days (see details in the Materials and methods section). The ELISA used to measure the anti-tau antibody relies on the plate-immobilized recombinant NH$_2$26-44aa tau which, being the minimal Alzheimer's disease-relevant (Borreca *et al.*, 2018) active moiety of the parental longer NH$_2$26-230 (Amadoro *et al.*, 2004, 2006), was used as catching peptide. Notice that a significant portion of the 12A12mAb in 3xTg brains is bound to endogenous NH$_2$htau and does non-specifically interact with the large amount of intracellular tau released during homogenization. Statistically significant differences (see details in the main text) were calculated by ANOVA followed by *post hoc* test for multiple comparisons among more than two groups. $P < 0.05$ was accepted as statistically significant.

checked by western blotting and ELISA (Supplementary Fig. 1).

Having ascertained that the NH$_2$htau accumulated into hippocampal synapses under pathological conditions in association with progressive disruption of animals' memory/learning function(s), we investigated whether the 12A12mAb could be exploited to systemic tau-directed immunization regimen. In particular, we ascertained whether 12A12mAb was able to gain access to the cerebral parenchyma after its peripheral administration, an optimal prerequisite for local engagement of the pathogenic target and its successful neutralization/clearance *in vivo*. To this aim, 6-month-old mice from these two different strains (Tg-Alzheimer's disease) were infused over 14 days with two weekly injections of 12A12mAb (30 μg/dose) administered on two alternate days to the lateral vein of the tail. Both age-matched WTs and 'naïve' (i.e. not-immunized) Tg Alzheimer's disease counterparts, which were sham-infused under the same experimental conditions with vehicle (saline) only, were also included as negative controls. By probing with anti-mouse IgG used as primary antibody, western blotting analysis (Fig. 1C) carried out on hippocampal protein extracts from the three experimental groups (WT, 'naïve' Tg-Alzheimer's disease, Tg-Alzheimer's disease + mAb which, importantly, were sacrificed and thoroughly perfused with PBS in order to make sure that their brains were free of blood contaminations) showed that 12A12mAb-injected 3xTg animals exhibited high levels of cerebral mouse IgG when compared to not-vaccinated, saline-treated controls. This qualitative finding is in line with previous reports on the ability of other, intravenously administered anti-tau antibodies to cross the blood–brain barrier of diseased Tg mice (about 0.1% of delivered total amount), likely owing to its age-related impairment and increased permeability (Asuni *et al.*, 2007; Blair *et al.*, 2015; Mably *et al.*, 2015; Bennett *et al.*, 2018).

Next, to confirm that peripherally delivered 12A12mAb was actually able to bind the NH$_2$htau *in vivo*, we carried out ELISA quantitative test on TBS-soluble fractions isolated from hippocampi of WT, 'naïve'3xTg and 3xTg + mAb animals after 14 days i.v. injection. Healthy, WT mice infused with 12A12mAb under the same experimental conditions (WT + mAb) were also included to ascertain whether 12A12mAb could enter the brain from periphery despite the intact blood–brain barrier and/or the lack of tau pathology into the CNS. It's worth underlying that: (i) the ELISA test aimed at assessing the cerebral amount of injected 12A12mAb is based on the plate-immobilized synthetic NH$_2$26-44aa which, being the minimal Alzheimer's disease-relevant (Borreca *et al.*, 2018) active moiety of the parental longer NH$_2$26-230 (Amadoro *et al.*, 2004, 2006), was used as catching peptide; (ii) only the free (i.e. unoccupied) antibody can readily bind to its immobilized specific antigen and be measured, whereas the tau-bound antibody is not detectable. As shown in Fig. 1D, a sizeable proportion of the injected 12A12mAb was unbound and biologically active (antigen-binding competent) in 3xTg brains, being able to recognize the synthetic plate-immobilized recombinant tau peptide. Interestingly, the levels of i.v.-administered 12A12mAb were significantly lower in 3xTg + mAb experimental group than in WT + mAb counterpart (two-way ANOVA analysis followed by Bonferroni's *post hoc* test for multiple comparisons, genotype × treatment interaction $F(1,24) = 28.92$, $P < 0.0001$; WT + saline versus Tg-Alzheimer's disease + saline *n*.s., $P > 0.99$; ****$P < 0.0001$ for all other pair comparisons), indicating that a higher fraction of this antibody is actually bound *in vivo* to the endogenously generated NH$_2$htau antigen—and thus less available for capture in *in vitro* ELISA assay—into the hippocampi from diseased animals than in healthy controls. Similar results were also found in 6-month-old Tg2576 animals from the other genetic background which were analysed and treated under the same experimental conditions (data not shown).

Collectively, these findings demonstrated that: (i) the pathological tau truncated at its N-terminal domain early accumulates into hippocampal synapses from Tg-Alzheimer's disease, suggesting that it might contribute to the age-dependent disruption of animals' memory and learning functions; (ii) after its i.v. injection, 12A12mAb can be actively up-taken into the brain because an appreciable percentage of free and antigen-binding competent form of antibody is present into the hippocampus both from healthy controls and 3xTg immunized mice, regardless of the integrity of their blood–brain barrier and/or the presence of tau pathology; (iii) 12A12mAb does not aspecifically interact, neither in WT nor in 3xTg, with the large amount of intracellular full-length normal tau which is routinely released during procedure of samples homogenization, in line with our previous *in vivo* observations advocating its cleavage-specificity towards the NH$_2$htau truncated fragment (Amadoro *et al.*, 2012, Supplementary Fig. 1); (iv) 12A12mAb is not in limiting amount and, thus, endowed with potential therapeutic effect (*in vivo* target-engagement) because after immunization it is locally detectable in its active/antigen-competent state into mouse brains, with higher level in the WT controls than in diseased 3xTg ones.

12A12mAb passive immunization reduces both pathological tau and APP/Aβ metabolisms into synaptic compartments from treated Alzheimer's disease Tg mice at the prodromal stage of neuropathology

Co-occurrence between tau and Aβ pathology has been described to take place within neuronal processes and nerve ending compartments at early stages of Alzheimer's disease (Takahashi *et al.*, 2010; Amadoro *et al.*, 2012;

Spires-Jones and Hyman, 2014; Rajmohan and Reddy, 2017). In the preclinical models of Tg2576 and 3xTg, Aβ exerts its synaptotoxicity, at least in part, via tau, but both separate and synergistic neurodegenerative mechanisms have been also described in these two experimental paradigms (Nisbet et al., 2015; Li and Gotz, 2017; Polanco et al., 2018). Recent in vitro and in vivo evidence have demonstrated that Aβ and tau pathology—in addition to their direct and/or indirect interaction (Castillo-Carranza et al., 2015; Dai et al., 2017, 2018; Rajamohamedsait et al., 2017)—can damage the synaptic terminals in an APP-dependent manner suggesting that its increased expression level per se should be considered as an additional therapeutic target to preserve the integrity and function of crucial neuronal networks (Gulisano et al., 2018; Kametani and Hasegawa, 2018; Schreurs et al., 2018).

In view of these considerations, we investigated whether the antibody-mediated neutralization of pathogenic NH_2-truncated tau following i.v. 12A12mAb infusion could mitigate in vivo the occurrence of neurochemical derivatives from the abnormal APP and tau metabolisms which are largely recognized to compromise the Alzheimer's disease nerve terminals at prodromal disease stages (Braak and Del Tredici, 2015). To this aim, western blotting sodium dodecyl sulphate-polyacrylamide gel electrophoresis analyses (Fig. 2, Tg2576; Fig. 3, 3xTg) were carried out on hippocampal synaptosomal preparations from the three experimental groups (WT, 'naïve' Tg-Alzheimer's disease, Tg-Alzheimer's disease + mAb) of both genetic backgrounds (3-month-old Tg2576 and 3xTg) by probing with both 12A12mAb and specific commercial antibodies detecting the Alzheimer's disease-like, site-specific tau hyperphosphorylation at Ser202/Thr205 epitope (AT8) (Goedert et al., 1995) and the accumulation of soluble 6E10-positive APP/Aβ derivatives (Teich et al., 2015). As shown in Figs 2A and 3A—and in line with Fig. 1A and B—the intensity signal of the neurotoxic 20–22 kDa NH_2htau truncated fragment was markedly increased in saline-treated, 'naïve' Tg-Alzheimer's disease mice when compared to non-Tg WT controls (one-way ANOVA followed by Bonferroni's post hoc test for multiple comparisons $F(2,18) = 117.5$, $P < 0.0001$, Tg2576; $F(2,18) = 34.54$, $P < 0.0001$, 3xTg; ****$P < 0.0001$, Tg2576 versus WT; ****$P < 0.0001$, 3xTg versus WT). Importantly, the 12A12mAb treatment significantly reduced the synaptic load of 20–22 kDa NH_2htau form(s) in Tg-Alzheimer's disease animals from both strains indicating that this antibody, after i.v. delivery, successfully engaged/intercepted its target into hippocampus with consequent neutralization/clearance in vivo (one-way ANOVA followed by Bonferroni's post hoc test ****$P < 0.0001$, Tg2576 + mAb versus Tg2576; ****$P < 0.0001$, 3xTg + mAb versus 3xTg). Following 12A12mAb immunization, the AT8 immunoreactivity was strongly inhibited in Tg-Alzheimer's disease animals (one-way ANOVA followed by Bonferroni's post hoc test $F(2,18) = 23.72$,

$P < 0.0001$, Tg2576; $F(2,18) = 42.18$, $P < 0.0001$, 3xTg; Tg2576 versus WT, ****$P < 0.0001$; Tg2576 + mAb versus WT n.s., $P = 0.7913$; Tg2575 + mAb versus Tg2576, ***$P < 0.0005$; 3xTg versus WT, ****$P < 0.0001$; 3xTg + mAb versus WT n.s., $P = 0.3747$; 3xTg + mAb versus 3xTg, ****$P < 0.0001$), proving that the anti-truncated tau antibody was able to down-regulate the extent of tau neuropathology in vivo (Figs 2C and 3C). A drastic decline and/or disappearance of the expression levels of 6E10-positive APP/Aβ specie(s) (i.e. 4 kDa Aβ monomer, 14 kDa low-molecular weight Aβ oligomers or APP C-terminal fragment (βCTF)) was also clearly observed in Tg-Alzheimer's disease hippocampal synapses from treated experimental groups of both genetic backgrounds (Figs 2E and 3E and F) (one-way ANOVA followed by Bonferroni's post hoc test $F(2,18) = 104.7$, $P < 0.0001$, Tg2576; $F(2,18) = 115.8$, $P < 0.0001$, 3xTg; Tg2576 versus WT, ****$P < 0.0001$; Tg2576 + mAb versus WT n.s., $P = 0.0536$; Tg2576 + mAb versus Tg2576, ****$P < 0.0001$; ****$P < 0.0001$ for all pair comparisons from 3xTg). Importantly, the steady-state expression level of total tau detected by probing with H150 and DC25 (Figs 2B and 3B), two commercial anti-pan tau antibodies binding both murine and human tau isoforms (Zilka et al., 2006; Lee et al., 2010; Um et al., 2011; Schroeder et al., 2016), was unchanged in synapses from Alzheimer's disease Tg animals after 12A12mAb immunization regimen, with significantly higher level of total tau detected in 3xTg in comparison with WT controls due to the presence of both endogenous and human Tg proteins (one-way ANOVA followed by Bonferroni's post hoc test $F(2,18) = 0.3014$, $P = 0.7434$ Tg2576; $F(2,18) = 22.8$ $P < 0.0001$ 3xTg; n.s. $P > 0.999$ for all pair comparisons from Tg2576; 3xTg versus WT ***$P < 0.0005$; 3xTg + mAb versus WT ****$P < 0.0001$; 3xTg + mAb versus 3xTg n.s. $P = 0.1577$). These findings are consistent with tau cleavage-specificity of 12A12mAb which selectively binds in vivo the neurotoxic NH_2htau truncated specie(s) (Amadoro et al., 2012; Corsetti et al., 2015) without showing any cross-reaction towards the full-length form of protein (Supplementary Fig. 1). Finally, as visualized by 22C11 commercial antibody (Figs 2D and 3D), 12A12mAb immunization resulted to act upstream on Aβ production by normalizing the disease-associated up-regulation in the expression level of APP full-length holoprotein in both Tg Alzheimer's disease mice models (one-way ANOVA followed by Bonferroni's post hoc test $F(2,18) = 46.07$ $P < 0.0001$ Tg2576; $F(2,18) = 97.33$ $P < 0.0001$ 3xTg; Tg2576 versus WT ****$P < 0.0001$; Tg2576 + mAb versus Tg2576 ****$P < 0.0001$; Tg2576 + mAb versus WT n.s. $P = 0.999$; ****$P < 0.0001$ 3xTg for all comparisons). Interestingly, this evidence supports more recent studies which suggest a prominent, causal role of APP accumulation in triggering synaptotoxicity and tauopathy (Kametani and Hasegawa, 2018; Schreurs et al., 2018).

Collectively, these results demonstrate that: (i) when i.v. administrated to young (3 months old) Tg2576 and 3xTg
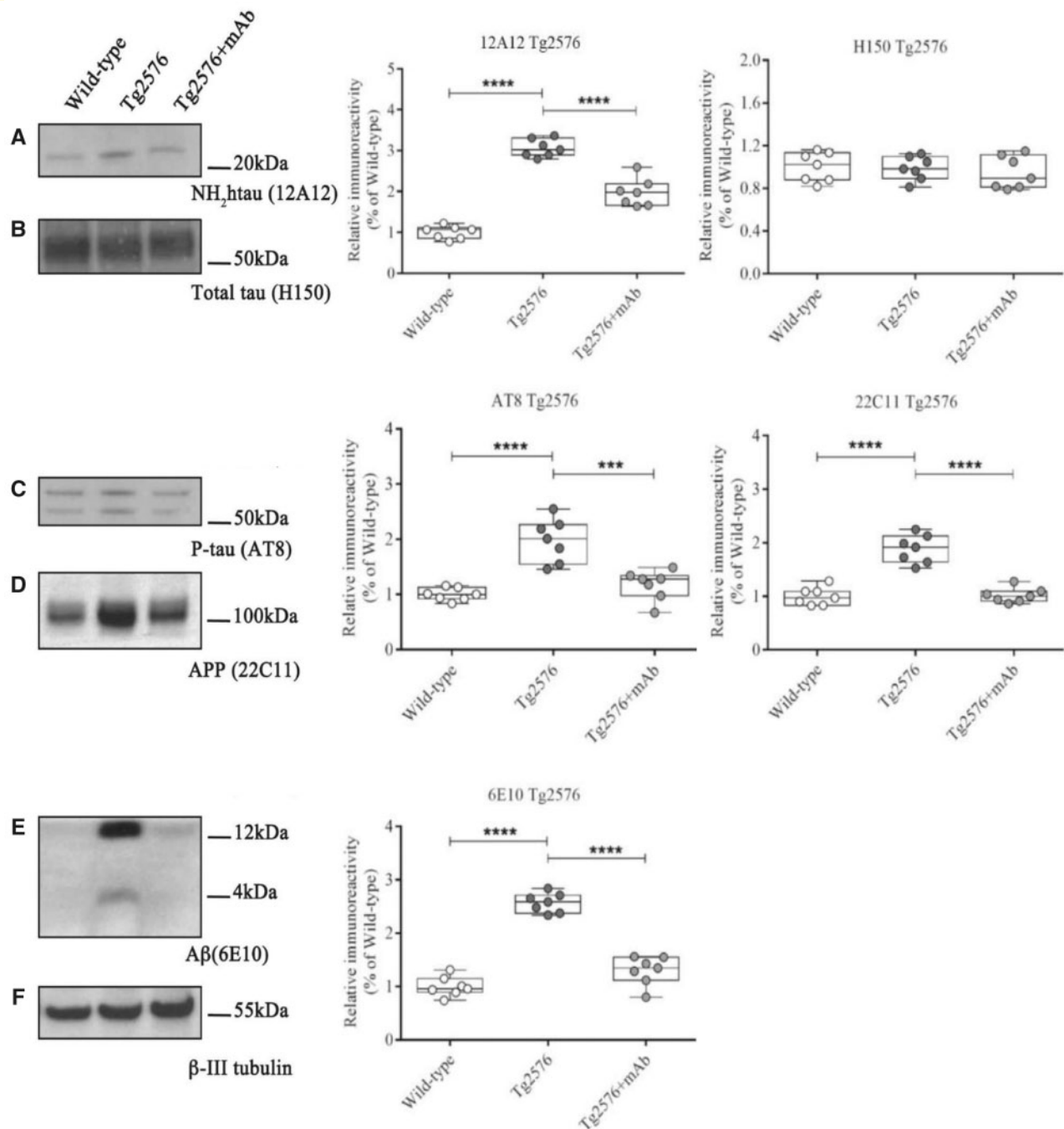
Figure 2 Reduction of the hippocampal NH₂htau in Tg-Alzheimer's disease (Tg2576) mice immunized with 12A12mAb ameliorates the disease-associated synaptic neuropathology. Representative blots ($n = 5$) of sodium dodecyl sulphate-polyacrylamide gel electrophoresis western blotting analysis (left) on isolated synaptosomal preparations from hippocampal region of animals from three experimental groups (WT, Tg-Alzheimer's disease and Tg-Alzheimer's disease + mAb) of Tg2576 strain to assess the content of the NH₂htau fragment (**A**), total tau full-length (**B**), AT8-phosphorylated tau (**C**), APP holoprotein (**D**) and Aβ monomeric and oligomeric species (**E**). Data were quantified for molecular weight size ranges for each antibody and normalized to β-III tubulin which was used as loading control (**F**) and relative densitometric quantifications are reported (right). Arrows on the right side indicate the molecular weight (kDa) of bands calculated from migration of standard proteins. Full uncropped blots are available in Supplementary Fig. 6. Notice that changes in levels of total tau are not statistically significant. Statistically significant differences (see details in the main text) were calculated by ANOVA followed by *post hoc* test for multiple comparisons among more than two groups. $P < 0.05$ was accepted as statistically significant (*$P < 0.05$; **$P < 0.01$; ***$P < 0.0005$; ****$P < 0.0001$).
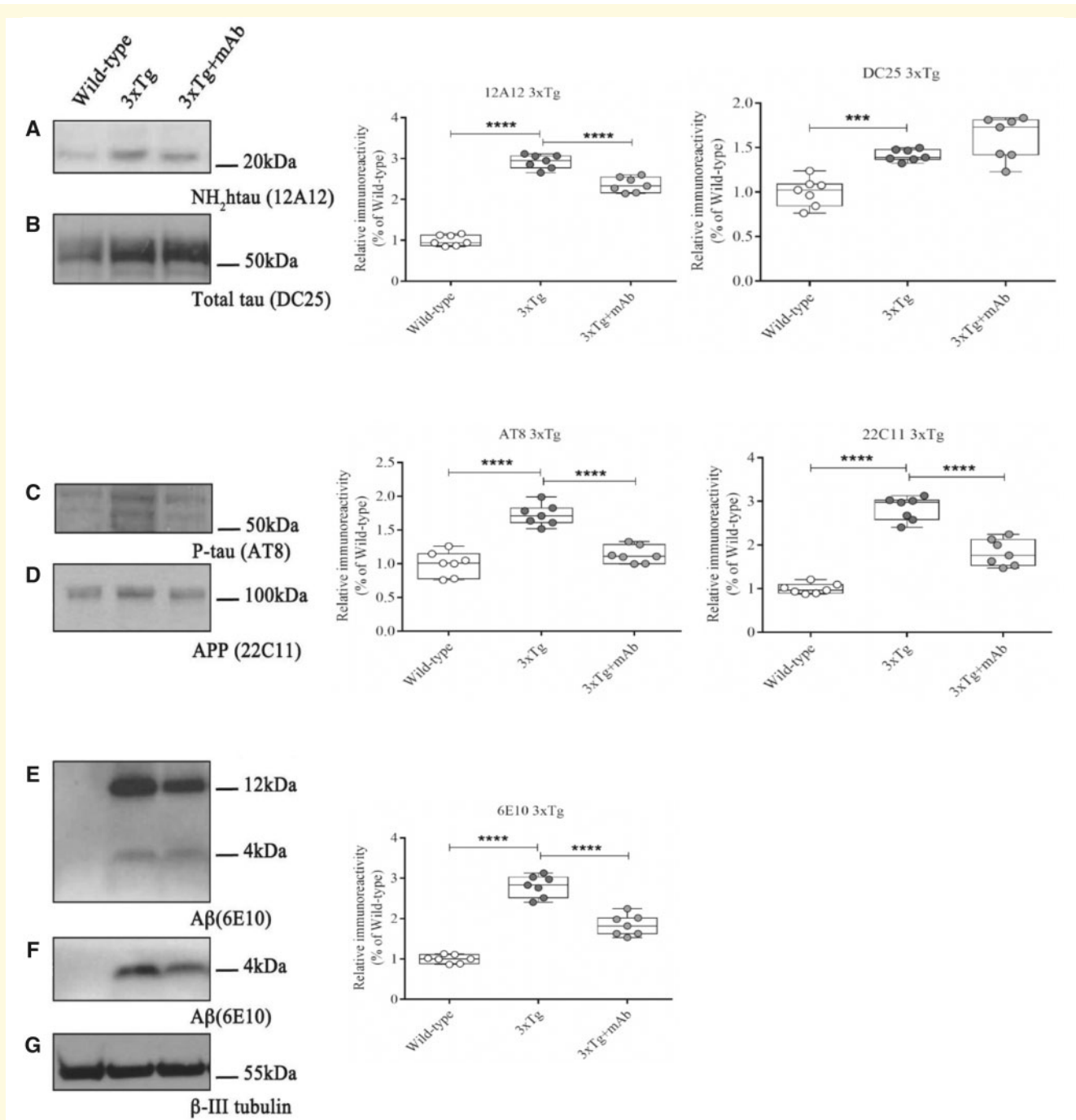
Figure 3 Reduction of the hippocampal NH₂htau in Tg-Alzheimer's disease mice (3xTg) immunized with 12A12mAb ameliorates the disease-associated synaptic neuropathology. (A–G) Representative blots (*n* = 5) of sodium dodecyl sulphate-polyacrylamide gel electrophoresis western blotting analysis (left) on isolated synaptosomal preparations from hippocampal region of animals from three experimental groups (WT, Tg-Alzheimer's disease and Tg-Alzheimer's disease + mAb) of 3xTg strain to assess the content of the NH₂htau fragment (**A**), total tau full-length (**B**), AT8-phosphorylated tau (**C**), APP holoprotein (**D**) and Aβ monomeric and oligomeric species (**E/F**). Data were quantified for molecular weight size ranges for each antibody and normalized to β-III tubulin which was used as loading control (**G**) and relative densitometric quantifications are reported (right). Arrows on the right side indicate the molecular weight (kDa) of bands calculated from migration of standard proteins. Full uncropped blots are available in Supplementary Fig. 7. Notice that changes in levels of total tau are not statistically significant. Statistically significant differences (see details in the main text) were calculated by ANOVA followed by *post hoc* test for multiple comparisons among more than two groups. *P* < 0.05 was accepted as statistically significant (*P < 0.05; **P < 0.01; ***P < 0.0005; ****P < 0.0001).

mice—two well-established Alzheimer's disease animal models showing tau-dependent neuropathology (Oddo et al., 2006; Castillo-Carranza et al., 2015; Amar et al., 2017)—the cleavage-specific 12A12mAb is able to reach an appreciable concentration into the hippocampal parenchyma ensuing an effective binding/degradation of the pathologic 20–22 kDa NH$_2$htau form(s); (ii) the *in vivo* antibody-mediated removal of the 20–22 kDa NH$_2$htau form(s) alleviates the detrimental alterations of both APP/Aβ and tau metabolisms (i.e. AT8 tau hyperphosphorylation, APP/Aβ species accumulation and processing) commonly occurring at the earliest stage of Alzheimer's disease progression into nerve endings; (ii) the 12A12mAb-mediated immunodepletion of the toxic 20–22 kDa NH$_2$htau form(s) takes place in the absence of any significant change in the stability/turnover of normal full-length tau protein which is known to be endowed with important physiological functions into synaptic compartments (Pooler et al., 2014; Regan et al., 2017) and whose reduction, even if partial, is extremely harmful in terminally differentiated post-mitotic neurons *in vivo* (Biundo et al., 2018; Velazquez et al., 2018).

Cognitive performance is significantly improved in symptomatic Alzheimer's disease Tg mice after i.v. 12A12mAb delivery

Having established that classical molecular determinants underlying the phenotypic Alzheimer's disease manifestations are strongly reduced at early/pre-symptomatic stages of neuropathology following peripheral administration of 12A12mAb, cognitive functioning of symptomatic Tg-Alzheimer's disease animals (6-month-old Tg2576 and 3xTg) was analysed under the same schedule of treatment by means of a comprehensive behavioural test battery (Fig. 4, Tg2576; Fig. 5, 3xTg).

The NOR task is a paradigm which is considered an appropriate readout for measures of learning/memory impairment in Tg and non-Tg animal models of tauopathies, including Alzheimer's disease (Polydoro et al. 2009; Lanté et al., 2015). Relevantly, the NOR behavioural task: (i) involves brain areas such as transentorhinal/entorhinal/perirhinal cortices and hippocampus which are pathologically relevant in this field, being affected by neurofibrillary tau changes at early stages of disease (Braak and Braak, 1991; Lasagna-Reeves et al., 2011, 2012; Bengoetxea et al., 2015; Sankaranarayanan et al., 2015); (ii) is a non-aversive learning paradigm, avoiding the potential confounds of using differential rewards or punishments, able to evaluate the hippocampal-dependent episodic memory (Antunes and Biala, 2012; Leger et al., 2013) which is the first type of memory affected in Alzheimer's disease patients (Reed et al., 1997; Zola and Squire, 2001; de Toledo-Morrell et al., 2007; Salmon and

Bondi, 2009; Grayson, et al., 2015). Owing to innate and spontaneous preference of mice towards novelty, any increase in exploration of the novel object (NO) during the test session is to be ascribed to the animal's ability in discriminating it from the familiar one (FO). This parameter was quantified as preference index (PI), which is calculated as the percentage of time spent exploring the new object over the total time spent exploring the two objects. In the recognition session, a PI for the NO >50% indicated that the NO was preferred, <50% that the FO was preferred and at 50% that no object was preferred (Hammond et al., 2004).

Interestingly (Figs 4A and 5A), Tg2576 and 3xTg mice receiving 12A12mAb showed a significant rescue in short-term memory deficits when tested in this hippocampal-dependent task, being able to distinguish NO from FO (Tg2576 + mAb PI = 58.6%; 3xTg + mAb PI = 66.41%) just as WT, healthy non-Tg mice (B6SJL PI = 59.44%; C57 PI = 68.0%, respectively). On the other hand, saline-treated/'naïve' Tg-Alzheimer's disease mice from both strains exhibited a poor performance when evaluated in NOR test because they spent the same time in exploring the NO versus the FO (Tg2576 PI = 48.51%; 3xTg PI = 50.48%, respectively). Accordingly, a two-way ANOVA of behavioural data (treatment × object discrimination) indicated significant difference between the three experimental groups of both strains ($F_{(1,32)} = 6.60$ $P = 0.01$ for Tg2576; $F_{(2,56)} = 3.4$ $P = 0.04$ for 3xTg) with the NO being preferred from 12A12mAb-infused Alzheimer's disease Tg animals (Fisher's *post hoc* test NO versus FO Tg2576 + mAb: **$P < 0.01$; 3xTg + mAb: ***$P < 0.0005$) which behaved in the same manner of WT, non-Tg ones (Fisher's *post hoc* test NO versus FO B6SJL: ***$P < 0.0005$; C57: ***$P < 0.0005$). Conversely, not-immunized Alzheimer's disease mice from both genetic backgrounds did not discriminate between NO and FO object and displayed defective mnestic abilities without any preference for NO (Fisher's *post hoc* test Tg2576: $P = 0.61$; 3xTg: $P = 0.32$). Furthermore, these results were not due to an intrinsic inability of animals to interact with the objects because no significant difference (treatment × object discrimination) was measured during training phase among the animals' cohorts from both strains which explored both objects for the same length of time and without any particular preference towards a side of the cage (two-way ANOVA analysis $F_{(2,32)} = 0.087$ $P = 0.916$ for Tg2576 background; $F_{(2,52)} = 1.09$: $P = 0.34$ for 3xTg mice; Fisher's *post hoc* test left object versus right object B6SJL: $P = 0.53$, Tg2576: $P = 0.20$, Tg2576 + mAb: $P = 0.30$; Fischer's *post hoc* test left object versus right object C57: $P = 0.72$, 3xTg: $P = 0.91$, 3xTg + mAb: $P = 0.11$).

In addition to the objects' recognition memory, the hippocampal formation is devoted to store information about places in the organism's environment, their spatial relations and the existence of specific objects in specific places (spatial memory) (O'Keefe and Conway, 1978;
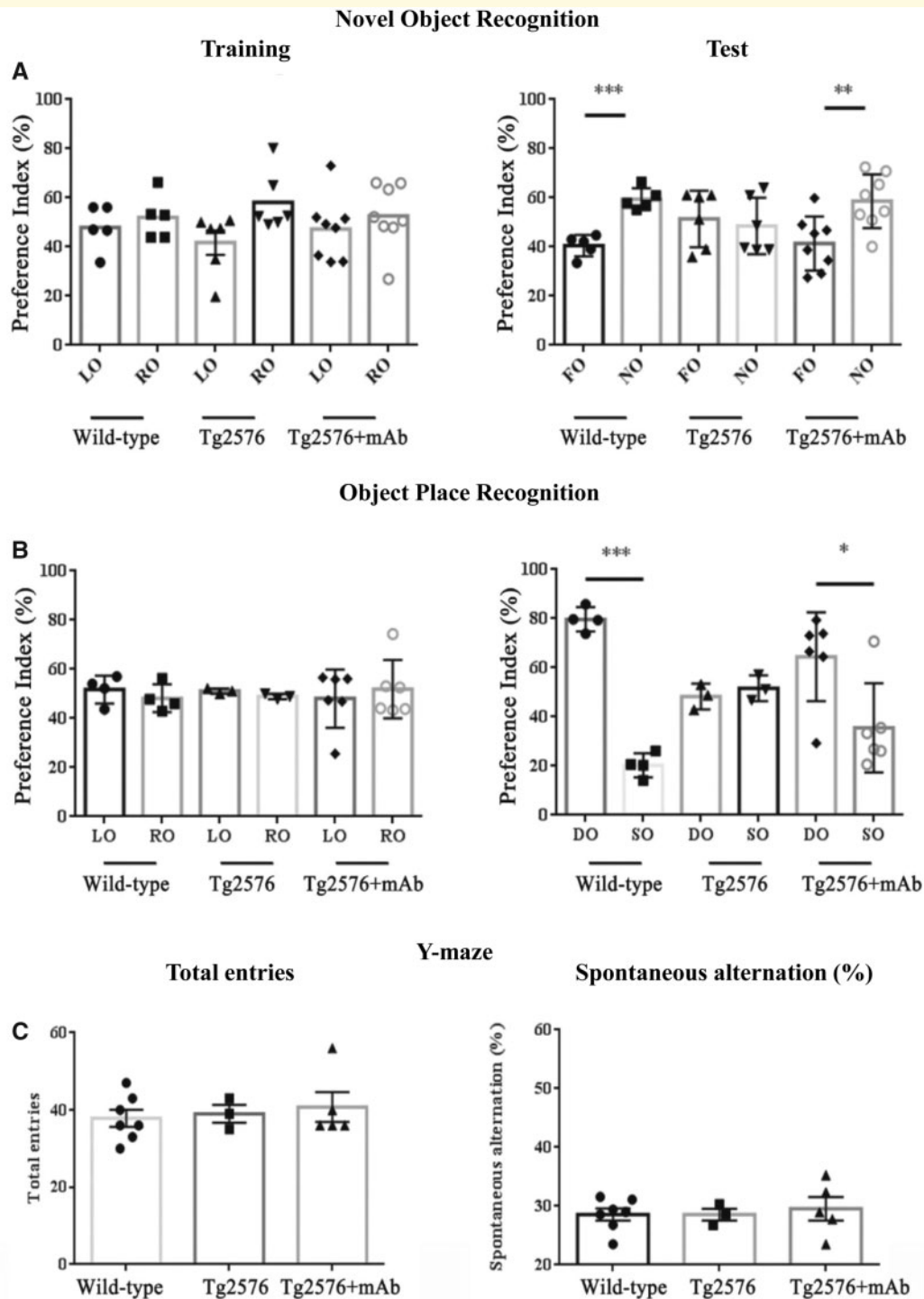
Figure 4 Improved cognition in Tg-Alzheimer's disease (Tg2576) mice immunized with 12A12mAb. (A–C) Fourteen days after i.v. 12A12mAb immunization, the *in vivo* effect of NH_2htau removal on cognitive performance was investigated in animals from the three experimental groups (WT, Tg-Alzheimer's disease and Tg-Alzheimer's disease + mAb) of Tg2576 genetic background in the NOR (**A**), OPR (**B**) and Y-maze (**C**) tasks (top to bottom). For NOR (**A**) and OPR (**B**): right and left histograms, respectively, represent the PI (%) of corresponding values measured during the test trial among animals from the different experimental groups (WT, Tg-Alzheimer's disease and Tg-Alzheimer's disease + mAb) of Tg2576 genetic background. The columns refer to objects presented during training and test trial. Analysis of PI (%) measured as time spending in the exploration of the novel/DO/(time spending in the exploration of novel/DO + time spending in the exploration of familiar/SO) × 100. Data were expressed as means ± SEM ($n = 6$–10). Values are means of at least three independent experiments and statistically significant differences (see details in the main text) were calculated by ANOVA followed by *post hoc* test for multiple comparisons among more than two groups. $P < 0.05$ was accepted as statistically significant (*$P < 0.05$; **$P < 0.01$; ***$P < 0.0005$; ****$P < 0.0001$). For Y-maze (**C**): right and left histograms, respectively, represent the total entries (the total arm entries correspond to the total number of arms entered) and the spontaneous alternation (the number of alternations corresponds to the successive entries into three different arms in

(continued)

Broadbent et al., 2004; Manns and Eichenbaum, 2009). Accordingly, immunized and not-immunized animals from the three experimental groups run the object place recognition task, another hippocampal-dependent paradigm which examines the memory/learning ability of mice in spatial relationships, rather than in objects recognition, by calculating the time spent in discriminating the spatially displaced 'old familiar' object relative to the stationary 'old familiar' object (Antunes and Biala, 2012; Vogel-Ciernia and Wood, 2014). Rodents normally display a clear preference for the object moved to a novel place [displaced object (DO)] in comparison to the object that remains in the same (familiar) place [stationary object (SO)], which confirms their proficiency for remembering which spatial locations have or have not been engaged earlier (Warburton et al., 2013).

Again (Figs 4B and 5B), cognitive impairment of mice from the two genetic backgrounds (Tg2576 and 3xTg) was relieved following i.v. 12A12mAb injection because immunized animals were able to distinguish DO from SO (Tg2576 PI = 73.26%; 3xTg PI = 69.07%) by performing in spatial novelty memory task just as WT, healthy non-Tg ones (B6SJL PI = 79.71%; C57 PI = 71.48%, respectively). On the other hand, saline-treated 'naïve' Alzheimer's disease Tg mice showed no preference for the moved object as they spent nearly equivalent amounts of time exploring the DO and SO which confirms that these not-immunized animals from both strains have object location memory dysfunction (Tg2576 home-cage PI = 48.29%; 3xTg home-cage PI = 52.53%, respectively). Consistently, a two-way ANOVA of behavioural data (treatment × object discrimination) indicated significant difference between the three animals' cohorts in both strains analysed ($F_{(2,20)}$ = 9.68 $P = 0.001$ for Tg2576; $F_{(2,50)}$ = 33.11 $P < 0.001$ for 3xTg) with the DO being preferred from 12A12mAb-immunized Alzheimer's disease mice (Fisher's post hoc test DO versus SO Tg2576 + mAb: $*P < 0.05$, 3xTg + mAb: $***P < 0.0005$) which behaved in the same manner of WT, non-Tg ones (Fisher's post hoc test DO versus SO B6SJL: $***P < 0.0005$, C57: $***P < 0.0005$). In contrast, 'naïve' Tg2576 and 3xTg mice displayed no difference between DO and SO object with no obvious preference for DO (Fisher's post hoc test Tg2576: $P = 0.76$; 3xTg: $P = 0.35$). Besides, regardless of the genetic background, no variation (treatment × object discrimination) was measured during the training phase among the three experimental

groups which explored both objects for the same length of time and without any particular preference towards a side of the cage (two-way ANOVA analysis $F_{(2,20)}$ = 0.47 $P = 0.63$ for Tg2576 background; $F_{(2,52)}$ = 0.79 $P = 0.46$ for 3xTg mice; Fisher's post hoc test left object versus right object B6SJL: $P = 0.58$, Tg2576: $P = 0.76$, Tg2576 + mAb: $P = 0.47$; Fischer's post hoc test left object versus right object C57: $P = 0.24$, 3xTg: $P = 0.86$, 3xTg + mAb: $P = 0.68$).

After assessing the object discrimination and spatial memory, we also tested mice in the spontaneous alternation by employing the Y-maze, an hippocampal-dependent episodic-like behavioural test for measuring their willingness to explore new environments (exploratory tendency). Animals are started from the base of the Y-shaped apparatus placed horizontally and allowed to freely explore all three arms. The number of arm entries and the number of triads are recorded in order to calculate the percentage of alternation (Deacon and Rawlins, 2006; Borchelt and Savonenko, 2008) which is based on the fact that the rodent tends to choose the arm not visited before, reflecting memory (spatial-based working memory) of the previous choice (Paul et al., 2009).

Interestingly (Fig. 4C), in line with previous literature findings (King and Arendash, 2002; Deacon et al., 2008; Yassine et al., 2013), the spontaneous alternation task did not reliably detect cognitive deficits in Tg2576 mice at 6 months of age because no difference was found in their working-memory performance in comparison to cognitively intact, WTs, both in spontaneous alternation and total entries into the arms (spontaneous alternation one-way ANOVA $F_{(2,12)}$ = 0.15 $P = 0.86$; Fisher's post hoc test WT versus Tg2576 $P = 0.99$; Tg2576 versus Tg2576 + mAb $P = 0.68$; Total Entries $F_{(2,12)}$ = 0.28 $P = 0.76$; Fisher's post hoc test WT versus Tg2576 $P = 0.81$; Tg2576 versus Tg2576 + mAb $P = 0.72$). All three groups of mice alternated between arms above chance level (22.2%), indicating that neither cohort showed impairment in this test. On the other hand (Fig. 5C) and in line with previous reports (Spires-Jones and Knafo, 2012; Ameen-Ali et al., 2017), although disability was clearly discernible in naïve, cognitively impaired 3xTg at 6 months of age when tested in comparison to age-matched WTs (Spontaneous alternation one-way ANOVA $F_{(2,28)}$ = 7.44 $P = 0.025$; Total entries $F_{(2,28)}$ = 18.01 $P = 0.00001$), no significant improvement in their reference and working-memory/learning abilities was detected

Figure 4 Continued
overlapping triplet sets) of animals from the different experimental groups (WT, Tg-Alzheimer's disease and Tg-Alzheimer's disease + mAb) of Tg2576 genetic background. The percentage alternation was calculated as the ratio between number of correct triplets (e.g. ABC) and total entrances minus 2, multiplied by 100. Values are means of at least three independent experiments and statistically significant differences (see details in the main text) were calculated by ANOVA followed by post hoc test for multiple comparisons among more than two groups. $P < 0.05$ was accepted as statistically significant ($*P < 0.05$; $**P < 0.01$; $***P < 0.0005$; $****P < 0.0001$). FO = familiar object; LO = left object; OPR = object place recognition; RO = right object.
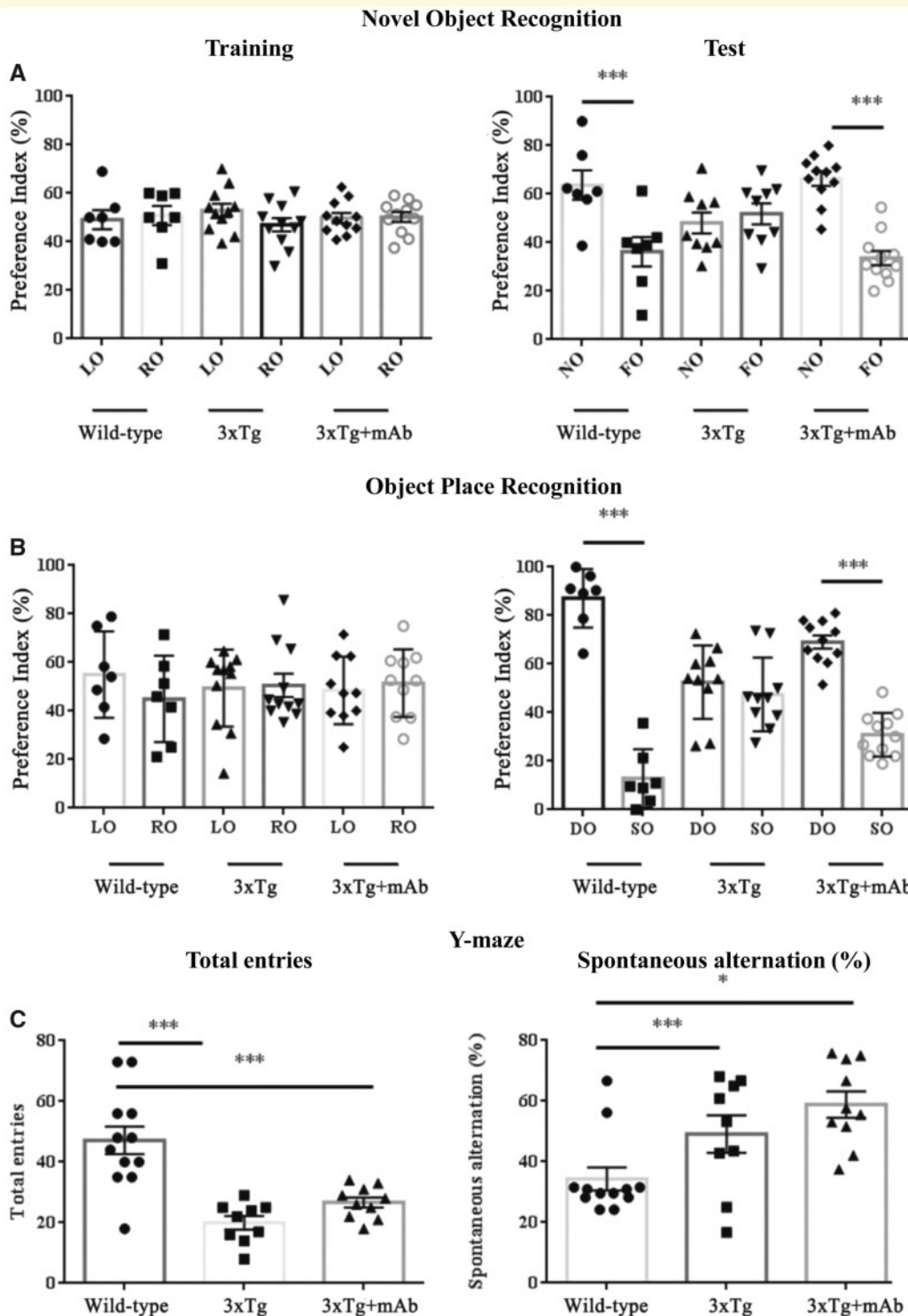
Figure 5 Improved cognition in Tg-Alzheimer's disease (3xTg) mice immunized with 12A12mAb. Fourteen days after i.v. 12A12mAb immunization, the *in vivo* effect of NH_2htau removal on cognitive performance was investigated in animals from the three experimental groups (WT, Tg-Alzheimer's disease and Tg-Alzheimer's disease + mAb) of 3xTg genetic background in the NOR (**A**), OPR (**B**) and Y-maze (**C**) tasks(top to bottom). For NOR (**A**) and OPR (**B**): right and left histograms, respectively, represent the PI (%) of corresponding values measured during the test trial among animals from the different experimental groups (WT, Tg-Alzheimer's disease and Tg-Alzheimer's disease + mAb) of 3xTg genetic background. The columns refer to objects presented during training and test trial. Analysis of PI (%) measured as time spending in the exploration of the novel/DO/(time spending in the exploration of novel/DO + time spending in the exploration of familiar/SO) × 100. Data were expressed as mean ± SEM (*n* = 6–10). Values are means of at least three independent experiments and statistically significant differences (see details in the main text) were calculated by ANOVA followed by *post hoc* test for multiple comparisons among more than two groups. $P < 0.05$ was accepted as statistically significant (*$P < 0.05$; **$P < 0.01$; ***$P < 0.0005$;

(continued)

following systemic injection with 12A12mAb (Fisher's *post hoc* test analysis, Total entries: WT versus 3xTg ***$P < 0.0005$; WT versus 3xTg + mAb ***$P < 0.0005$; 3xTg versus 3xTg + mAb $P = 0.19$; Spontaneous alternation WT versus 3xTg ***$P < 0.0005$; WT versus 3xTg + mAb *$P < 0.05$; 3xTg versus 3xTg + mAb $P = 0.17$). In this framework, it is worth stressing that, in contrast to 3xTg characterized by genetically driven tau pathology, Tg2576 mice express human APP (K670N/M671L)PS1(M146V) transgene in endogenous background of murine not-mutated tau. Therefore, the discrepancy in results between two different Tg Alzheimer's disease rodent models, each having its own characteristics, may be due to the aggressive phenotype of the human tau-overexpressing 3xTg strain, which is likely to require a more optimized immunization regimen (antibody dosage, time of treatment, timing of administration) in order to fully prevent and/or delay its robust cognition symptomatology. Alternatively, the reversible nature of *in vivo* tau neuropathology could be restricted within strain-specific temporal window(s) because of the complex and multifactorial feature of Alzheimer's disease pathology involving a wide range of inflammatory, oxidative, neurodegenerative causative mechanisms (Webster *et al.*, 2014; Velazquez *et al.*, 2018).

Finally, to rule out the possibility that the *in vivo* enhancement of cognitive skills in immunized animals involved an effect of 12A12mAb treatment on body energy homeostasis known to influence their sensorial-motor abilities, metabolic rate (EE) from vehicle- or antibody-infused non-Tg WT mice was assessed by means of indirect calorimetry during 2 days of continuous analysis/recording. As shown in Supplementary Fig. 2A, an unpaired *t*-test of EE data revealed no significant difference between the two experimental groups [vehicle-treated animals: ($M = 25.29$; SEM $= \pm0.61$) or mAb-treated animals: ($M = 24.92$; SEM $= \pm0.64$ $t_{(142)} = 0.42$)]. Furthermore, the EE analysis in resting conditions (REE)—i.e. by considering only the EE values generated in the absence of motor activity (i.e. 0–2 counts)—did not show any variation in heat production from 12A12mAb-treated healthy WT mice, thus corroborating the important finding that intra-caudal injection either with vehicle alone ($M = 18.51$; SEM $= \pm0.43$), or with antibody ($M = 18.08$; SEM $= \pm0.52$ $t_{(142)} = 0.42$), was

ineffective in altering the whole body REE, whatever the physical motor activity involved ($t_{(118)} = 0.63$) (Supplementary Fig. 2B).

In keeping with this finding, no change in recognition memory performance was detected when vehicle- or 12A12mAb-treated WT mice were evaluated in the NOR paradigm (Supplementary Fig. 2C and D), further indicating that the immunization regimen *per se* did not affect cognitive functions under non-pathological settings. Two-way ANOVA of time (s) of exploration of FO versus NO showed no significant difference for treatment factor ($F(1,12) = 0.28$ $P =$ ns), significant object novelty factor ($F(1,12) = 18.74$ $P < 0.001$) and no significant effect of the interaction between treatment and object novelty ($F(1,12) = 0.08$ $P =$ ns). *Post hoc* Tukey's test for object novelty (FO versus NO) further confirmed that both vehicle-treated (**$P < 0.01$) and mAb-treated (**$P < 0.01$) WT animals exhibited intact recognition memory (Supplementary Fig. 2C). No difference was found between the PI of vehicle-treated and mAb-treated WT groups (unpaired sample *t*-test: vehicle-treated and mAb-treated ones, $t_{(6)} = 1.672$, $P =$ ns, Supplementary Fig. 2D), thus demonstrating that 12A12mAb-induced injection did not impair recognition memory in non-Tg mice. In agreement with the cleavage-selectivity of antibody (Supplementary Fig. 1), the 12A12mAb treatment appeared to be avoid of potential adverse side-effects in discriminatory skills when injected in healthy animals, notwithstanding its ability of penetrating the animals' blood–brain barrier and/or successfully accessing to hippocampus in biologically active state (Fig. 1D).

Likewise, no difference in cognitive performance was detected when sham-immunized 6-month-old Tg2576 mice (i.e., animals administered with IgG isotype control, at the same dosage and period of time) were tested for performance in NOR paradigm in comparison with their vehicle-treated counterparts. Two-way ANOVA analysis on time (s) of exploration of FO versus NO displayed no significant difference for object factor ($F(1,8) = 0.66$ $P =$ ns) and treatment factor ($F(1,8) = 0.67$ $P =$ ns) in vehicle- and IgG-treated Tg mice (Supplementary Fig. 3A). Moreover, the unpaired sample *t*-test of PI data showed that neither vehicle nor IgG administration improved the deficit of recognition memory (compare Supplementary

Figure 5 Continued
****$P < 0.0001$). For Y-maze (**C**): right and left histograms, respectively, represent the total entries (the total arm entries correspond to the total number of arms entered) and the spontaneous alternation (the number of alternations corresponds to the successive entries into three different arms in overlapping triplet sets) of animals from the different experimental groups (WT, Tg-Alzheimer's disease and Tg-Alzheimer's disease + mAb) of 3xTg genetic background. The percentage alternation was calculated as the ratio between number of correct triplets (e.g. ABC) and total entrances minus 2, multiplied by 100. Values are means of at least three independent experiments and statistically significant differences (see details in the main text) were calculated by ANOVA followed by *post hoc* test for multiple comparisons among more than two groups. $P < 0.05$ was accepted as statistically significant (*$P < 0.05$; **$P < 0.01$; ***$P < 0.0005$; ****$P < 0.0001$). FO = familiar object; LO = left object; OPR = object place recognition; RO = right object.

Fig. 3B with Supplementary Fig.2C), thus confirming the lack of ability of Tg animals in discriminating between FO and NO ($t_{(4)}$ = 0.05, P = ns). Similar results were detected following IgG infusion in 6-month-old 3xTg mice when compared to not-immunized Tg counterparts (data not shown).

Active behaviour, such as exploring a novel environment, induces the expression of the immediate-early gene Arc (activity-regulated cytoskeletal-associated protein, or Arc/Arg3.1) in several brain regions, including the hippocampus. Activity-regulated cytoskeleton-associated protein messenger RNA is quickly induced and dynamically up-regulated by behavioural experience and the protein is selectively translated into activated dendrites, being required for the memory consolidation of an early initial potentiation of synaptic transmission into a lasting form of long-term potentiation (LTP) (Ramirez-Amaya et al., 2005, 2013; Plath et al., 2006; Korb and Finkbeiner, 2011). Interestingly and consistent with their cognitive enhancement in behavioural assessments (Figs 4 and 5), western blotting analyses performed on hippocampal synaptosomal-enriched preparations isolated from post-trained animals (Supplementary Fig. 4A and B) showed that the stimulus-driven, steady-state expression level of activity-regulated cytoskeleton-associated protein was significantly up-regulated in 12A12mAb-immunized Tg2576 and 3xTg mice when compared to their saline-treated cognitively impaired counterparts (one-way ANOVA followed by Bonferroni's *post hoc* test $F(2,18)$ = 34.81 $P < 0.0001$ Tg2576; $F(2,18)$ = 33.32 $P < 0.0001$ 3xTg; Tg2576 + mAb versus Tg2576 ****$P < 0.0001$; Tg2576 + mAb versus WT n.s. $P = 0.1441$; 3xTg + mAb versus 3xTg ***$P < 0.0005$; 3xTg + mAb versus WT **$P < 0.01$). Conversely and in line with their scarce performance in novelty-based cognitive tasks (Figs 4 and 5), *naïve* Alzheimer's disease Tg animals—which were not systemically infused with 12A12mAb—displayed marked defects in the experience-dependent induction of activity-regulated cytoskeleton-associated protein expression, and then in their processes of memory/learning trace consolidation following its initial acquisition, as shown by the finding that immunoreactivity signal of protein in their synaptic fractions was significantly lower than that from healthy WT controls (one-way ANOVA followed by Bonferroni's *post hoc* test ****$P < 0.0001$ for Tg2576 versus WT and for 3xTg versus WT).

Collectively, these experiments indicate that passive immunization with 12A12mAb, which selectively targets the neurotoxic NH_2htau fragment(s) *in vivo*, significantly improves cognition in symptomatic (6 months old) Tg-Alzheimer's disease animals by rescuing their instinctual and innate preference for novelty (object recognition and object location skills) when tested in two pathologically relevant, hippocampal-dependent behavioural tasks.

Loss in dendritic spine density is prevented in hippocampal CA1 region from 12A12mAb-infused 6-month-old Tg-Alzheimer's disease animals

Dendritic spines, the sites of excitatory synapses protruding from dendritic shafts, are cellular morphological specializations devoted to memory-forming processes in neurons (Segal, 2005). Being extremely dynamic structures, modification in their number, size and/or shape is an important index of synaptic plasticity occurring in response to external environmental inputs (Pignataro et al., 2015). As a consequence, loss of dendritic arbourization (length/complexity) in vulnerable neuronal networks, although occurring along different spatio-temporal patterns among commonly used Tg animal models, undoubtedly represents one of the earliest changes of structural plasticity which critically contributes over time to the disruption of neuronal network with consequent appearance of cognitive dysfunction in Alzheimer's disease and other related dementias (Knobloch and Mansuy, 2008; Spires-Jones and Knafo, 2012; Cochran et al., 2014; Dorostkar et al., 2015). Therefore, in order to complement our behavioural findings, we assessed the neuroanatomical effect of passive immunization with 12A12mAb on dendritic connectivity from 6-month-old Alzheimer's disease animals. To this aim, hippocampal sections from mice of the three experimental groups were stained by Golgi-Cox impregnation procedure followed by quantitative assessment of dendritic spine density (number of spines per unit length) along both apical and basal compartments of individual CA1 pyramidal neurons (Fig. 6).

As shown in Fig. 6A and in line with previous works reporting in Tg2576 an early decline of dendritic boutons which undergo dystrophy and shrinkage (Lanz et al., 2003; Jacobsen et al., 2006; D'Amelio et al., 2011), the spine loss was detectable at the age of 6 months in apical compartments of CA1 hippocampal neurons from this genetic background when animals were compared to non-Tg controls. Importantly, in 12A12mAb-immunized Alzheimer's disease group the apical spine density was significantly ameliorated up to the level of saline-injected cognitively intact WTs (one-way ANOVA followed by Fisher's *post hoc* test $F(2,8)$ = 10.828, P = 0.00530; **$P < 0.01$ WT versus Tg2576; **$P < 0.01$ Tg2576 + mAb versus Tg2576), indicating that treatment was strongly effective in blocking/preventing the dendritic degeneration. Interestingly, no difference was detected when spines were counted in the basal compartment of CA1 neurons from the three experimental cohorts (one-way ANOVA $F(2,8)$ = 0.71926, $P = 0.51611$), suggesting that age-related spine changes in Tg2576 mice initially involve the apical dendritic arbours with no apparent effect on basal dendrites of CA1 pyramidal neurons which are more likely to be affected only later, when their
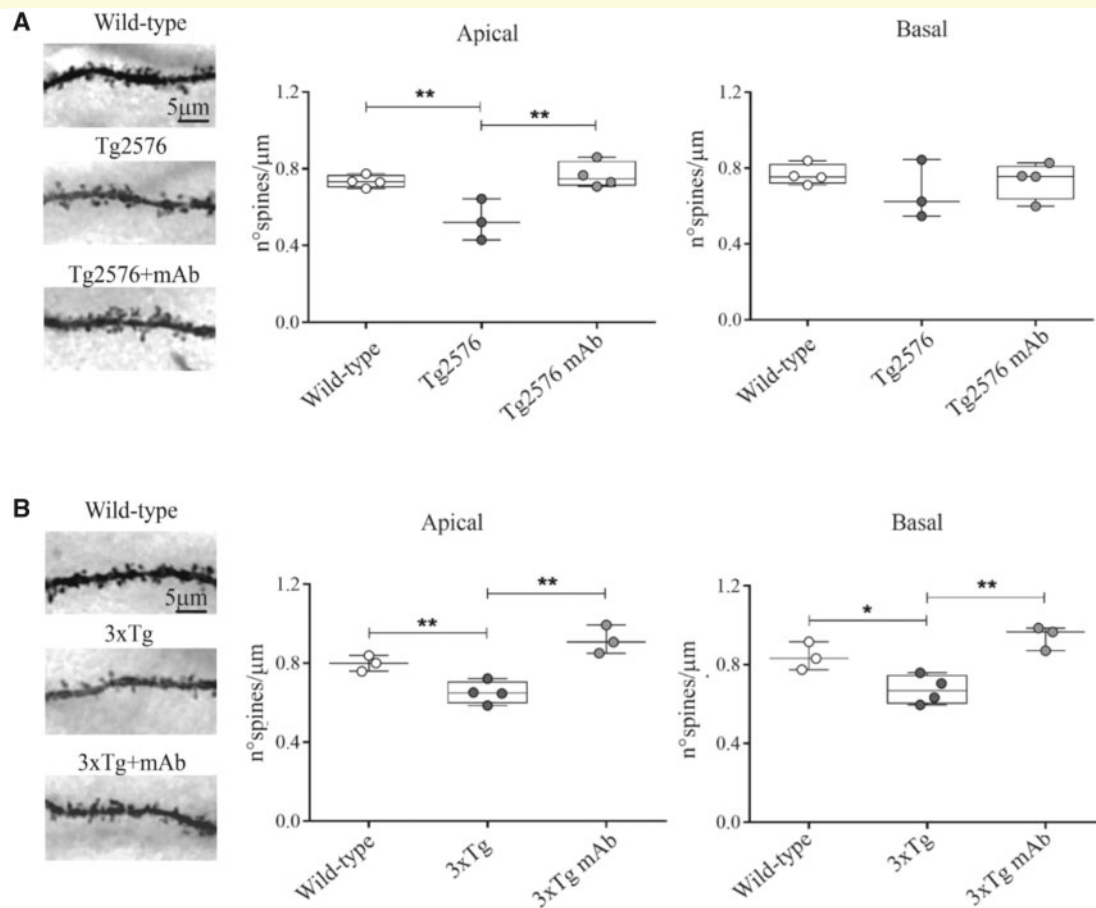
Figure 6 Immunization with 12A12mAb in Tg-Alzheimer's disease mice is protective against the dendritic spines density loss which affects the memory and learning processes. (**A**, **B**) Comparative photomicrographs of Golgi-stained hippocampal CA1 neurons showing dendritic segments from animals from three experimental groups (WT, Tg-Alzheimer's disease and Tg-Alzheimer's disease + mAb) of both strains (Tg2576, 3xTg) (left, refers to CA1 pyramidal neurons dendrites scale bar: 5 μm). Box-and-whisker plots (right) depict the morphometric analysis of the dendritic spine density from the three experimental groups. Values are expressed as number of spines per 1 μm segment. Statistically significant differences (comparisons were made on single mouse values obtained by averaging the number of spines counted on neurons of the same mouse) were calculated by ANOVA followed by *post hoc* test for multiple comparison among more than two groups. *P* < 0.05 was accepted as statistically significant (*P < 0.05; **P < 0.01; ***P < 0.0005; ****P < 0.0001).

structural plasticity and stability (formation and elimination) is completely impaired (Spires-Jones *et al.*, 2007).

On the other hand and in stark contrast with previous literature findings (BIttner *et al.*, 2010), we found out (Fig. 6B) that the reduction in the spines density, both in apical and basal compartments of individual CA1 pyramidal neurons, already started from the age of 6 months in cognitively impaired 3xTg mice (one-way ANOVA followed by Fisher's *post hoc* test apical: $F(2,7) = 18.697$, $P = 0.00156$; basal: $F(2,7) = 13.404$, $P = 0.00404$) which exhibited lower values in dendritic protrusions counts when compared with their age-matched, non-Tg WTs. Remarkably, degeneration of dendritic spine structures was robustly decreased in immunized 3xTg mice (apical: **$P < 0.01$ 3xTg + mAb versus 3xTg; **$P < 0.01$ WT versus 3xTg; basal: **$P < 0.01$ 3xTg + mAb versus 3xTg; *$P < 0.05$ WT versus 3xTg) pointing out that—possibly as

result of increased afferent inputs to the CA1 from other neighbouring hippocampal areas and/or as a local positive effect in the CA1 region—12A12mAb treatment was able to mitigate the age-related pathology of post-synaptic connections from symptomatic 6-month-old 3xTg mice, both in their apical and basal compartments.

Systemic administration of 12A12mAb also normalizes the Alzheimer's disease-related electrophysiological alterations of Tg-Alzheimer's disease animal models

In order to investigate whether 12A12mAb immunization, in addition to its protective actions on Alzheimer's

disease-related behavioural and neurochemical and neuroanatomical abnormalities, was also able to exert an effect on electrophysiological correlate(s) of the memory/learning processes, hippocampal synaptic transmission and plasticity in the Schaffer collateral pathway were compared between Tg and WT animals from both genetic backgrounds (Fig. 7A–D for Tg2576; Fig. 7E–H for 3xTg).

We first recorded basal synaptic transmission and the strength of pre-synaptic Schaffer collaterals activation (i.e. axonal depolarization) from CA3-to-CA1 synapses in acute brain slices from 6-month-old WT and age-matched Tg2576 animals treated with saline vehicle or 12A12mAb, respectively. To this aim, we first generated input/output curves by measuring the field excitatory post-synaptic potentials elicited in the stratum radiatum of the CA1 area after stimulation of the Schaffer collaterals at increasing intensities. As shown in Fig. 7A and B and in line with previous investigations reporting no change in basal synaptic transmission in this Tg Alzheimer's disease model at 6 months of age (Chapman *et al.*, 1999; Nobili *et al.*, 2017), the input/output curves displayed a similar trend among the three experimental groups (two-way repeated-measures ANOVA for stimulus intensity × experimental group followed by Bonferroni's *post hoc* test $F_{(12,282)} = 0.8409$ $P = 0.6082$; n.s. $P > 0.05$ for all comparisons).

Next, we investigated the pre-synaptic function by assessing paired-pulse facilitation, a short-term plasticity paradigm which inversely depends on Ca^{2+}-dependent pre-synaptic changes in neurotransmitter release probability at nerve endings (Manabe *et al.*, 1993; Debanne *et al.*, 1996; Dobrunz and Stevens, 1997; Dobrunz *et al.*, 1997; Thomson, 2000; Zucker and Regehr, 2002). Again (Fig. 7C), short-term potentiation was almost identical among the three animals' cohorts (two-way repeated-measures ANOVA for paired-pulse interval × experimental group, followed by Bonferroni's *post hoc* test $F_{(10,170)} = 0.51$ $P = 0.8839$; n.s. $P > 0.05$ for all comparisons), consistent with previous results referring no significant dissimilarity in paired-pulse facilitation between 6-month-old Tg2576 and WT littermates (Jung *et al.*, 2011; Nobili *et al.*, 2017).

In contrast to the basic synaptic transmission (input–output relationship and paired-pulse facilitation), the 'classical' N-methyl-D-aspartate (NMDA) receptor-dependent LTP paradigm at Schaffer collaterals/CA1 synapses—a long-lasting enhancement of the strength/efficacy of excitatory synaptic transmission which is widely used in investigations on numerous APP/Aβ models of Alzheimer's disease (Rowan *et al.*, 2003; Shankar *et al.*, 2008)—turned out to be significantly compromised in 6-month-old Tg2576 mice in comparison to age-matched WTs (Fig. 7D). Following the induction of LTP by delivery of trains of high-frequency stimulation at half-maximal intensity, field excitatory post-synaptic potential slopes appeared to decay down to baseline in 6-month-

old Tg2576 animals so that no persistent, activity-driven potentiation was measurable starting from 30 min after induction which was indicative of an impaired function of hippocampal Schaffer collaterals/CA1 synapses. Importantly and in keeping with improvement of cognitive performance in hippocampal-dependent behavioural assessments, peripheral administration of 12A12mAb was able to mitigate *in vivo* the disease-related LTP deficiency of symptomatic Tg2576 animals, as shown by the fact that the LTP amplitude calculated after application of high-frequency stimulation was significantly increased in immunized experimental group when compared to 'naïve' cognitively impaired counterpart (one-way ANOVA followed by Bonferroni's *post hoc* test $F_{(2,21)} = 19.38$ $P < 0.0001$; ***$P < 0.0005$ Tg2576 versus WT; *$P < 0.05$ Tg2576 + mAb versus Tg2576; Tg2576 + mAb versus WT **$P < 0.01$). Moreover, these electrophysiological investigations further corroborated the finding that the disruption of synaptic plasticity in hippocampal Schaffer collateral commissural pathway from this Alzheimer's disease model was more likely due to altered post-synaptic signalling pathways, given that no alteration in paired-pulse facilitation was contextually detected in Tg animals at 6 months of age (Chapman *et al.*, 1999; Jacobsen *et al.*, 2006; Jung *et al.*, 2011; Nobili *et al.*, 2017).

In contrast with results from symptomatic Tg2576 mice, in 3xTg paradigm the input/output relationship revealed a significant reduction of field excitatory post-synaptic potential slopes evoked by increasing stimulation intensities (Fig. 7E and F) when 6-month-old Tg animals were compared to WT counterparts (two-way repeated-measures ANOVA for stimulus intensity × experimental group followed by Bonferroni's *post hoc* test $F_{(12,204)} = 5.812$ $P < 0.0001$; *$P < 0.05$ and **$P < 0.01$ WT versus 3xTg for paired comparisons). Most importantly, cumulative distributions of field excitatory post-synaptic potential slopes within the range of 100 and 300 μA of stimulus amplitude were shifted to higher values in 12A12mAb-immunized Alzheimer's disease group in contrast to 'naïve', cognitively impaired counterpart, indicating that antibody treatment positively influenced the fast glutamatergic transmission in this genetic background (#$P < 0.05$, ##$P < 0.01$, ###$P < 0.001$ for 3xTg versus 3xTg + mAb for paired comparisons with Bonferroni's *post hoc* test). No change in paired-pulse facilitation short-term plasticity (Fig. 7G) was found among the three experimental cohorts (two-way ANOVA paired-pulse interval × genotype followed by Bonferroni's *post hoc* test $F_{(12,198)} = 0.3464$ $P = 0.9792$ n.s. $P > 0.05$ for all comparisons), consistent with previous data showing that the abnormalities in pre-synaptic release machinery were not discernible between 6-month-old 3xTg and age-matched WTs when measured in a facilitation electrophysiological paradigm (Oddo *et al.*, 2003). In a way similar to Tg2576, hippocampal slices from 6-month-old 12A12mAb-injected 3xTg animals displayed a strong potentiation after high-frequency stimulation bout, pointing
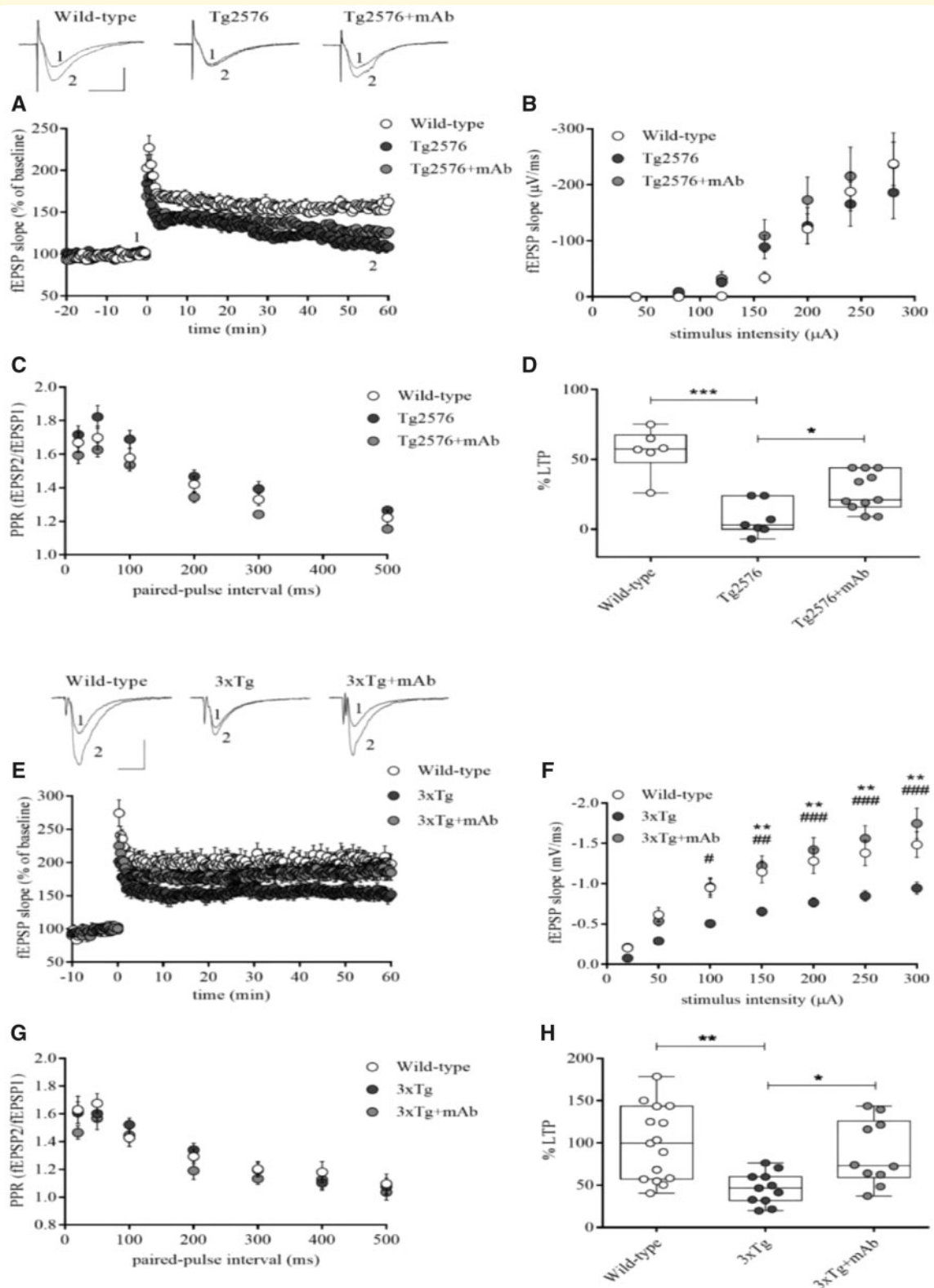
Figure 7 Reduction of cognitive deficits in 12A12mAb-immunized Tg-Alzheimer's disease mice correlates with an increased LTP. (**A, D**) For Tg2576; (**E, H**) for 3xTg) time plot of average fEPSP responses (**A, E**) and changes in magnitude of LTP at CA3-Ca1 synapses (**D, H**) were calculated among animals (n = 6–10) from three experimental groups (WT, Tg-Alzheimer's disease and Tg-Alzheimer's disease + mAb) of both strains. At least seven slices from six different mice were recorded for each experimental condition. Data are presented as the mean (±SEM). The traces above the plot show fEPSPs at baseline (1) and at 60 min after LTP induction (2). The box-whisker plots show pooled data. Statistically significant differences (see details in the main text) were calculated by ANOVA followed by *post hoc* test for multiple comparisons among more than two groups. $P < 0.05$ was accepted as statistically significant (*$P < 0.05$; **$P < 0.01$; ***$P < 0.0005$;

(continued)

to a strong protective action evoked *in vivo* by the antibody treatment on the cellular/molecular correlate(s) of their memory/learning processes (one-way ANOVA followed by Bonferroni's *post hoc* test $F_{(2,33)} = 7.018$ $P = 0.0029$; $**P < 0.01$ 3xTg versus WT; $*P < 0.05$ 3xTg + mAb versus 3xTg; 3xTg + mAb versus WT n.s. $P > 0.05$). Notably, when LTP was calculated in 6-month-old 3xTg mice (Fig. 7H), a lower post-tetanic potentiation was found against WTs suggesting that, in this Alzheimer's disease strain, the LTP reduction in magnitude and persistence was more likely due to deficits of induction (either pre- and/or post-synaptic), in line with structural and functional modifications observed both in their basal synaptic transmission and dendritic spine density (Fig. 6B).

Taken together, these electrophysiological recordings indicate that disruption of excitatory synaptic transmission and plasticity detected at 6 months of age in hippocampal CA3-CA1 circuit of these two genetically distinct Tg-Alzheimer's disease animal models, although manifests at different rate and involves non-overlapping causative mechanism(s), was significantly rescued following *in vivo* peripheral administration of 12A12mAb.

Expression levels of inflammatory astroglial and microglial markers are also down-regulated in 6-month-old 12A12mAb-immunized Tg-Alzheimer's disease animals

The inflammatory response—which is one of the earliest manifestations of neurodegenerative tauopathies, including Alzheimer's disease (Bellucci *et al.*, 2004; Yoshiyama *et al.*, 2007; Wes *et al.*, 2014; Leyns *et al.*, 2017; Ishikawa *et al.*, 2018)—may act as a double-edged sword being either detrimental or protective depending on the context (Schlachetzki and Hull, 2009). On the one hand, activated glial cells contribute to the Alzheimer's disease pathogenesis by means of diverse mechanisms including complement-mediated synapse removal, non-cell autonomous spreading of pathological seeds/conformers, extracellular release of inflammatory mediators such as pro-inflammatory cytokines, complement components, chemokines, free radicals and gliotransmitters which, in turn, trigger neurodegeneration.

On the other hand, astro- and microglial reactions are endowed with beneficial role in Alzheimer's disease environment by stimulating the digestion/clearance of pathogenic Aβ and tau species and, then, by preventing their accumulation into insoluble cerebral lesions, the senile plaques and neurofibrillary tangles.

To get further insights into protective effect evoked by i.v. 12A12mAb-based immunization in Tg-Alzheimer's disease mice, the extent of inflammatory response was assessed on hippocampi from 6-month-old Tg2576 and 3xTg mice of the three experimental groups (WT, 'naïve' Tg-Alzheimer's disease, Tg-Alzheimer's disease + mAb). Western blotting analysis (Fig. 8) were carried out on animals' total extracts by probing with antibodies which detect the glial fibrillary acidic protein and Iba1, whose cell type-specific steady-state expression levels are recognized as indicative of active astrogliosis and microgliosis, respectively (Sydow *et al.*, 2016). As shown in Fig. 8A and B and regardless of the different genetic background, the immunoreactivity signals of these two classical inflammatory markers were strongly increased in saline-treated, 'naïve' Tg-Alzheimer's disease mice in comparison to WT controls, in line with previous findings reporting a prominent astrocytic and microglial activation in hippocampal parenchyma from these animal models (Olabarria *et al.*, 2010, 2011; Vogels *et al.*, 2019). Remarkably, the gliosis detected in 12A12mAb-injected Tg-Alzheimer's disease mice turned out to be significantly down-regulated compared to their *naïve* counterparts (one-way ANOVA followed by Bonferroni's *post hoc* test glial fibrillary acidic protein: $F_{(2,21)} = 169.4$ $P < 0.0001$ Tg2576 $****P < 0.0001$ for all comparisons; $F_{(2,18)} = 53.88$ $P < 0.0001$ 3xTg; $****P < 0.0001$ 3xTg versus WT; $****P < 0.0001$ 3xTg + mAb versus 3xTg; n.s. $P > 0.05$ 3xTg + mAb versus WT; Iba1: $F_{(2,21)} = 38.43$ $P < 0.0001$ Tg2576 $****P < 0.0001$ Tg2576 versus WT; $****P < 0.0001$ Tg2576 + mAb versus Tg2576; n.s. $P > 0.05$ Tg2576 + mAb versus WT; $F_{(2,18)} = 273$ $P < 0.0001$ 3xTg $****P < 0.0001$ for all comparisons), indicating that: (i) the neuron-derived, extracellularly released 20–22 kDa NH$_2$htau form(s) is more likely to be endowed with non-cell autonomous action by contributing to the glial cells activation; (ii) the neuroprotective effect of 12A12mAb appears to be, at least in part, due to its modulatory role at the glia-neurons interplay.

Figure 7 Continued
$****P < 0.0001$). (**B, C**) For Tg2576; (**F, G**) for 3xTg) input/output curves show the fEPSP slopes plotted against the corresponding stimulus intensities recorded from hippocampal slices of animals ($n = 6$–10) from three experimental groups (WT, Tg-Alzheimer's disease and Tg-Alzheimer's disease + mAb) of both strains (**B, F**). Comparison of PPF in animals ($n = 6$–10) from three experimental groups (WT, Tg-Alzheimer's disease and Tg-Alzheimer's disease + mAb) of both strains (Tg2576, 3xTg) was also determined (**C, G**). PPF was induced by pairs of stimuli delivered at increasing interpulse intervals (20, 50, 100, 200, 300, 500 ms). Data are presented as the mean ($\pm$SEM) facilitation ratio of the second response relative to the first response. Statistically significant differences (see details in the main text) were calculated by ANOVA followed by *post hoc* test for multiple comparisons among more than two groups. $P < 0.05$ was accepted as statistically significant ($*P < 0.05$; $**P < 0.01$; $***P < 0.0005$; $****P < 0.0001$). fEPSP = field excitatory post-synaptic potential; PPF = paired-pulse facilitation.
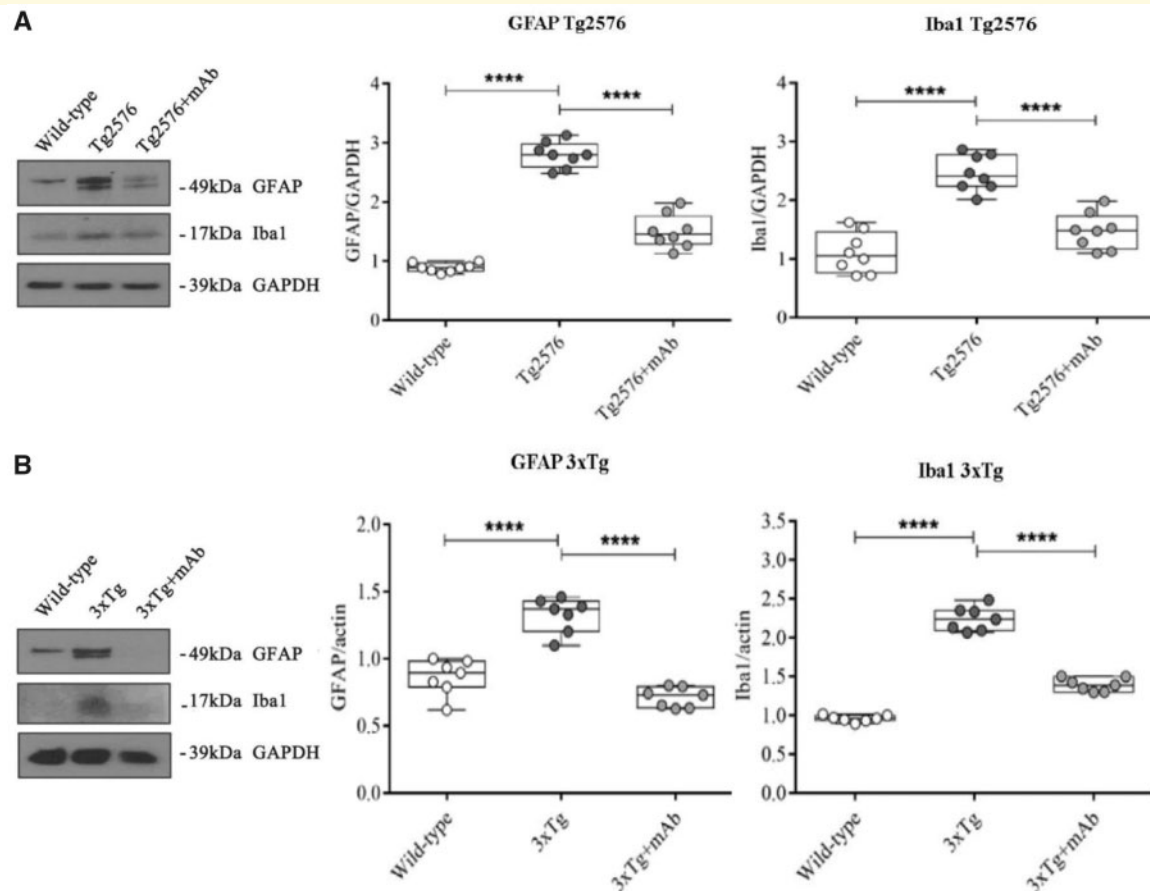
Figure 8 Inflammatory response (activation of astrocytes and microglia) is strongly down-regulated in 12A12mAb-immunized Tg-Alzheimer's disease mice. (**A**, **B**) Neuroinflammation processes (activation of astrocytes and microglia) were assessed on hippocampal extracts from animals from three experimental groups (WT, Tg-Alzheimer's disease and Tg-Alzheimer's disease + mAb) of both strains (Tg2576, 3xTg) by western blotting analysis (left) for inflammatory proteins (glial fibrillary acidic protein, Iba1). Relative densitometric quantification of intensity signals (right) indicates lower levels of glial fibrillary acidic protein and Iba1 in Tg-Alzheimer's disease mice + mAb compared to not-immunized Tg-Alzheimer's disease. GAPDH housekeeping expression serves as loading control. Arrows on the right side indicate the molecular weight (kDa) of bands calculated from migration of standard proteins. Full uncropped blots are available in Supplementary Fig. 8. Values are from at least three independent experiments and statistically significant differences (see details in the main text) were calculated by ANOVA followed by *post hoc* test for multiple comparisons among more than two groups. $P < 0.05$ was accepted as statistically significant ($*P < 0.05$; $**P < 0.01$; $***P < 0.0005$; $****P < 0.0001$). GAPDH = glyceraldehyde-3-phosphate dehydrogenase; GFAP = glial fibrillary acidic protein.

Taken together these findings indicate that sub-chronic i.v. delivery of 12A12mAb into the hippocampus is devoid of potentially adverse inflammatory effects associated to classical immunization regimen by limiting the local activation of neuroglia which is *per se* both a consequence to the disease process and a contributor to the synaptic pathology and neuronal damage (Block *et al.*, 2007; Yoshiyama *et al.*, 2007; Edison *et al.*, 2008; Perry *et al.*, 2010; Schwab *et al.*, 2010; Zotova *et al.*, 2010).

Discussion

Accumulating evidence have suggested that the detrimental effects of Aβ are dependent on tau pathology (Rapoport *et al.*, 2002; King *et al.*, 2006; Roberson *et al.*, 2007; Ittner *et al.*, 2010; Vossel *et al.*, 2010; Desikan *et al.*, 2011; Shipton *et al.*, 2011; Nussbaum *et al.*, 2012; Bloom, 2014) and that tau, rather than Aβ (Murray *et al.*, 2015), serves a prominent role in early synaptic decline and cognitive impairment (Arriagada *et al.*, 1992; Ashe and Zahs, 2010; Nelson *et al.*, 2012; Pontecorvo *et al.*, 2017; Busche *et al.*, 2019). Independently of its ability of seeding aggregation, abnormal extracellular/intracellular tau is *per se* neurotoxic (Diaz-Hernandez *et al.*, 2010; Medina and Avila, 2014a, b; Hu *et al.*, 2018) and propagates trans-synaptically along interconnected neuronal networks in a stereotypical manner which strongly correlates with the development of clinical symptoms during Alzheimer's disease

progression (Mohamed *et al.*, 2013; Pooler *et al.*, 2013; Yamada *et al.*, 2017). These pathologically relevant findings represent the rationale which advocates the employment of tau-based strategies (Li and Gotz, 2017; Congdon and Sigurdsson, 2018) as promising disease-modifying intervention of slow progressing Alzheimer's disease and other human dementias (Novak *et al.*, 2018a; Jadhav *et al.*, 2019), especially in view of the disappointing outcomes from Aβ-targeting pharmacological and immunological approaches (Sigurdsson, 2008; Giacobini and Gold, 2013; Doody *et al.*, 2014; Salloway *et al.*, 2014; Schroeder *et al.*, 2016; Agadjanyan *et al.*, 2017). In this connection, tau-directed passive immunotherapy—which relies on the specific, epitope-directed antibody-mediated depletion/clearance of its toxic species (Sigurdsson, 2008; Pedersen and Sigurdsson, 2015; Li and Gotz, 2017; Congdon and Sigurdsson, 2018)—has been recently recognized as a feasible, valuable approach to reduce the neuropathology and to improve the memory/learning abilities of experimental animal models of tauopathies (Boutajangout *et al.*, 2011; Chai *et al.*, 2011; d'Abramo *et al.*, 2013; Yanamandra *et al.*, 2013, 2015; Castillo-Carranza *et al.*, 2014; Dai *et al.*, 2015, 2018; Subramanian *et al.*, 2017). However, several reasons have hindered the clinical success of tau-targeting approaches which are currently under investigation (Giacobini and Gold, 2013; Novak *et al.*, 2018a; Elmaleh *et al.*, 2019). To this regard, recent reports of ongoing trials indicate that the potential flaws include: (i) study design with the medical care given too late when neuronal damage is already present in a considerable extent so that drugs/modulators are unable to compensate adequately for the detrimental effects; (ii) systemic toxicity owing to long-term and multiple administrations of drugs/modulators used at high doses which can interfere with the neuronal physiology (i.e. affect the normal cellular metabolism and/or impact on the immune surveillance); (iii) inadequate brain bioavailability of medicaments against the target substrate and/or the biochemical pathway, even after crossing the blood–brain barrier; (iv) adverse risks of inflammatory response, such as cerebral microhaemorrhages (Elmaleh *et al.*, 2019).

Here, we show that systemic administration with 12A12mAb—which selectively recognizes the human tau at D_{25}(DRKD$_{26}$QGGYTMHQDQEGDTDAGLK$_{44}$), a known N-terminal truncation protein site (Quinn *et al.*, 2018) previously identified both in cellular and animal Alzheimer's disease paradigms (Corsetti *et al.*, 2008) and in human Alzheimer's disease brains (Rohn *et al.*, 2002; Amadoro *et al.*, 2012; Corsetti *et al.*, 2015)—rescues the neurochemical, anatomical, behavioural and electrophysiological alterations underlying the Alzheimer's disease phenotype in two well-established Tg mouse strains, such as preclinical Tg2576 and 3xTg models. Of particular relevance is the fact that the Tg Tg2576 mice expressing human mutant APP (K670N/M671L), in contrast to 3xTg harbouring PS1(M146V), APP(Swe) and tau(P301L)

transgenes, display an endogenous genetic background of murine not-mutated tau. Furthermore, since treatments started when synaptic deterioration is evident but extensive neurodegeneration has not yet developed turn out to be the most effective in preventing the disease-associated brain atrophy and related cognitive impairment (Bokde *et al.*, 2009; Elmaleh *et al.*, 2019), our experimental evaluations are carried out on symptomatic animals which are employed at early-middle stages (6 months old) of pathology progression, when their hippocampi are not largely compromised with massive neuronal loss. It is also worth underlining that the 12A12mAb we employed in the present study is specific for the pathological truncated tau because it selectively binds *in vivo* the neurotoxic Alzheimer's disease-linked NH$_2$26-230 fragment (i.e. NH$_2$htau) without showing any significant cross-reaction towards the intact, physiological form of protein, in line with our previous investigations (Amadoro *et al.*, 2012). To this point, biochemical and functional outcomes *in vivo* measures further confirm that 12A12mAb: (i) does not specifically interact with the abundant intracellular pool of endogenous normal full-length tau protein whose steady-state level is unchanged in hippocampus after its i.v. delivery in Tg-Alzheimer's disease mice regardless of the genetic backgrounds; (ii) is harmless when injected in healthy, cognitive-intact WT mice, despite the ability of successfully penetrating/reaching the brain in its biologically active (antigen-competent) state under physiological settings. Remarkably, the cleavage-specific 12A12mAb—which selectively binds 20–22 kDa NH$_2$htau without unproductive and deleterious cross-reaction towards the physiological intact tau—appears to be potent tool by providing measurable changes on Alzheimer's disease brain physiopathology which result in significant improvement of the synaptic and cognitive deficits in affected animals, even after its short-term (14 days) i.v. delivery. Conversely, there is proof that the use of other therapeutic anti-tau antibodies binding all forms of tau is more likely to result in considerable reduction of its effective dose available *in vivo* against the target toxic tau species with consequent requirement of more aggressive and prolonged applications (Novak *et al.*, 2018a). Furthermore, our results may have important clinical implications by prospecting the non-invasive i.v. delivery route of 12A12mAb as effective and safe disease-modifying approach in contrasting the earliest neuropathological and cognitive alterations of subjects which suffer the chronically developing human Alzheimer's disease and non-Alzheimer's disease tauopathies characterized by an increased burden of tau truncation. In postmitotic neurons, tau is endowed with important functions beyond the control of microtubule integrity and dynamics (Sotiropoulos *et al.*, 2017) and the treatment with tau-targeting antibodies may have undesirable adverse side-effects due to 'loss of function' of full-length protein (Rosenmann *et al.*, 2006; Rozenstein-Tsalkovich *et al.*, 2013; Bakota *et al.*, 2017). Although we cannot rule out

the later development of gliosis following prolonged immunization regimen, from a translational perspective another interesting finding of the present study is that the sub-chronic i.v. treatment with 12A12mAb is sufficient *per se* to drive a robust therapeutic effect in the absence of increased microglia and astrocyte activation which, on the contrary, appears to be critical for the mechanism of action of at least a few Aβ-directed antibodies (Bard et al., 2000; Wilcock et al., 2004) leading as byproduct to excessive deleterious stimulation of local inflammatory response (Lemere, 2013; Wisniewski and Goni, 2015). We find no obvious evidence of neuroinflammatory response which is known to cause mortality in WT mice when actively immunized with various fragments of tau (Rosenmann et al., 2006; Rozenstein-Tsalkovich et al., 2013). Furthermore, the evidence that passive immunization with 12A12mAb can normalize *in vivo* the APP/Aβ dysmetabolism in two independent genetic backgrounds overexpressing human mutated APP (K670N/M671L) not only unveils a novel and potential connection between tau and APP/Aβ, whereby toxic tau can upstream affect APP/Aβ pathology in damaging synapses, but also—and more importantly—highlights the 20–22 kDa NH_2-terminal tau fragment as crucial target for Alzheimer's disease therapy starting from its earliest stages which are characterized by initial disruption of synaptic functions in the absence of frank neuronal loss. Therefore, this study prospects the peripheral administration of the humanized counterpart of murine 12A12mAb as a novel, promising multi-targeted intervention in preventing disease-associated cognitive deterioration in human beings suffering Alzheimer's disease-related dementias, being endowed with higher clinical potentialities than those altering either neuropathology alone (Oddo et al., 2006; Rosenmann et al., 2006; Lambracht-Washington and Rosenberg, 2013; Bakota et al., 2017).

Concerning the mechanism(s) of action involved in the beneficial power of 12A12mAb immunization, in the present study, we are unable to anticipate whether tau-directed therapeutic effects offered by i.v. delivery of 12A12mAb involve only the extracellular or both intracellular and extracellular pool of toxic truncated tau because we did not collect and analyse the level of NH_2htau fragment in CSF or interstitial fluid and plasma. It is worth noting that the N-terminal, but not C-terminal, fragments of tau including the 20–22 kDa NH_2htau form(s), are mainly secreted from synaptosomes of Alzheimer's disease brains (Sokolow et al., 2015) and detected both in CSF from Alzheimer's disease patients (Johnson et al., 1997; Portelius et al., 2008; Meredith et al., 2013; Amadoro et al., 2014; Chen et al., 2019; Cicognola et al., 2019) and in conditioned media from patient-derived induced pluripotent stem cells cortical neurons (Bright et al., 2015; Kanmert et al., 2015; Sato et al., 2018). The $NH_2$26-44 amino acidic stretch, which is the minimal biological active moiety of parental 20–22 kDa NH_2-truncated tau form(s) (Amadoro et al., 2010,

2012; Corsetti et al., 2015) has been recently recognized as one among the potentially targetable tau epitopes for promising Alzheimer's disease immunotherapeutic interventions, being largely represented into CSF samples (Barthélemy et al., 2016a, b; Sato et al., 2018) and in autoptic specimens from affected subjects (Borreca et al., 2018). Interestingly, previous *in vitro*, *ex vivo* and *in vivo* experiments from our research group have demonstrated that this short peptide when extracellularly administered to hippocampal neurons dynamically perturbs the plasma membranes—mainly of distal axonal compartments (Perini et al., 2019)—by exerting a deleterious action on synaptic connectivity and plasticity being more likely internalized only after prolonged incubation times (Florenzano et al., 2017; Borreca et al., 2018). Moreover, studies have shown that tau antibodies can be readily taken up by neurons, promote the intracellular sequestration/clearance of pathological species by means of different mechanisms and prevent their release into the extracellular space followed by consequent spreading throughout the brain (Asuni et al., 2007; Krishnamurthy et al., 2011; Congdon et al., 2013; Gu et al., 2013; Collin et al., 2014; Pedersen and Sigurdsson, 2015; Shamir et al., 2016). After its i.v. administration in both healthy and disease mice, the 12A12mAb in circulation seems to be able to successfully penetrate the hippocampus and engage *in vivo* its target at a sufficient level to exert biologically relevant neuroprotective effects. The N-terminal region of tau, despite the lack of the microtubule binding domains which abnormally aggregate to form paired helical filaments, is able to undergo higher order of oligomerization (Feinstein et al., 2016) and, in this framework, the binding of 12A12mAb to the NH_2htau may also prevent the trans-synaptic propagation of detrimental insoluble tau. Therefore, both extracellular and intracellular interaction between 12A12mAb and the NH_2htau might be plausible routes by which immunization directed against this harmful, Alzheimer's disease-relevant N-truncated tau specie(s) operates *in vivo*. Furthermore, although the immune system has been increasingly recognized as an important player in the immunotherapeutic approaches (Congdon and Sigurdsson, 2018; Katsinelos et al., 2019), the finding that the cognitive skills improvement of 12A12mAb-injected Alzheimer's disease Tg mice are paralleled by a strong and concomitant reduction of the disease-associated cerebral level of reactive gliosis further supports recent results showing that (i) antibody-mediated targeting of pathological tau *in vivo* does not necessarily required engagement of microglia that may *per se* induce deleterious neuroinflammation (Lee et al., 2016); (ii) the neuroprotective mechanism action evoked by tau-based immunotherapy is more likely to rely on the direct neutralization of toxic extracellular species and/or on preventing their uptake by neurons (Congdon et al., 2013; Gu et al., 2013). In this regard, glial activation and neuroinflammation have been reported to severely impact on tau pathology

directly, by participating to tau aggregation and degradation and spreading (Asai *et al.*, 2015; Yuan *et al.*, 2016; Bolos *et al.*, 2017; Hopp *et al.*, 2018), or indirectly, through a non-cell autonomous effect on neuronal signalling via cytokine and complement factor and gliotransmitter secretion (Liddelow *et al.*, 2017; Piacentini *et al.*, 2017; Litvinchuk *et al.*, 2018) and up-regulation of senescence-associated genes (Bussian *et al.*, 2018) and synapses pruning (Marttinen *et al.*, 2018; Vogels *et al.*, 2019).

Another challenging question is whether the neuroprotection offered by 12A12mAb can be further ameliorated *in vivo* following its prolonged administration, especially in more severe 3xTg animal model, or sustained even after its discontinuing immunization. Further investigations will be needed to better clarify the dose-dependent effect of 12A12mAb treatment on pathology and cognitive performance of Alzheimer's disease Tg mice and how long the beneficial effect can last beyond the period of the immunization.

It is also worth stressing that—although mouse and human tau amino acidic sequences are similar—there are 14 amino acid differences in the N-terminal region (Andorfer *et al.*, 2003; Bright *et al.*, 2015; Hernandez *et al.*, 2019). Nevertheless, the extreme N-terminal sequence of tau protein starting at D25 encompasses a not-canonical caspase(s) cleavage-site sequence (McStay *et al.*, 2008; Kumar *et al.*, 2014) which has been identified both in cellular (human SY5Y and rat PC12) and animal (Alzheimer's disease11 mice) Alzheimer's disease models (Rohn *et al.*, 2002; Corsetti *et al.*, 2008) and in human Alzheimer's disease brains (Rohn *et al.*, 2002; Amadoro *et al.*, 2012; Quinn *et al.*, 2018). Moreover results from *in vitro* experiments and Tg animal models have shown that truncation plays a causative role in remodelling the highly flexible conformational ensemble of intrinsically disordered protein tau into Alzheimer's disease-like pathological conformations (Novak *et al.*, 2018b). Conformational changes involving the amino-terminus of tau early occur in Alzheimer's disease and other related tauopathies (Garcia-Sierra *et al.*, 2003). Consistently, Mukrasch *et al.*, have demonstrated that—although the largest part of tau441 amino acid sequence is devoid of any ordered structure—the N-terminal 50 residues of protein favour a compact conformation, as indicated by strong contacts within the residue stretch 1–20 and from this region to residues 30–50 (Mukrasch *et al.*, 2009). Therefore it is reasonable to hypothesize that, although the amino acid sequence of human and murine tau surrounding this epitope is divergent, 12A12mAb is more likely to recognize the newly generated, sequence- and structural-based immunoreactive determinants whose formation requires pathological truncation occurring under Alzheimer's disease conditions at D25 residue both in human and rodent tau (Rohn *et al.*, 2002; Corsetti *et al.*, 2008; Quinn *et al.*, 2018; Amadoro *et al.*, 2019). In support of this finding and in line with the experimental evidence that temporary secondary structures occur in

causal relation with tau neuropathology progression, both in isolated domains of the full-length protein and of some of its fragments (Mukrasch *et al.*, 2009; Avila *et al.*, 2016b; Fichou *et al.*, 2019), by means of molecular dynamics (MD) simulations and SAXS experiments, we have recently demonstrated that the short sequence including the 26–44 of N-terminal region of human tau—but not its reverse counterpart (tau44-26 peptide)—undergoes isolated β-bridges, α-helices and 3-helix which involve the Y29, T30, Q33, D34, Q35, E36 amino acid residues (Perini *et al.*, 2019). Importantly, these amino acid residues are present both in murine and primate tau sequence. Besides, the fact that 12A12mAb does not change the expression level of full-length tau but selectively reduces the endogenously produced 20–22 kDa tau fragment in both Alzheimer's disease strains, as we showed in western blotting Figs 2 and 3, further strengthens the notion that a local conformational element (i.e. sequence- and structure-based immunoreactive epitope) is more likely to underlie its *in vivo* specificity in targeting the neo-epitope of the N-derived truncated pathological tau specie(s), both in human and mouse. Finally, since the epitopes cannot be predicted reliably from antigen primary amino acid sequences because some novel epitopes can arise exclusively due to the alteration of the molecule's conformation (Opuni *et al.*, 2018), further experiments of immunoprecipitation followed by mass spectrometry and alanine epitope scanning mapping are needed to identify the crucial binding residues and the precise structure of N-terminal of tau protein that are directly involved in the interaction with 12A12mAb.

Concerning the interplay occurring *in vivo* between APP/Aβ and tau pathologies, according to the classical Aβ cascade hypothesis aberrant changes of tau metabolism are considered downstream of Aβ pathology which acts as initial trigger (Hardy and Selkoe, 2002; De Strooper and Karran, 2016). Consistently, compelling studies have demonstrated that Aβ can potentiate tau abnormalities (Gotz *et al.*, 2001; Lewis *et al.*, 2001; Oddo *et al.*, 2004; Bolmont *et al.*, 2007) and that an enhanced neuropathology occurs following *in vivo* interaction between Aβ and tau (Gotz *et al.*, 2001; Lewis *et al.*, 2001; Hurtado *et al.*, 2010; Bennett *et al.*, 2017; Pontecorvo *et al.*, 2017; He *et al.*, 2018; Jacobs *et al.*, 2018; Quiroz *et al.*, 2018). In this regard, our findings highlighting a novel mechanistic interplay between APP/Aβ and tau at synapses fit more well with other studies showing that changes in tau metabolism precede Aβ pathology in aged and Alzheimer's disease brains (Braak and Del Tredici, 2004; Schonheit *et al.*, 2004; Braak *et al.*, 2013; Jack *et al.*, 2013) and that the removal of pathogenetic species of tau can prevent *in vivo* the deleterious effect of both Aβ and tau (Oddo *et al.*, 2006; Castillo-Carranza *et al.*, 2015; Dai *et al.*, 2017, 2018; Rajamohamedsait *et al.*, 2017). Remarkably, the spreading/propagation of tau neuropathology into the Aβ plaque-bearing cerebral cortex is associated with the

transition from the preclinical (asymptomatic) to the clinical (symptomatic) stage of Alzheimer's disease (Delacourte *et al.*, 1999; Wang *et al.*, 2016; Pontecorvo *et al.*, 2017). Furthermore, although the tau pathology to evolve to full-blown Alzheimer's disease requires the concomitant presence of Aβ pathology (Braak and Del Tredici, 2011; Duyckaerts, 2011; Jack *et al.*, 2013; Crary *et al.*, 2014), the failure of anti-Aβ therapies in preventing the disease progression suggests that Alzheimer's disease pathogenesis might be driven by tau independently of Aβ (Giacobini and Gold, 2013). However, whether Aβ is necessary for tau neurotoxicity or whether the reverse is true is still an open question (Ashe and Zahs, 2010). On the other hand, recent data also suggest that tau and Aβ may be independent processes and reciprocally interact over the evolution of Alzheimer's disease (Small and Duff, 2008; Mondragón-Rodríguez *et al.*, 2010). In this context, co-occurrence between tau and Aβ within neuronal processes and synaptic compartments has been described in Alzheimer's disease (Hoover *et al.*, 2010; Ittner *et al.*, 2010; Zempel *et al.*, 2010; Amadoro *et al.*, 2012; Miller *et al.*, 2014) and synaptic abnormalities occur in aging Tg2576 and 3xTg mice (Spires-Jones *et al.*, 2007; Nisticò *et al.*, 2012; Ameen-Ali *et al.*, 2017). Aβ and tau pathologies exert synergistic effects on neuronal morphology/function (Rhein *et al.*, 2009) particularly at synapses (Hoover *et al.*, 2010; Ittner *et al.*, 2010; Takahashi *et al.*, 2010; Amadoro *et al.*, 2012) believed to initiate Alzheimer's disease progression (Selkoe, 2002), indicating that passive immunization with 12A12mAb can contribute to improve disease-associated mnestic disabilities at its early phases by preventing both pathognomonic toxic proteins from damaging synaptic connectivity in pathologically relevant vulnerable neuronal circuits. Furthermore, a recent hypothesis also suggests that synaptic dysfunction in Alzheimer's disease is triggered by impairment of APP metabolism which further progresses via tau pathology (Gulisano *et al.*, 2018; Kametani and Hasegawa, 2018; Schreurs *et al.*, 2018). Consistently, an increased level of APP and/or its C-terminal fragments are able to induce axonal and synaptic defects (Rusu *et al.*, 2007; Rodrigues *et al.*, 2012; Deyts *et al.*, 2016; Xu *et al.*, 2016) associated with mis-localization of tau (Blurton-Jones and Laferla, 2006; Hochgrafe *et al.*, 2013). Overexpression of APP promotes *per se* the seeded aggregation of intracellular tau in cultured cell, suggesting that APP, rather than Aβ, can work as a receptor of abnormal tau fibrils (Takahashi *et al.*, 2015) by accelerating *in vivo* internalization in neurons (Holmes *et al.*, 2013; Mirbaha *et al.*, 2015) followed by pathological accumulation and propagation. Besides, both soluble/prefibrillar extracellular toxic Aβ and tau can damage the synaptic terminals in APP-dependent manner (Puzzo *et al.*, 2017; Wang *et al.*, 2017), suggesting a translation potential of 12A12mAb for APP-targeted therapy in patients.

Concerning the routes by which the 12A12mAb-mediated removal of the NH_2htau can affect the cross-talk between Aβ and tau neuropathology or interfere upstream with APP metabolism and/or its processing *in vivo*, both cell- and non-cell autonomous action mechanisms (Alasmari *et al.*, 2018) should be taken into account by operating in alternative but not mutually exclusive manners and by acting at different transcriptional (Bright *et al.*, 2015; Zhang *et al.*, 2018), translation (Asuni *et al.*, 2014; Borreca *et al.*, 2016; Meier *et al.*, 2016; Koren *et al.*, 2019) and post-translational (Amadoro *et al.*, 2012) levels. Furthermore, variations in the type of mechanism(s) engaged *in vivo* by 12A12mAb in two APP mouse models analysed and/or dissimilarity in their temporal progression of plaque deposition (Ameen-Ali *et al.*, 2017) are more likely to account for the difference in the magnitude of antibody effect(s) on APP/Aβ mis-processing. At the present, *in vitro*, *ex vivo* and *in vivo* experiments are being performed by our research group to better clarify this important issue.

In conclusion, the present investigation not only highlights a novel dynamic positive feed-forward regulation between APP/Aβ and N-truncated tau *in vivo* by reinforcing the concept of pathological tau as main therapeutic target of Alzheimer's disease but also hopefully helps to design more efficacious and safety tau-directed interventions by prospecting the 12A12mAb as beneficial and disease-modifying approach for the cure of Alzheimer's disease and other tauopathies.

Supplementary material

Supplementary material is available at *Brain Communications* online.

Acknowledgements

Funding

funders had no role in study design, data collection and analysis, decision to publish or preparation of manuscript.

Competing interests

References

Agadjanyan MG, Zagorski K, Petrushina I, Davtyan H, Kazarian K, Antonenko M, et al. Humanized monoclonal antibody armanezumab specific to N-terminus of pathological tau: characterization and therapeutic potency. Mol Neurodegener 2017; 12: 33.

Akkerman S, Prickaerts J, Steinbusch HW, Blokland A. Object recognition testing: statistical considerations. Behav Brain Res 2012; 232: 317–22.

Akkerman S, Blokland A, Reneerkens O, van Goethem NP, Bollen E, Gijselaers HJ, et al. Object recognition testing: methodological considerations on exploration and discrimination measures. Behav Brain Res 2012; 232: 335–47.

Alasmari F, Alshammari MA, Alasmari AF, Alanazi WA, Alhazzani K. Neuroinflammatory cytokines induce amyloid beta neurotoxicity through modulating amyloid precursor protein levels/metabolism. Biomed Res Int 2018; 2018: 1–8.

Amadoro G, Latina V, Corsetti V, Calissano P. N-terminal tau truncation in the pathogenesis of Alzheimer's Disease (AD): developing a novel diagnostic and therapeutic approach. Biochim Biophys Acta 2020; 1866: 165584.

Amadoro G, Corsetti V, Sancesario GM, Lubrano A, Melchiorri G, Bernardini S, et al. Cerebrospinal fluid levels of a 20-22 kDa NH$_2$ fragment of human tau provide a novel neuronal injury biomarker in Alzheimer's disease and other dementias. J Alzheimers Dis 2014; 42: 211–26.

Amadoro G, Corsetti V, Atlante A, Florenzano F, Capsoni S, Bussani R, et al. Interaction between NH$_{(2)}$-tau fragment and Aβ in Alzheimer's disease mitochondria contributes to the synaptic deterioration. Neurobiol Aging 2012; 33: 833.e1–25.

Amadoro G, Corsetti V, Stringaro A, Colone M, D'Aguanno S, Meli G, et al. A NH$_2$ tau fragment targets neuronal mitochondria at AD synapses: possible implications for neurodegeneration. J Alzheimers Dis 2010; 21: 445–70.

Amadoro G, Ciotti MT, Costanzi M, Cestari V, Calissano P, Canu N. NMDA receptor mediates tau-induced neurotoxicity by calpain and ERK/MAPK activation. Proc Natl Acad Sci USA 2006; 103: 2892–7.

Amadoro G, Serafino AL, Barbato C, Ciotti MT, Sacco A, Calissano P, et al. Role of N-terminal tau domain integrity on the survival of cerebellar granule neurons. Cell Death Differ 2004; 11: 217–30.

Amar F, Sherman MA, Rush T, Larson M, Boyle G, Chang L, et al. The amyloid-β oligomer Aβ*56 induces specific alterations in neuronal signaling that lead to tau phosphorylation and aggregation. Sci Signal 2017; 10: eaal2021.

Ameen-Ali KE, Wharton SB, Simpson JE, Heath PR, Sharp P, Berwick J. Review: neuropathology and behavioural features of transgenic murine models of Alzheimer's disease. Neuropathol Appl Neurobiol 2017; 43: 553–70.

Andorfer C, Kress Y, Espinoza M, de Silva R, Tucker KL, Barde YA, et al. Hyperphosphorylation and aggregation of tau in mice expressing normal human tau isoforms. J Neurochem 2003; 86: 582–90.

Antunes M, Biala G. The novel object recognition memory: neurobiology, test procedure, and its modifications. Cogn Process 2012; 13: 93–110.

Arriagada PV, Growdon JH, Hedley-Whyte ET, Hyman BT. Neurofibrillary tangles but not senile plaques parallel duration and severity of Alzheimer's disease. Neurology 1992; 42: 631–9.

Asai H, Ikezu S, Tsunoda S, Medalla M, Luebke J, Haydar T, et al. Depletion of microglia and inhibition of exosome synthesis halt tau propagation. Nat Neurosci 2015; 18: 1584–93.

Ashe KH, Zahs KR. Probing the biology of Alzheimer's disease in mice. Neuron 2010; 66: 631–45.

Asuni AA, Guridi M, Pankiewicz JE, Sanchez S, Sadowski MJ. Modulation of amyloid precursor protein expression reduces β-amyloid deposition in a mouse model. Ann Neurol 2014; 75: 684–99.

Asuni AA, Boutajangout A, Quartermain D, Sigurdsson EM. Immunotherapy targeting pathological tau conformers in a tangle mouse model reduces brain pathology with associated functional improvements. J Neurosci 2007; 27: 9115–29.

Avila J, Pallas N, Bolós M, Sayas CL, Hernandez F. Intracellular and extracellular microtubule associated protein tau as a therapeutic target in Alzheimer disease and other tauopathies. Expert Opin Ther Targets 2016; 20: 653–61.

Avila J, Jiménez JS, Sayas CL, Bolós M, Zabala JC, Rivas G, et al. Tau structures. Front Aging Neurosci 2016b; 8: 262.

Bakota L, Ussif A, Jeserich G, Brandt R. Systemic and network functions of the microtubule-associated protein tau: Implications for tau-based therapies. Mol Cell Neurosci 2017; 84: 132–41.

Bard F, Cannon C, Barbour R, Burke RL, Games D, Grajeda H, et al. Peripherally administered antibodies against amyloid beta-peptide enter the central nervous system and reduce pathology in a mouse model of Alzheimer's disease. Nat Med 2000; 6: 916–9.

Barthélemy NR, Fenaille F, Hirtz C, Sergeant N, Schraen-Maschke S, Vialaret J, et al. Tau protein quantification in human cerebrospinal fluid by targeted mass spectrometry at high sequence coverage provides insights into its primary structure heterogeneity. J Proteome Res 2016a; 15: 667–76.

Barthélemy NR, Gabelle A, Hirtz C, Fenaille F, Sergeant N, Schraen-Maschke S, et al. Differential mass spectrometry profiles of tau protein in the cerebrospinal fluid of patients with Alzheimer's disease, progressive supranuclear palsy, and dementia with lewy bodies. J Alzheimers Dis 2016b; 51: 1033–43.

Bellucci A, Westwood AJ, Ingram E, Casamenti F, Goedert M, Spillantini MG. Induction of inflammatory mediators and microglial activation in mice transgenic for mutant human P301S tau protein. Am J Pathol 2004; 165: 1643–52.

Bengoetxea X, Rodriguez-Perdigon M, Ramirez M. Object recognition test for studying cognitive impairments in animal models of Alzheimer's disease. Front Biosci 2015; 7: 10–29.

Bennett IJ, Stark SM, Stark C. Recognition memory dysfunction relates to hippocampal subfield volume: a study of cognitively normal and mildly impaired older adults. J Gerontol B Psychol Sci Soc Sci 2019; 74: 1132–41.

Bennett RE, DeVos SL, Dujardin S, Corjuc B, Gor R, Gonzalez J, et al. Enhanced tau aggregation in the presence of amyloid β. Am J Pathol 2017; 187: 1601–12.

Bevins RA, Besheer J. Object recognition in rats and mice: a one-trial non-matching-to-sample learning task to study 'recognition memory'. Nat Protoc 2006; 1: 1306–11.

Bittner T, Fuhrmann M, Burgold S, Ochs SM, Hoffmann N, Mitteregger G, et al. Multiple events lead to dendritic spine loss in triple transgenic Alzheimer's disease mice. PLoS One 2010; 5: e15477.

Biundo F, Del Prete D, Zhang H, Arancio O, D'Adamio LA. Role for tau in learning, memory and synaptic plasticity. Sci Rep 2018; 8: 3184.

Blair LJ, Frauen HD, Zhang B, Nordhues BA, Bijan S, Lin YC, et al. Tau depletion prevents progressive blood-brain barrier damage in a mouse model of tauopathy. Acta Neuropathol Commun 2015; 3: 8.

Block ML, Zecca L, Hong JS. Microglia-mediated neurotoxicity: uncovering the molecular mechanisms. Nat Rev Neurosci 2007; 8: 57–69.

Bloom GS. Amyloid-β and tau: the trigger and bullet in Alzheimer disease pathogenesis. JAMA Neurol 2014; 71: 505–8.

Blurton-Jones M, Laferla FM. Pathways by which Abeta facilitates tau pathology. Curr Alzheimer Res 2006; 3: 437–48.

Bokde AL, Ewers M, Hampel H. Assessing neuronal networks: understanding Alzheimer's disease. Prog Neurobiol 2009; 89: 125–33.

Bolmont T, Clavaguera F, Meyer-Luehmann M, Herzig MC, Radde R, Staufenbiel M, et al. Induction of tau pathology by intracerebral infusion of amyloid-beta -containing brain extract and by amyloid-beta deposition in APP x Tau transgenic mice. Am J Pathol 2007; 171: 2012–20.

Bolós M, Perea JR, Avila J. Alzheimer's disease as an inflammatory disease. Biomol Concepts 2017; 8: 37–43.

Borchelt DR, Savonenko AV. Transgenic mouse models of Alzheimer's disease and episodic-like memory. In: Ekrem Dere AELN, Joseph PH, editors. Handbook of behavioral neuroscience. Elsevier; 2008. p.553–73.

Borreca A, Latina V, Corsetti V, Middei S, Piccinin S, Della Valle F, et al. AD-related N-terminal truncated tau is sufficient to recapitulate in vivo the early perturbations of human neuropathology: implications for immunotherapy. Mol Neurobiol 2018; 55: 8124–53.

Borreca A, Gironi K, Amadoro G, Ammassari-Teule M. Opposite dysregulation of fragile-X mental retardation protein and heteronuclear ribonucleoprotein C protein associates with enhanced APP translation in Alzheimer disease. Mol Neurobiol 2016; 53: 3227–34.

Borroni B, Gardoni F, Parnetti L, Magno L, Malinverno M, Saggese E, et al. Pattern of tau forms in CSF is altered in progressive supranuclear palsy. Neurobiol Aging 2009; 30: 34–40.

Boutajangout A, Ingadottir J, Davies P, Sigurdsson EM. Passive immunization targeting pathological phospho-tau protein in a mouse model reduces functional decline and clears tau aggregates from the brain. J Neurochem 2011; 118: 658–67.

Braak H, Braak E. Neuropathological staging of Alzheimer-related changes. Acta Neuropathol 1991; 82: 239–59.

Braak H, Del Tredici K. The preclinical phase of the pathological process underlying sporadic Alzheimer's disease. Brain 2015; 138: 2814–33.

Braak H, Del Tredici K. The pathological process underlying Alzheimer's disease in individuals under thirty. Acta Neuropathol 2011; 121: 171–81.

Braak H, Del Tredici K. Alzheimer's disease: intraneuronal alterations precede insoluble amyloid-beta formation. Neurobiol Aging 2004; 25: 713–8; discussion 743–6

Braak H, Zetterberg H, Del Tredici K, Blennow K. Intraneuronal tau aggregation precedes diffuse plaque deposition, but amyloid-β changes occur before increases of tau in cerebrospinal fluid. Acta Neuropathol 2013; 126: 631–41.

Brandt R, Léger J, Lee G. Interaction of tau with the neural plasma membrane mediated by tau's amino-terminal projection domain. J Cell Biol 1995; 131: 1327–40.

Bright J, Hussain S, Dang V, Wright S, Cooper B, Byun T, et al. Human secreted tau increases amyloid-b production. Neurobiol Aging 2015; 36: 693–709.

Broadbent NJ, Squire LR, Clark RE. Spatial memory, recognition memory, and the hippocampus. Proc Natl Acad Sci USA 2004; 101: 14515–20.

Busche MA, Wegmann S, Dujardin S, Commins C, Schiantarelli J, Klickstein N, et al. Tau impairs neural circuits, dominating amyloid-β effects, in Alzheimer models in vivo. Nat Neurosci 2019; 22: 57–64.

Bussian TJ, Aziz A, Meyer CF, Swenson BL, van Deursen JM, Baker DJ. Clearance of senescent glial cells prevents tau-dependent pathology and cognitive decline. Nature 2018; 562: 578–82.

Canu N, Dus L, Barbato C, Ciotti MT, Brancolini C, Rinaldi AM, et al. Tau cleavage and dephosphorylation in cerebellar granule neurons undergoing apoptosis. J Neurosci 1998; 18: 7061–74.

Castellani RJ, Perry G, Tau Biology T. Traumatic brain injury, and diagnostic challenges. J Alzheimers Dis 2019; 67: 447–67.

Castillo-Carranza DL, Guerrero-Muñoz MJ, Sengupta U, Hernandez C, Barrett AD, Dineley K, et al. Tau immunotherapy modulates both pathological tau and upstream amyloid pathology in an Alzheimer's disease mouse model. J Neurosci 2015; 35: 4857–68.

Castillo-Carranza DL, Sengupta U, Guerrero-Muñoz MJ, Lasagna-Reeves CA, Gerson JE, Singh G, et al. Passive immunization with Tau oligomer monoclonal antibody reverses tauopathy phenotypes without affecting hyperphosphorylated neurofibrillary tangles. J Neurosci 2014; 34: 4260–72.

Chai X, Wu S, Murray TK, Kinley R, Cella CV, Sims H, et al. Passive immunization with anti-Tau antibodies in two transgenic models: reduction of Tau pathology and delay of disease progression. J Biol Chem 2011; 286: 34457–67.

Chapman PF, White GL, Jones MW, Cooper-Blacketer D, Marshall VJ, Irizarry M, et al. Impaired synaptic plasticity and learning in aged amyloid precursor protein transgenic mice. Nat Neurosci 1999; 2: 271–6.

Chen Z, Mengel D, Keshavan A, Rissman RA, Billinton A, Perkinton M, et al. Learnings about the complexity of extracellular tau aid development of a blood-based screen for Alzheimer's disease. Alzheimers Dement 2019; 15: 487–96.

Cicognola C, Brinkmalm G, Wahlgren J, Portelius E, Gobom J, Cullen NC, et al. Novel tau fragments in cerebrospinal fluid: relation to tangle pathology and cognitive decline in Alzheimer's disease. Acta Neuropathol 2019; 137: 279–96.

Cochran JN, Hall AM, Roberson ED. The dendritic hypothesis for Alzheimer's disease pathophysiology. Brain Res Bull 2014; 103: 18–28.

Collin L, Bohrmann B, Göpfert U, Oroszlan-Szovik K, Ozmen L, Grüninger F. Neuronal uptake of tau/pS422 antibody and reduced progression of tau pathology in a mouse model of Alzheimer's disease. Brain 2014; 137: 2834–46.

Combs B, Kanaan NM. Exposure of the amino terminus of tau is a pathological event in multiple tauopathies. Am J Pathol 2017; 187: 1222–9.

Combs B, Hamel C, Kanaan NM. Pathological conformations involving the amino terminus of tau occur early in Alzheimer's disease and are differentially detected by monoclonal antibodies. Neurobiol Dis 2016; 94: 18–31.

Congdon EE, Sigurdsson EM. Tau-targeting therapies for Alzheimer disease. Nat Rev Neurol 2018; 14: 399–415.

Congdon EE, Gu J, Sait HB, Sigurdsson EM. Antibody uptake into neurons occurs primarily via clathrin-dependent Fcγ receptor endocytosis and is a prerequisite for acute tau protein clearance. J Biol Chem 2013; 288: 35452–65.

Corsetti V, Florenzano F, Atlante A, Bobba A, Ciotti MT, Natale F, et al. NH$_2$-truncated human tau induces deregulated mitophagy in neurons by aberrant recruitment of Parkin and UCHL-1: implications in Alzheimer's disease. Hum Mol Genet 2015; 24: 3058–81.

Corsetti V, Amadoro G, Gentile A, Capsoni S, Ciotti MT, Cencioni MT, et al. Identification of a caspase-derived N-terminal tau fragment in cellular and animal Alzheimer's disease models. Mol Cell Neurosci 2008; 38: 381–92.

Crary JF, Trojanowski JQ, Schneider JA, Abisambra JF, Abner EL, Alafuzoff I, et al. Primary age-related tauopathy (PART): a common pathology associated with human aging. Acta Neuropathol 2014; 128: 755–66.

d'Abramo C, Acker CM, Jimenez HT, Davies P. Tau passive immunotherapy in mutant P301L mice: antibody affinity versus specificity. PLoS One 2013; 8: e62402.

Dai CL, Hu W, Tung YC, Liu F, Gong CX, Iqbal K. Tau passive immunization blocks seeding and spread of Alzheimer hyperphosphorylated Tau-induced pathology in 3 × Tg-AD mice. Alzheimers Res Ther 2018; 10: 13.

Dai CL, Tung YC, Liu F, Gong CX, Iqbal K. Tau passive immunization inhibits not only tau but also Aβ pathology. Alzheimers Res Ther 2017; 9: 1.

Dai C-L, Chen X, Kazim SF, Liu F, Gong C-X, Grundke-Iqbal I, et al. Grundke-Iqbal I, Iqbal K. Passive immunization targeting the N-terminal projection domain of tau decreases tau pathology and improves cognition in a transgenic mouse model of Alzheimer disease and tauopathies. J Neural Transm 2015; 122: 607–17.

Deacon RM, Cholerton LL, Talbot K, Nair-Roberts RG, Sanderson DJ, Romberg C, et al. Age-dependent and -independent behavioral deficits in Tg2576 mice. Behav Brain Res 2008; 189: 126–38.

Deacon RM, Rawlins JN. T-maze alternation in the rodent. Nat Protoc 2006; 1: 7–12.

Debanne D, Guérineau NC, Gähwiler BH, Thompson SM. Paired-pulse facilitation and depression at unitary synapses in rat hippocampus: quantal fluctuation affects subsequent release. J Physiol 1996; 491: 163–76.

Delacourte A, David JP, Sergeant N, Buée L, Wattez A, Vermersch P, et al. The biochemical pathway of neurofibrillary degeneration in aging and Alzheimer's disease. Neurology 1999; 52: 1158–65.

Desikan RS, McEvoy LK, Thompson WK, Holland D, Roddey JC, Blennow K, et al. Alzheimer's disease neuroimaging initiative. Amyloid-*β* associated volume loss occurs only in the presence of phospho-tau. Ann Neurol 2011; 70: 657–61.

De Strooper B, Karran E. The cellular phase of Alzheimer's disease. Cell 2016; 164: 603–15.

deToledo-Morrell L, Stoub TR, Wang C. Hippocampal atrophy and disconnection in incipient and mild Alzheimer's disease. Prog Brain Res 2007; 163: 741–53.

Deyts C, Thinakaran G, Parent AT. APP receptor? To be or not to be. Trends Pharmacol Sci 2016; 37: 390–411.

Díaz-Hernández M, Gómez-Ramos A, Rubio A, Gómez-Villafuertes R, Naranjo JR, Miras-Portugal MT, et al. Tissue-nonspecific alkaline phosphatase promotes the neurotoxicity effect of extracellular tau. J Biol Chem 2010; 285: 32539–48.

Dobrunz LE, Stevens CF. Heterogeneity of release probability, facilitation, and depletion at central synapses. Neuron 1997a; 18: 995–1008.

Dobrunz LE, Huang EP, Stevens CF. Very short-term plasticity in hippocampal synapses. Proc Natl Acad Sci USA 1997; 94: 14843–7.

Doody RS, Thomas RG, Farlow M, Iwatsubo T, Vellas B, Joffe S, et al. Alzheimer's disease cooperative study steering committee; solanezumab study group. phase 3 trials of solanezumab for mild-to-moderate Alzheimer's disease. N Engl J Med 2014; 370: 311–21.

Dorostkar MM, Zou C, Blazquez-Llorca L, Herms J. Analyzing dendritic spine pathology in Alzheimer's disease: problems and opportunities. Acta Neuropathol 2015; 130: 1–19.

Duyckaerts C. Tau pathology in children and young adults: can you still be unconditionally baptist? Acta Neuropathol 2011; 121: 145–7.

Edison P, Archer HA, Gerhard A, Hinz R, Pavese N, Turkheimer FE, et al. Microglia, amyloid, and cognition in Alzheimer's disease: An [11C](R)PK11195-PET and [11C]PIB-PET study. Neurobiol Dis 2008; 32: 412–9.

Elmaleh DR, Farlow MR, Conti PS, Tompkins RG, Kundakovic L, Tanzi RE. Developing effective Alzheimer's disease therapies: clinical experience and future directions. J Alzheimers Dis 2019; 71: 715–32.

Fá M, Puzzo D, Piacentini R, Staniszewski A, Zhang H, Baltrons MA, et al. Extracellular tau oligomers produce an immediate impairment of LTP and memory. Sci Rep 2016; 6: 19393.

Feinstein HE, Benbow SJ, LaPointe NE, Patel N, Ramachandran S, Do TD, et al. Oligomerization of the microtubule-associated protein tau is mediated by its N-terminal sequences: implications for normal and pathological tau action. J Neurochem 2016; 137: 939–54.

Fichou Y, Al-Hilaly YK, Devred F, Smet-Nocca C, Tsvetkov PO, Verelst J, et al. The elusive tau molecular structures: can we translate the recent breakthroughs into new targets for intervention? Acta Neuropathol Commun 2019; 7: 31.

Florenzano F, Veronica C, Ciasca G, Ciotti MT, Pittaluga A, Olivero G, et al. Extracellular truncated tau causes early presynaptic dysfunction associated with Alzheimer's disease and other tauopathies. Oncotarget 2017; 8: 64745–78.

García-Sierra F, Ghoshal N, Quinn B, Berry RW, Binder LI. Conformational changes and truncation of tau protein during tangle evolution in Alzheimer's disease. J Alzheimers Dis 2003; 5: 65–77.

Giacobini E, Gold G. Alzheimer disease therapy–moving from amyloid-*β* to tau. Nat Rev Neurol 2013; 9: 677–86.

Gibb R, Kolb B. A method for vibratome sectioning of Golgi-Cox stained whole rat brain. J Neurosci Methods 1998; 79: 1–4.

Goedert M, Jakes R, Qi Z, Wang JH, Cohen P. Protein phosphatase 2A is the major enzyme in brain that dephosphorylates tau protein phosphorylated by proline-directed protein kinases or cyclic AMP-dependent protein kinase. J Neurochem 1995; 65: 2804–7.

Gómez-Isla T, Price JL, McKeel DW Jr, Morris JC, Growdon JH, Hyman BT. Profound loss of layer II entorhinal cortex neurons occurs in very mild Alzheimer's disease. J Neurosci 1996; 16: 4491–500.

Götz J, Chen F, van Dorpe J, Nitsch RM. Formation of neurofibrillary tangles in P301l tau transgenic mice induced by Abeta 42 fibrils. Science 2001; 293: 1491–5.

Grayson B, Leger M, Piercy C, Adamson L, Harte M, Neill JC. Assessment of disease-related cognitive impairments using the novel object recognition (NOR) task in rodents. Behav Brain Res 2015; 285: 176–93.

Gu J, Congdon EE, Sigurdsson EM. Two novel Tau antibodies targeting the 396/404 region are primarily taken up by neurons and reduce Tau protein pathology. J Biol Chem 2013; 288: 33081–95.

Guillozet AL, Weintraub S, Mash DC, Mesulam MM. Neurofibrillary tangles, amyloid, and memory in aging and mild cognitive impairment. Arch Neurol 2003; 60: 729–36.

Gulisano W, Melone M, Li Puma DD, Tropea MR, Palmeri A, Arancio O, et al. The effect of amyloid-*β* peptide on synaptic plasticity and memory is influenced by different isoforms, concentrations, and aggregation status. Neurobiol Aging 2018; 71: 51–60.

Hammond RS, Tull LE, Stackman RW. On the delay-dependent involvement of the hippocampus in object recognition memory. Neurobiol Learn Mem 2004; 82: 26–34.

Hardy J, Selkoe DJ. The amyloid hypothesis of Alzheimer's disease: progress and problems on the road to therapeutics. Science 2002; 297: 353–6.

He Z, Guo JL, McBride JD, Narasimhan S, Kim H, Changolkar L, et al. Amyloid-*β* plaques enhance Alzheimer's brain tau-seeded pathologies by facilitating neuritic plaque tau aggregation. Nat Med 2018; 24: 29–38.

Hernández F, Cuadros R, Ollá I, García C, Ferrer I, Perry G, et al. Differences in structure and function between human and murine tau. Biochim Biophys Acta Mol Basis Dis 2019; 1865: 2024–30.

Hiramatsu M, Sasaki M, Nabeshima T, Kameyama T. Effects of dynorphin A (1-13) on carbon monoxide-induced delayed amnesia in mice. Pharmacol Biochem Behav 1997; 56: 73–9.

Hochgräfe K, Sydow A, Mandelkow EM. Regulatable transgenic mouse models of Alzheimer disease: onset, reversibility and spreading of Tau pathology. FEBS J 2013; 280: 4371–81.

Holmes BB, DeVos SL, Kfoury N, Li M, Jacks R, Yanamandra K, et al. Heparan sulfate proteoglycans mediate internalization and propagation of specific proteopathic seeds. Proc Natl Acad Sci USA 2013; 110: E3138–E3147.

Honer WG, Dickson DW, Gleeson J, Davies P. Regional synaptic pathology in Alzheimer's disease. Neurobiol Aging 1992; 13: 375–82.

Hoover BR, Reed MN, Su J, Penrod RD, Kotilinek LA, Grant MK, et al. Tau mislocalization to dendritic spines mediates synaptic dysfunction independently of neurodegeneration. Neuron 2010; 68: 1067–81.

Hopp SC, Lin Y, Oakley D, Roe AD, DeVos SL, Hanlon D, et al. The role of microglia in processing and spreading of bioactive tau seeds in Alzheimer's disease. J Neuroinflammation 2018; 15: 269.

Horner CH, Arbuthnott E. Methods of estimation of spine density–are spines evenly distributed throughout the dendritic field? J Anat 1991; 177: 179–84.

Hsiao K, Chapman P, Nilsen S, Eckman C, Harigaya Y, Younkin S, et al. Correlative memory deficits, Abetaelevation, and amyloid plaques in transgenic mice. Science 1996; 274: 99–102.

Hu NW, Corbett GT, Moore S, Klyubin I, O'Malley TT, Walsh DM, et al. Extracellular forms of A*β* and tau from iPSC models of

Alzheimer's disease disrupt synaptic plasticity. Cell Rep 2018; 23: 1932–8.

Hurtado DE, Molina-Porcel L, Iba M, Aboagye AK, Paul SM, Trojanowski JQ, et al. A{beta} accelerates the spatiotemporal progression of tau pathology and augments tau amyloidosis in an Alzheimer mouse model. Am J Pathol 2010; 177: 1977–88.

Ishikawa A, Tokunaga M, Maeda J, Minamihisamatsu T, Shimojo M, Takuwa H, et al. *In Vivo* visualization of tau accumulation, microglial activation, and brain atrophy in a mouse model of tauopathy rTg4510. J Alzheimers Dis 2018; 61: 1037–52.

Ittner LM, Ke YD, Delerue F, Bi M, Gladbach A, van Eersel J, et al. Dendritic function of tau mediates amyloid-beta toxicity in Alzheimer's disease mouse models. Cell 2010; 142: 387–97.

Jack CR Jr, Knopman DS, Jagust WJ, Petersen RC, Weiner MW, Aisen PS, et al. Tracking pathophysiological processes in Alzheimer's disease: an updated hypothetical model of dynamic biomarkers. Lancet Neurol 2013; 12: 207–16.

Jacobs HIL, Hedden T, Schultz AP, Sepulcre J, Perea RD, Amariglio RE, et al. Structural tract alterations predict downstream tau accumulation in amyloid-positive older individuals. Nat Neurosci 2018; 21: 424–31.

Jacobsen JS, Wu CC, Redwine JM, Comery TA, Arias R, Bowlby M, et al. Early-onset behavioral and synaptic deficits in a mouse model of Alzheimer's disease. Proc Natl Acad Sci USA 2006; 103: 5161–6.

Jadhav S, Avila J, Schöll M, Kovacs GG, Kövari E, Skrabana R, et al. A walk through tau therapeutic strategies. Acta Neuropathol Commun 2019; 7: 22.

Johnson GV, Seubert P, Cox TM, Motter R, Brown JP, Galasko D. The tau protein in human cerebrospinal fluid in Alzheimer's disease consists of proteolytically derived fragments. J Neurochem 1997; 68: 430–3.

Jung JH, An K, Kwon OB, Kim HS, Kim JH. Pathway-specific alteration of synaptic plasticity in Tg2576 mice. Mol Cells 2011; 32: 197–201.

Kametani F, Hasegawa M. Reconsideration of amyloid hypothesis and tau hypothesis in Alzheimer's disease. Front Neurosci 2018; 12: 25.

Kanmert D, Cantlon A, Muratore CR, Jin M, O'Malley TT, Lee G, et al. C-terminally truncated forms of tau, but not full-length tau or its C-terminal fragments, are released from neurons independently of cell death. J Neurosci 2015; 35: 10851–65.

Katsinelos T, Tuck BJ, Mukadam AS, McEwan WA. The role of antibodies and their receptors in protection against ordered protein assembly in neurodegeneration. Front Immunol 2019; 10: 1139.

Kim W, Lee S, Hall GF. Secretion of human tau fragments resembling CSF-tau in Alzheimer's disease is modulated by the presence of the exon 2 insert. FEBS Lett 2010; 584: 3085–8.

King DL, Arendash GW. Behavioral characterization of the Tg2576 transgenic model of Alzheimer's disease through 19 months. Physiol Behav 2002; 75: 627–42.

King ME, Kan HM, Baas PW, Erisir A, Glabe CG, Bloom GS. Tau-dependent microtubule disassembly initiated by prefibrillar beta-amyloid. J Cell Biol 2006; 175: 541–6.

Knobloch M, Mansuy IM. Dendritic spine loss and synaptic alterations in Alzheimer's disease. Mol Neurobiol 2008; 37: 73–82.

Kontsekova E, Zilka N, Kovacech B, Skrabana R, Novak M. Identification of structural determinants on tau protein essential for its pathological function: novel therapeutic target for tau immunotherapy in Alzheimer's disease. Alzheimers Res Ther 2014 6: 45.

Korb E, Finkbeiner S. Arc in synaptic plasticity: from gene to behavior. Trends Neurosci 2011; 34: 591–8.

Kordower JH, Chu Y, Stebbins GT, DeKosky ST, Cochran EJ, Bennett D, et al. Loss and atrophy of layer II entorhinal cortex neurons in elderly people with mild cognitive impairment. Ann Neurol 2001; 49: 202–13.

Koren SA, Hamm MJ, Meier SE, Weiss BE, Nation GK, Chishti EA, et al. Tau drives translational selectivity by interacting with ribosomal proteins. Acta Neuropathol 2019; 137: 571–83.

Krishnamurthy PK, Deng Y, Sigurdsson EM. Mechanistic studies of antibody-mediated clearance of tau aggregates using an ex vivo brain slice model. Front Psychiatry 2011; 2: 59.

Kumar S, van Raam BJ, Salvesen GS, Cieplak P. Caspase cleavage sites in the human proteome: CaspDB, a database of predicted substrates. PLoS One 2014; 9: e110539.

Lambracht-Washington D, Rosenberg RN. Anti-amyloid beta to tau-based immunization: developments in immunotherapy for Alzheimer disease. Immunotargets Ther 2013; 2013: 105–14.

Lanté F, Chafai M, Raymond EF, Pereira AR, Mouska X, Kootar S, et al. Subchronic glucocorticoid receptor inhibition rescues early episodic memory and synaptic plasticity deficits in a mouse model of Alzheimer's disease. Neuropsychopharmacology 2015; 40: 1772–81.

Lanz TA, Carter DB, Merchant KM. Dendritic spine loss in the hippocampus of young PDAPP and Tg2576 mice and its prevention by the ApoE2 genotype. Neurobiol Dis 2003; 13: 246–53.

Lasagna-Reeves CA, Castillo-Carranza DL, Sengupta U, Guerrero-Munoz MJ, Kiritoshi T, Neugebauer V, et al. Alzheimer brain-derived tau oligomers propagate pathology from endogenous tau. Sci Rep 2012; 2: 700.

Lasagna-Reeves CA, Castillo-Carranza DL, Sengupta U, Clos AL, Jackson GR, Kayed R. Tau oligomers impair memory and induce synaptic and mitochondrial dysfunction in wild-type mice. Mol Neurodegener 2011; 6: 39.

Lee DC, Rizer J, Selenica ML, Reid P, Kraft C, Johnson A, et al. LPS-induced inflammation exacerbates phospho-tau pathology in rTg4510 mice. J Neuroinflammation 2010; 7: 56.

Lee SH, Le Pichon CE, Adolfsson O, Gafner V, Pihlgren M, Lin H, et al. Antibody-mediated targeting of tau *in vivo* does not require effector function and microglial engagement. Cell Rep 2016; 16: 1690–700.

Leger M, Quiedeville A, Bouet V, Haelewyn B, Boulouard M, Schumann-Bard P, et al. Object recognition test in mice. Nat Protoc 2013; 8: 2531–7.

Lemere CA. Immunotherapy for Alzheimer's disease: hoops and hurdles. Mol Neurodegener 2013; 8: 36.

Lesburguères E, Tsokas P, Sacktor TC, Fenton AA. The object context-place-location paradigm for testing spatial memory in mice. Bio Protoc 2017; 7. pii: e2231.

Leuner B, Falduto J, Shors TJ. Associative memory formation increases the observation of dendritic spines in the hippocampus. J Neurosci 2003; 23: 659–65.

Lewis J, Dickson DW, Lin WL, Chisholm L, Corral A, Jones G, Yen SH, et al. Enhanced neurofibrillary degeneration in transgenic mice expressing mutant tau and APP. Science 2001; 293: 1487–91.

Leyns CEG, Holtzman DM. Glial contributions to neurodegeneration in tauopathies. Mol Neurodegener 2017; 12: 50.

Li C, Götz J. Tau-based therapies in neurodegeneration: opportunities and challenges. Nat Rev Drug Discov 2017; 16: 863–83.

Liddelow SA, Guttenplan KA, Clarke LE, Bennett FC, Bohlen CJ, Schirmer L, et al. Neurotoxic reactive astrocytes are induced by activated microglia. Nature 2017; 541: 481–7.

Litvinchuk A, Wan YW, Swartzlander DB, Chen F, Cole A, Propson NE, et al. Complement C3aR inactivation attenuates tau pathology and reverses an immune network deregulated in tauopathy models and Alzheimer's disease. Neuron 2018; 100: 1337–53.e5.

Mably AJ, Kanmert D, Mc Donald JM, Liu W, Caldarone BJ, Lemere CA, et al. Tau immunization: a cautionary tale? Neurobiol Aging 2015; 36: 1316–32.

Manabe T, Wyllie DJ, Perkel DJ, Nicoll RA. Modulation of synaptic transmission and long-term potentiation: effects on paired pulse facilitation and EPSC variance in the CA1 region of the hippocampus. J Neurophysiol 1993; 70: 1451–9.

Manns JR, Eichenbaum H. A cognitive map for object memory in the hippocampus. Learn Mem 2009; 16: 616–24.

Markesbery WR. Neuropathologic alterations in mild cognitive impairment: a review. J Alzheimers Dis 2010; 19: 221–8.

Markesbery WR, Schmitt FA, Kryscio RJ, Davis DG, Smith CD, Wekstein DR. Neuropathologic substrate of mild cognitive impairment. Arch Neurol 2006; 63: 38–46.

Marttinen M, Takalo M, Natunen T, Wittrahm R, Gabbouj S, Kemppainen S, et al. Molecular mechanisms of synaptotoxicity and neuroinflammation in Alzheimer's disease. Front Neurosci 2018; 12: 963.

McStay GP, Salvesen GS, Green DR. Overlapping cleavage motif selectivity of caspases: implications for analysis of apoptotic pathways. Cell Death Differ 2008; 15: 322–31.

Medina M, Avila J. New perspectives on the role of tau in Alzheimer's disease. Implications for therapy. Biochem Pharmacol 2014a; 88: 540–7.

Medina M, Avila J. The role of extracellular Tau in the spreading of neurofibrillary pathology. Front Cell Neurosci 2014b; 8: 113.

Meier S, Bell M, Lyons DN, Rodriguez-Rivera J, Ingram A, Fontaine SN, et al. Pathological tau promotes neuronal damage by impairing ribosomal function and decreasing protein synthesis. J Neurosci 2016; 36: 1001–7.

Meredith JE Jr, Sankaranarayanan S, Guss V, Lanzetti AJ, Berisha F, Neely RJ, et al. Characterization of novel CSF Tau and ptau biomarkers for Alzheimer's disease. PLoS One 2013; 8: e76523.

Miller EC, Teravskis PJ, Dummer BW, Zhao X, Huganir RL, Liao D. Tau phosphorylation and tau mislocalization mediate soluble Aβ oligomer-induced AMPA glutamate receptor signaling deficits. Eur J Neurosci 2014; 39: 1214–24.

Mirbaha H, Holmes BB, Sanders DW, Bieschke J, Diamond MI. Tau trimers are the minimal propagation unit spontaneously internalized to seed intracellular aggregation. J Biol Chem 2015; 290: 14893–903.

Mondragón-Rodríguez S, Basurto-Islas G, Lee HG, Perry G, Zhu X, Castellani RJ, et al. Causes versus effects: the increasing complexities of Alzheimer's disease pathogenesis. Expert Rev Neurother 2010; 10: 683–91.

Mohamed NV, Herrou T, Plouffe V, Piperno N, Leclerc N. Spreading of tau pathology in Alzheimer's disease by cell-to-cell transmission. Eur J Neurosci 2013; 37: 1939–48.

Mukrasch MD, Bibow S, Korukottu J, Jeganathan S, Biernat J, Griesinger C, et al. Structural polymorphism of 441-residue tau at single residue resolution. PLoS Biol 2009; 7: e34.

Murray ME, Lowe VJ, Graff-Radford NR, Liesinger AM, Cannon A, Przybelski SA, et al. Clinicopathologic and 11C-Pittsburgh compound B implications of Thal amyloid phase across the Alzheimer's disease spectrum. Brain 2015; 138: 1370–81.

Nelson PT, Alafuzoff I, Bigio EH, Bouras C, Braak H, Cairns NJ, et al. Correlation of Alzheimer disease neuropathologic changes with cognitive status: a review of the literature. J Neuropathol Exp Neurol 2012; 71: 362–81.

Nisbet RM, Polanco JC, Ittner LM, Götz J. Tau aggregation and its interplay with amyloid-β. Acta Neuropathol 2015; 129: 207–20.

Nisticò R, Pignatelli M, Piccinin S, Mercuri NB, Collingridge G. Targeting synaptic dysfunction in Alzheimer's disease therapy. Mol Neurobiol 2012; 46: 572–87.

Nobili A, Latagliata EC, Viscomi MT, Cavallucci V, Cutuli D, Giacovazzo G, et al. Dopamine neuronal loss contributes to memory and reward dysfunction in a model of Alzheimer's disease. Nat Commun 2017; 8: 14727.

Novak P, Kontsekova E, Zilka N, Novak M. Ten years of tau-targeted immunotherapy: the path walked and the roads ahead. Front Neurosci 2018a; 12: 798.

Novak P, Cehlar O, Skrabana R, Novak M. Tau conformation as a target for disease-modifying therapy: the role of truncation. J Alzheimers Dis 2018b; 64: S535–46.

Nussbaum JM, Schilling S, Cynis H, Silva A, Swanson E, Wangsanut T, et al. Prion-like behaviour and tau-dependent cytotoxicity of pyroglutamylated amyloid-β. Nature 2012; 485: 651–5.

Oddo S, Caccamo A, Tran L, Lambert MP, Glabe CG, Klein WL, et al. Temporal profile of amyloid-beta (Abeta) oligomerization in an *in vivo* model of Alzheimer disease. A link between Abeta and tau pathology. J Biol Chem 2006; 281: 1599–604.

Oddo S, Billings L, Kesslak JP, Cribbs DH, LaFerla FM. Abeta immunotherapy leads to clearance of early, but not late, hyperphosphorylated tau aggregates via the proteasome. Neuron 2004; 43: 321–32.

Oddo S, Caccamo A, Shepherd JD, Murphy MP, Golde TE, Kayed R, et al. Triple-transgenic model of Alzheimer's disease with plaques and tangles: intracellular Abeta and synaptic dysfunction. Neuron 2003; 39: 409–21.

O'Keefe J, Conway DH. Hippocampal place units in the freely moving rat: why they fire where they fire. Exp Brain Res 1978; 31: 573–90.

Olabarria M, Noristani HN, Verkhratsky A, Rodríguez JJ. Age-dependent decrease in glutamine synthetase expression in the hippocampal astroglia of the triple transgenic Alzheimer's disease mouse model: mechanism for deficient glutamatergic transmission? Mol Neurodegener 2011; 6: 55.

Olabarria M, Noristani HN, Verkhratsky A, Rodríguez JJ. Concomitant astroglial atrophy and astrogliosis in a triple transgenic animal model of Alzheimer's disease. Glia 2010; 58: 8.

Opuni KFM, Al-Majdoub M, Yefremova Y, El-Kased RF, Koy C, Glocker MO. Mass spectrometric epitope mapping. Mass Spec Rev 2018; 37: 229–41.

Quiroz YT, Sperling RA, Norton DJ, Baena A, Arboleda-Velasquez JF, Cosio D, Schultz A, et al. Association between amyloid and tau accumulation in young adults with autosomal dominant Alzheimer disease. JAMA Neurol 2018; 75: 548–56.

Panza F, Solfrizzi V, Seripa D, Imbimbo BP, Lozupone M, Santamato A, et al. Tau-based therapeutics for Alzheimer's disease: active and passive immunotherapy. Immunotherapy 2016; 8: 1119–34.

Paul CM, Magda G, Abel S. Spatial memory: Theoretical basis and comparative review on experimental methods in rodents. Behav Brain Res 2009; 203: 151–64.

Pedersen JT, Sigurdsson EM. Tau immunotherapy for Alzheimer's disease. Trends Mol Med 2015; 21: 394–402.

Perini G, Ciasca G, Minelli E, Papi M, Palmieri V, Maulucci G, et al. Dynamic structural determinants underlie the neurotoxicity of the N-terminal tau 26-44 peptide in Alzheimer's disease and other human tauopathies. Int J Biol Macromol 2019; 141: 278–89.

Perry VH, Nicoll JA, Holmes C. Microglia in neurodegenerative disease. Nat Rev Neurol 2010; 6: 193–201.

Piacentini R, Li Puma DD, Mainardi M, Lazzarino G, Tavazzi B, Arancio O, et al. Reduced gliotransmitter release from astrocytes mediates tau-induced synaptic dysfunction in cultured hippocampal neurons. Glia 2017; 65: 1302–16.

Pignataro A, Borreca A, Ammassari-Teule M, Middei S. CREB regulates experience-dependent spine formation and enlargement in mouse barrel cortex. Neural Plast 2015; 2015: 1–11.

Planel E, Tatebayashi Y, Miyasaka T, Liu L, Wang L, Herman M, et al. Insulin dysfunction induces *in vivo* tau hyperphosphorylation through distinct mechanisms. J Neurosci 2007; 27: 13635–48.

Plath N, Ohana O, Dammermann B, Errington ML, Schmitz D, Gross C, et al. Arc/Arg3.1 Is essential for the consolidation of synaptic plasticity and memories. Neuron 2006; 52: 437–44.

Plouffe V, Mohamed NV, Rivest-McGraw J, Bertrand J, Lauzon M, Leclerc N. Hyperphosphorylation and cleavage at D421 enhance tau secretion. PLoS One 2012; 7: e36873.

Podda MV, Cocco S, Mastrodonato A, Fusco S, Leone L, Barbati SA, et al. Anodal transcranial direct current stimulation boosts synaptic plasticity and memory in mice via epigenetic regulation of Bdnf expression. Sci Rep 2016; 6: 22180.

Polanco JC, Li C, Bodea LG, Martinez-Marmol R, Meunier FA, Götz J. Amyloid-β and tau complexity—towards improved biomarkers and targeted therapies. Nat Rev Neurol 2018; 14: 22–39.

Polydoro M, Acker CM, Duff K, Castillo PE, Davies P. Age-dependent impairment of cognitive and synaptic function in the htau mouse model of tau pathology. J Neurosci 2009; 29: 10741–9.

Pontecorvo MJ, Devous MD Sr, Navitsky M, Lu M, Salloway S, Schaerf FW, et al. 18F-AV-1451-A05 investigators. Relationships

between flortaucipir PET tau binding and amyloid burden, clinical diagnosis, age and cognition. Brain 2017; 140: 748–63.

Pooler AM, Noble W, Hanger DP. A role for tau at the synapse in Alzheimer's disease pathogenesis. Neuropharmacology 2014 76: 1–8.

Pooler AM, Polydoro M, Wegmann S, Nicholls SB, Spires-Jones TL, Hyman BT. Propagation of tau pathology in Alzheimer's disease: identification of novel therapeutic targets. Alzheimers Res Ther 2013; 5: 49.

Portelius E, Hansson SF, Tran AJ, Zetterberg H, Grognet P, Vanmechelen E, et al. Characterization of tau in cerebrospinal fluid using mass spectrometry. J Proteome Res 2008; 7: 2114–20.

Puzzo D, Piacentini R, Fá M, Gulisano W, Li Puma DD, Staniszewski A, et al. LTP and memory impairment caused by extracellular Aβ and Tau oligomers is APP-dependent. Elife 2017; 6: pii: e26991.

Quinn JP, Corbett NJ, Kellett KAB, Hooper NM. Tau proteolysis in the pathogenesis of tauopathies: neurotoxic fragments and novel biomarkers. J Alzheimers Dis 2018; 63: 13–33.

Qureshi IA, Tirucherai G, Ahlijanian MK, Kolaitis G, Bechtold C, Grundman M. A randomized, single ascending dose study of intravenous BIIB092 in healthy participants. Alzheimers Dement 2018; 4: 746–55.

Rajamohamedsait H, Rasool S, Rajamohamedsait W, Lin Y, Sigurdsson EM. Prophylactic active tau immunization leads to sustained reduction in both tau and amyloid-β pathologies in 3xTg mice. Sci Rep 2017; 7: 17034.

Rajmohan R, Reddy PH. Amyloid-beta and phosphorylated tau accumulations cause abnormalities at synapses of Alzheimer's disease neurons. J Alzheimers Dis 2017; 57: 975–99.

Ramirez-Amaya V, Angulo-Perkins A, Chawla MK, Barnes CA, Rosi S. Sustained transcription of the immediate early gene Arc in the dentate gyrus after spatial exploration. J Neurosci 2013; 33: 1631–9.

Ramírez-Amaya V, Vazdarjanova A, Mikhael D, Rosi S, Worley PF, Barnes CA. Spatial exploration-induced Arc mRNA and protein expression: evidence for selective, network-specific reactivation. J Neurosci 2005; 25: 1761–8.

Rapoport M, Dawson HN, Binder LI, Vitek MP, Ferreira A. Tau is essential to beta-amyloid-induced neurotoxicity. Proc Natl Acad Sci USA 2002; 99: 6364–9.

Reed JM, Squire LR. Impaired recognition memory in patients with lesions limited to the hippocampal formation. Behav Neurosci 1997; 111: 667–75.

Regan P, Whitcomb DJ, Cho K. Physiological and pathophysiological implications of synaptic tau. Neuroscientist 2017; 23: 137–51.

Rhein V, Song X, Wiesner A, Ittner LM, Baysang G, Meier F, et al. Amyloid-beta and tau synergistically impair the oxidative phosphorylation system in triple transgenic Alzheimer's disease mice. Proc Natl Acad Sci USA 2009; 106: 20057–62.

Roberson ED, Scearce-Levie K, Palop JJ, Yan F, Cheng IH, Wu T, et al. Reducing endogenous tau ameliorates amyloid beta-induced deficits in an Alzheimer's disease mouse model. Science 2007; 316: 750–4.

Rodrigues EM, Weissmiller AM, Goldstein LS. Enhanced β-secretase processing alters APP axonal transport and leads to axonal defects. Hum Mol Genet 2012; 21: 4587–601.

Rohn TT, Rissman RA, Davis MC, Kim YE, Cotman CW, Head E. Caspase-9 activation and caspase cleavage of tau in the Alzheimer's disease brain. Neurobiol Dis 2002; 11: 341–54.

Rosenmann H, Grigoriadis N, Karussis D, Boimel M, Touloumi O, Ovadia H, et al. Tauopathy-like abnormalities and neurologic deficits in mice immunized with neuronal tau protein. Arch Neurol 2006; 63: 1459–67.

Rosoklija GB, Petrushevski VM, Stankov A, Dika A, Jakovski Z, Pavlovski G, Davcheva N, et al. Reliable and durable Golgi staining of brain tissue from human autopsies and experimental animals. J Neurosci Methods 2014; 230: 20–9.

Rowan MJ, Klyubin I, Cullen WK, Anwyl R. Synaptic plasticity in animal models of early Alzheimer's disease. Phil Trans R Soc Lond B 2003; 358: 821–8.

Rozenstein-Tsalkovich L, Grigoriadis N, Lourbopoulos A, Nousiopoulou E, Kassis I, Abramsky O, et al. Repeated immunization of mice with phosphorylated-tau peptides causes neuroinflammation. Exp Neurol 2013; 248: 451–6.

Rusu P, Jansen A, Soba P, Kirsch J, Löwer A, Merdes G, et al. Axonal accumulation of synaptic markers in APP transgenic Drosophila depends on the NPTY motif and is paralleled by defects in synaptic plasticity. Eur J Neurosci 2007; 25: 1079–86.

Salloway S, Sperling R, Fox NC, Blennow K, Klunk W, Raskind M, et al. Bapineuzumab 301 and 302 Clinical Trial Investigators. Two phase 3 trials of bapineuzumab in mild-to-moderate Alzheimer's disease. N Engl J Med 2014; 370: 322–33.

Salmon DP, Bondi MW. Neuropsychological assessment of dementia. Annu Rev Psychol 2009; 60: 257–82.

Saman S, Kim W, Raya M, Visnick Y, Miro S, Saman S, et al. Exosome-associated tau is secreted in tauopathy models and is selectively phosphorylated in cerebrospinal fluid in early Alzheimer disease. J Biol Chem 2012; 287: 3842–9.

Sankaranarayanan S, Barten DM, Vana L, Devidze N, Yang L, Cadelina G, et al. Passive immunization with phospho-tau antibodies reduces tau pathology and functional deficits in two distinct mouse tauopathy models. PLoS One 2015 May 1; 10: e0125614.

Sato C, Barthélemy NR, Mawuenyega KG, Patterson BW, Gordon BA, Jockel-Balsarotti J, et al. Tau kinetics in neurons and the human central nervous system. Neuron 2018; 97: 1284–98.e7.

Scheff SW, Price DA, Schmitt FA, Mufson EJ. Hippocampal synaptic loss in early Alzheimer's disease and mild cognitive impairment. Neurobiol Aging 2006a; 27: 1372–84.

Scheff SW, Price DA. Alzheimer's disease-related alterations in synaptic density: neocortex and hippocampus. J Alzheimers Dis 2006b; 9: 101–15.

Schlachetzki JC, Hüll M. Microglial activation in Alzheimer's disease. Curr Alzheimer Res 2009; 6: 554–63.

Schönheit B, Zarski R, Ohm TG. Spatial and temporal relationships between plaques and tangles in Alzheimer-pathology. Neurobiol Aging 2004; 25: 697–711.

Schreurs A, Latif-Hernandez A, Uwineza A. Commentary: APP as a mediator of the synapse pathology in Alzheimer's disease. Front Cell Neurosci 2018; 12: 150. doi: 10.3389/fncel.2018.00150.

Schroeder SK, Joly-Amado A, Gordon MN, Morgan D. Tau-directed immunotherapy: a promising strategy for treating Alzheimer's disease and other tauopathies. J Neuroimmune Pharmacol 2016; 11: 9–25.

Schwab C, Klegeris A, McGeer PL. Inflammation in transgenic mouse models of neurodegenerative disorders. Biochim Biophys Acta 2010; 1802: 889–902.

Sebastián-Serrano Á, de Diego-García L, Díaz-Hernández M. The neurotoxic role of extracellular tau protein. Int J Mol Sci 2018; 19: 998.pii: E998.

Segal M. Dendritic spines and long-term plasticity. Nat Rev Neurosci 2005; 6: 277–84.

Selkoe DJ. Alzheimer's disease is a synaptic failure. Science 2002; 298: 789–91.

Shamir DB, Rosenqvist N, Rasool S, Pedersen JT, Sigurdsson EM. Internalization of tau antibody and pathological tau protein detected with a flow cytometry multiplexing approach. Alzheimers Dement 2016; 12: 1098–107.

Shankar GM, Li S, Mehta TH, Garcia-Munoz A, Shepardson NE, Smith I, et al. Amyloid-beta protein dimers isolated directly from Alzheimer's brains impair synaptic plasticity and memory. Nat Med 2008; 14: 837–42.

Shipton OA, Leitz JR, Dworzak J, Acton CE, Tunbridge EM, Denk F, et al. Tau protein is required for amyloid {beta}-induced impairment of hippocampal long-term potentiation. J Neurosci 2011; 31: 1688–92.

Sigurdsson EM. Immunotherapy targeting pathological tau protein in Alzheimer's disease and related tauopathies. J Alzheimers Dis 2008; 15: 157–68.

Small SA, Duff K. Linking Abeta and tau in late-onset Alzheimer's disease: a dual pathway hypothesis. Neuron 2008; 60: 534–42.

Sokolow S, Henkins KM, Bilousova T, Gonzalez B, Vinters HV, Miller CA, et al. Pre-synaptic C-terminal truncated tau is released from cortical synapses in Alzheimer's disease. J Neurochem 2015; 133: 368–79.

Sotiropoulos I, Galas MC, Silva JM, Skoulakis E, Wegmann S, Maina MB, et al. Atypical, non-standard functions of the microtubule associated Tau protein. Acta Neuropathol Commun 2017; 5: 91.

Spires-Jones TL, Hyman BT. The intersection of amyloid beta and tau at synapses in Alzheimer's disease. Neuron 2014; 82: 756–71.

Spires-Jones T, Knafo S. Spines, plasticity, and cognition in Alzheimer's model mice. Neural Plast 2012; 2012: 1–10.

Spires-Jones TL, Meyer-Luehmann M, Osetek JD, Jones PB, Stern EA, Bacskai BJ, et al. Impaired spine stability underlies plaque-related spine loss in an Alzheimer's disease mouse model. Am J Pathol 2007; 171: 1304–11.

Subramanian S, Savanur G, Madhavadas S. Passive immunization targeting the N-terminal region of phosphorylated tau (residues 68-71) improves spatial memory in okadaic acid induced tauopathy model rats. Biochem Biophys Res Commun 2017; 483: 585–9.

Sydow A, Hochgräfe K, Könen S, Cadinu D, Matenia D, Petrova O, et al. Age-dependent neuroinflammation and cognitive decline in a novel Ala152Thr-Tau transgenic mouse model of PSP and AD. Acta Neuropathol Commun 2016; 4: 17.

Takahashi M, Miyata H, Kametani F, Nonaka T, Akiyama H, Hisanaga S, et al. Extracellular association of APP and tau fibrils induces intracellular aggregate formation of tau. Acta Neuropathol 2015; 129: 895–907.

Takahashi RH, Capetillo-Zarate E, Lin MT, Milner TA, Gouras GK. Co-occurrence of Alzheimer's disease ß-amyloid and τ pathologies at synapses. Neurobiol Aging 2010; 31: 1145–52.

Teich AF, Nicholls RE, Puzzo D, Fiorito J, Purgatorio R, Fa' M, et al. Synaptic therapy in Alzheimer's disease: a CREB-centric approach. Neurotherapeutics 2015; 12: 29–41.

Thomson AM. Facilitation, augmentation and potentiation at central synapses. Trends Neurosci 2000; 23: 305–12.

Um HS, Kang EB, Koo JH, Kim HT, J-L Kim, EJYang CH, et al. Treadmill exercise represses neuronal cell death in an aged transgenic mouse model of Alzheimer's disease. Neurosci Res 2011; 69: 161–73.

Velazquez R, Ferreira E, Tran A, Turner EC, Belfiore R, Branca C, et al. Acute tau knockdown in the hippocampus of adult mice causes learning and memory deficits. Aging Cell 2018; 17: e12775.

Vogel-Ciernia A, Wood MA. Examining object location and object recognition memory in mice. Curr Protoc Neurosci 2014; 69: 8.31.1–17.

Vogels T, Murgoci AN, Hromádka T. Intersection of pathological tau and microglia at the synapse. Acta Neuropathol Commun 2019; 7: 109.

Vossel KA, Zhang K, Brodbeck J, Daub AC, Sharma P, Finkbeiner S, et al. Tau reduction prevents Abeta-induced defects in axonal transport. Science 2010; 330: 198.

Wall PM, Messier C. Infralimbic kappa opioid and muscarinic M1 receptor interactions in the concurrent modulation of anxiety and memory. Psychopharmacology (Berl). 2002; 160: 233–44.

Wang L, Benzinger TL, Su Y, Christensen J, Friedrichsen K, Aldea P, et al. Evaluation of tau imaging in staging Alzheimer disease and revealing interactions between β-amyloid and tauopathy. JAMA Neurol 2016; 73: 1070–7.

Wang Y, Garg S, Mandelkow EM, Mandelkow E. Proteolytic processing of tau. Biochem Soc Trans 2010; 38: 955–61.

Wang Z, Jackson RJ, Hong W, Taylor WM, Corbett GT, Moreno A, et al. Human brain-derived Aβ oligomers bind to synapses and disrupt synaptic activity in a manner that requires APP. J Neurosci 2017; 37: 11947–66.

Warburton EC, Barker GR, Brown MW. Investigations into the involvement of NMDA mechanisms in recognition memory. Neuropharmacology 2013; 74: 41–7.

Webster SJ, Bachstetter AD, Nelson PT, Schmitt FA, Van Eldik LJ. Using mice to model Alzheimer's dementia: an overview of the clinical disease and the preclinical behavioral changes in 10 mouse models. Front Genet 2014; 5: 88.

Wes PD, Easton A, Corradi J, Barten DM, Devidze N, DeCarr LB, et al. Tau overexpression impacts a neuroinflammation gene expression network perturbed in Alzheimer's disease. PLoS One 2014; 9: e106050.

West MJ, Coleman PD, Flood DG, Troncoso JC. Differences in the pattern of hippocampal neuronal loss in normal ageing and Alzheimer's disease. Lancet 1994; 344: 769–72.

Wilcock DM, Rojiani A, Rosenthal A, Levkowitz G, Subbarao S, Alamed J, et al. Passive amyloid immunotherapy clears amyloid and transiently activates microglia in a transgenic mouse model of amyloid deposition. J Neurosci 2004; 24: 6144–51.

Wisniewski T, Goñi F. Immunotherapeutic approaches for Alzheimer's disease. Neuron 2015; 85: 1162–76.

Xu W, Weissmiller AM, White JA, Fang F, Wang X, Wu Y, et al. Amyloid precursor protein-mediated endocytic pathway disruption induces axonal dysfunction and neurodegeneration. J Clin Invest 2016; 126: 1815–33.

Yamada K. Extracellular tau and its potential role in the propagation of tau pathology. Front Neurosci 2017; 11: 667.

Yanamandra K, Jiang H, Mahan TE, Maloney SE, Wozniak DF, Diamond MI, et al. Anti-tauantibody reduces insoluble tau and decreases brain atrophy. Ann Clin Transl Neurol 2015; 2: 278–88.

Yanamandra K, Kfoury N, Jiang H, Mahan TE, Ma S, Maloney SE, et al. Anti-tau antibodies that block tau aggregate seeding *in vitro* markedly decrease pathology and improve cognition *in vivo*. Neuron 2013; 80: 402–14.

Yassine N, Lazaris A, Dorner-Ciossek C, Després O, Meyer L, Maitre M, et al. Detecting spatial memory deficits beyond blindness in tg2576 Alzheimer mice. Neurobiol Aging 2013; 34: 716–30.

Yoshiyama Y, Higuchi M, Zhang B, Huang SM, Iwata N, Saido TC, et al. Synapse loss and microglial activation precede tangles in a P301S tauopathy mouse model. Neuron 2007; 53: 337–51.

Yuan P, Condello C, Keene CD, Wang Y, Bird TD, Paul SM, et al. TREM2 haplodeficiency in mice and humans impairs the microglia barrier function leading to decreased amyloid compaction and severe axonal dystrophy. Neuron 2016; 90: 724–39.

Zempel H, Thies E, Mandelkow E, Mandelkow EM. Abeta oligomers cause localized Ca (2+) elevation, missorting of endogenous Tau into dendrites, Tau phosphorylation, and destruction of microtubules and spines. J Neurosci 2010; 30: 11938–950.

Zhang Z, Li XG, Wang ZH, Song M, Yu SP, Kang SS, et al. δ-Secretase-cleaved tau stimulates Aβ production via upregulating STAT1-BACE1 signaling in Alzheimer's disease. Mol Psychiatry 2018; doi: 10.1038/s41380-018-0286-z.

Zhou L, McInnes J, Wierda K, Holt M, Herrmann AG, Jackson RJ, et al. Tau association with synaptic vesicles causes presynaptic dysfunction. Nat Commun 2017; 8: 15295.

Zilka N, Filipcik P, Koson P, Fialova L, Skrabana R, Zilkova M, et al. Truncated tau from sporadic Alzheimer's disease suffices to drive neurofibrillary degeneration *in vivo*. FEBS Lett 2006; 580: 3582–8.

Zola SM, Squire LR. Relationship between magnitude of damage to the hippocampus and impaired recognition memory in monkeys. Hippocampus 2001; 11: 92–8.

Zotova E, Nicoll JA, Kalaria R, Holmes C, Boche D. Inflammation in Alzheimer's disease: relevance to pathogenesis and therapy. Alzheimers Res Ther 2010; 2: 1.

Zucker RS, Regehr WG. Short-term synaptic plasticity. Annu Rev Physiol 2002; 64: 355–405.